Cape Peninsula
University of Technology

A SIMPLIFIED ANALYSIS OF THE VIBRATION OF VARIABLE LENGTH BLADE AS MIGHT BE USED IN WIND TURBINE SYSTEMS

by

KWANDA TARTIBU

Dissertation submitted in fulfilment of the requirements for the degree

MASTER OF TECHNOLOGY: Mechanical Engineering

in the

FACULTY OF ENGINEERING

at the

CAPE PENINSULA UNIVERSITY OF TECHNOLOGY

Supervisor: MARK KILFOIL
Co-supervisor: Dr ALETTA VAN DER MERWE

Cape Town
November 2008

DECLARATION

I, **KWANDA TARTIBU**, declare that the contents of this thesis represent my own unaided work, and that the dissertation/thesis has not previously been submitted for academic examination towards any qualification. Furthermore, it represents my own opinions and not necessarily those of the Cape Peninsula University of Technology.

Signed **Date**

ABSTRACT

Vibration is an inherent phenomenon in dynamic mechanical systems. The work undertaken in this thesis is to identify natural frequencies of a variable length blade. Therefore designers can ensure that natural frequencies will not be close to the frequency (or integer multiples) of the main excitation forces in order to avoid resonance. For a wind turbine blade, the frequency range between 0.5 Hz and 30 Hz is relevant. The turbine blade is approximated by a cantilever, therefore, it is fully constrained where attached to a turbine shaft/hub. Flap-wise, edge-wise and torsional natural frequencies are calculated.

The MATLAB program “BEAMANALYSIS.m” has been developed for the finite element analysis of a one dimensional model of the beam. Similarly, a three dimensional model of the beam has been developed in a finite element program Unigraphics NX5. The results found using the MATLAB program are compared with those found with NX5. Satisfactory agreement between the results is found for frequencies up to almost 500 Hz. Additionally, the frequencies one might expect in an experiment are identified.

Experimental modal analysis has been performed on a uniform and stepped beam made of mild steel to extract the first five flap-wise natural frequencies. The results found have been compared to numerical results and the exact solution of an Euler-Bernoulli beam. Concurrence is found for the frequency range of interest. Although, some discrepancies exist at higher frequencies (above 500 Hz), finite element analysis proves to be reliable for calculating natural frequencies.

Finally, the fixed portion and moveable portion of the variable length blade are approximated respectively by a hollow and a solid beam which can be slid in and out. Ten different configurations of the variable length blade, representing ten different positions of the moveable portion are investigated. A MATLAB program named VARIBLADEANALYSIS.m was developed to predict natural frequencies. Similarly three dimensional models of the variable length blade have been developed in the finite element program Unigraphics NX5.

ACKNOWLEDGEMENTS

I want to express my heartfelt appreciation to all individuals who have in one way or the other contributed to the success of this project and my studies:

Firstly to my parents, you made me who I am and for that I thank them. I'd like to thank also my family for their confidence in me that enabled me to complete this work. I should also acknowledge some of my relatives for their motivation.

I received a Postgraduate Award scholarship to conduct my research and I am grateful for this financial support. Dr. Oswald Franks is acknowledged for his help in obtaining funding for me.

Part of the thesis work was done while I was performing my experiment at IDEAS Solutions. It is a pleasure to thank Farid Hafez-Ismail for his support.

Finally, I would like to sincerely thank my supervisors. Mark Kilfoil and Dr. Van Der Merwe were ideal supervisors. They gave me the direction I needed whilst allowing me the freedom I desired. Their experience and knowledge was an asset. I can only hope that some of it wore off onto me.

DEDICATION

To my family

TABLE OF CONTENTS

DECLARATION ii
ABSTRACT iii
ACKNOWLEDGEMENTS iv
DEDICATION v
TABLE OF CONTENTS vi
LIST OF FIGURES ix
LIST OF TABLES xi
LIST OF APPENDICES xii
GLOSSARY xiii
CHAPTER 1 1
INTRODUCTION 1
1.1 Thesis Structure 1
1.2 Wind turbine technology and design concepts 2
1.2.1 Wind energy 2
1.2.2 Types of wind turbines 3
1.2.3 Components of wind energy systems 3
1.2.4 Working principle of a wind turbine 6
1.3 Wind turbine power output and variable length blade concept 8
1.4 Vibration and Resonance 12
1.5 Problem statement 14
1.6 Aims and objectives 14
CHAPTER 2 16
LITERATURE REVIEW 16
2.1. Vibration 16
2.1.1 Classification of previous research 16
2.1.2 Presenting natural frequency data 16
2.2 Beam models 18
2.3 Rotating beams/ blades 19
2.4 Extendable blades 20
2.5 Summary and Conclusion 21
CHAPTER 3 22
STRUCTURAL DYNAMIC CONSIDERATIONS IN WIND TURBINE DESIGN 22
3.1. Introduction 22
3.2. Fundamentals of vibration analysis 22
3.3. Turbine loadings and their origins 26
3.4. Rotor excitations and resonances 28
3.5. Beam: theory and background 29

3.5.1 Equation of motion for a uniform beam 29
3.5.2 Natural frequencies and modes shapes 31
3.6 Summary 33
CHAPTER 4 34
EXPERIMENTAL VERIFICATION 34
4.1. Introduction 34
4.2 Theory of experimental modal analysis 34
4.2.1 Discrete blade motion 34
4.2.2 Extraction of modal properties 36
4.3 Experimental setup 38
4.3.1 Measurement method 38
4.3.2 Exciting modes with impact testing 39
4.3.3 Determination of natural frequencies 39
4.4 Modal analysis technique 43
4.5 Summary 43
CHAPTER 5 44
NUMERICAL SIMULATION 44
5.1 Introduction 44
5.2 Modelling theory 44
5.3 Euler-Bernoulli beam element 44
5.4 One-dimensional models: MATLAB 47
5.4 Three-dimensional model: NX5 49
5.5 Summary 50
CHAPTER 6 51
RESULTS AND DISCUSSION 51
6.1 Introduction 51
6.2 Convergence test for finite element models 51
6.3 Results for uniform beam 53
6.3.1 Exact solution 54
6.3.2 MATLAB program 56
6.3.3 NX5 model 56
6.3.4 Experimental modal analysis results 57
6.3.5 Comparison of natural frequencies 58
6.4 Results for stepped beam 60
6.4.1 MATLAB program 60
6.4.2 NX5 model 61
6.4.3 Experimental modal analysis results 62
6.4.4 Comparison of natural frequencies 63

6.5 Results for variblade 64
6.5.1 NX5 and MATLAB results comparison for variblade 64
6.5.2 Influence of blade length 67
6.5.3 Effect of rotation 68
6.6. Contextualization of the findings 69
CHAPTER 7 71
CONCLUSIONS AND RECOMMENDATIONS FOR FUTURE WORK 71
7.1 Conclusions 71
7.2 Recommendations 72
7.2.1 Finite element analysis 72
7.2.2 Experimental modal analysis 73
BIBLIOGRAPHY/REFERENCES 74
APPENDICES 80

LIST OF FIGURES

Figure 1.1: Two basic wind turbines, horizontal axis and vertical axis 3
Figure 1.2: Major components of a horizontal axis wind turbine 4
Figure 1.3: Hub options 5
Figure 1.4: Lift and drag on the rotor of a wind turbine 6
Figure 1.5: Blade element force-velocity diagram 7
Figure 1.6: Power output from a wind turbine as a function of wind speed 8
Figure 1.7: Wind turbine schematic 9
Figure 1.8: Wind turbine with variable length blades with the blades extended and retracted 12
Figure 1.9: Terms used for representing displacements, loads and stresses on the rotor. 13
Figure 1.10: Edge-wise and flap-wise vibrations of the blade 15

Figure 2.1: Campbell Diagram for a hypothetical wind turbine 17
Figure 2.2: Mod-1 system natural frequencies 18
Figure 2.3: Typical fibreglass blade cross-section 19

Figure 3.1: Single degree of freedom mass-spring-damper system 22
Figure 3.2: Quasi-static response. Solid line: excitation force, and dashed line: simulated response. 23
Figure 3.3: Resonant response. Solid line: excitation force, and dashed line: simulated response. 23
Figure 3.4: Inertia dominated response. Solid line: excitation force, and dashed line: simulated response. 24
Figure 3.5: Frequency response function. Upper figure: magnitude versus frequency, and lower figure: phase lag versus frequency. 25
Figure 3.6: Sources of wind turbine loads 27
Figure 3.7: Exciting forces and degrees of vibrational freedom of a wind turbine 28
Figure 3.8: Soft to stiff frequency intervals of a three-bladed, constant rotational speed wind turbine 29
Figure 3.9: A beam in bending 30

Figure 4.1: The degrees of freedom for a wind turbine blade 35
Figure 4.2: Impact testing 39
Figure 4.3: Dimensions of the uniform beam used in the experiment 40
Figure 4.4: Dimensions of the uniform and stepped beam used in the experiment 40
Figure 4.5: Clamping details 41
Figure 4.6: Impact hammer 41

Figure 4.7: Accelerometer 42
Figure 4.8: Dynamic signal analyser 42

Figure 5.1: Euler-Bernoulli beam element 45
Figure 5. 2: Variblade 48
Figure 5.3: Ten configurations of variblade 49
Figure 5.4: Simulation part with constraint 50

Figure 6.1: MATLAB program convergence test results 52
Figure 6.2: NX convergence test results 53
Figure 6.3: Uniform beam deflections 57
Figure 6.4: Measured transfer functions imported into Vib-Graph 58
Figure 6.5: Stepped beam deflections 61
Figure 6.6: Measured transfer functions imported into Vib-Graph 62
Figure 6.7: Flap-wise, edge-wise and torsional deflection for configuration 1 65
Figure 6.8: Flap-wise, edge-wise and torsional deflection for configuration 5 65
Figure 6.9: Flap-wise, edge-wise and torsional deflection for configuration 10 66
Figure 6.10: MATLAB and NX5 results comparison 67
Figure 6.11: Natural frequencies 68

LIST OF TABLES

Table 3.1: Frequency equation and mode shape for the transverse vibration of a cantilever 33

Table 6.1: Material and geometric properties of the beam 52
Table 6.2: Material and geometric properties of the uniform beam 53
Table 6.3: MATLAB natural frequencies 56
Table 6.4: NX5 natural frequencies 57
Table 6.5: Measured and computed natural frequencies 59
Table 6.6: Material and geometric properties of the stepped beam 60
Table 6.7: MATLAB natural frequencies 61
Table 6.8: NX5 natural frequencies 62
Table 6.9: Measured and computed natural frequencies 63
Table 6.10: Material and geometric properties of the variblade 64
Table 6.11: Computed natural frequencies (NX5) 67
Table 6.12: Computed natural frequencies (MATLAB) 68
Table 6.13: Natural frequencies of the rotating variblade 69

LIST OF APPENDICES

Appendix A: Instrument specifications 80
Appendix B: MATLAB program for uniform and stepped beam 82
Appendix C: MATLAB Program explanation: 3 elements mesh 88
Appendix D: MATLAB program for VARIBLADE 101
Appendix E: NX5 results 109
Appendix F: NX5 and MATLAB results comparison 119

GLOSSARY

Terms/Acronyms/Abbreviations	Definition/Explanation
a' and *a*	Rotational and axial interference factors
A	Cross-section area
BC	Before Christ
C	Damping matrices
C_P	Power capture efficiency
$C_{P.Betz}$	Betz's Coefficient
C_t	Rotor thrust coefficient
D	Resultant drag force
DOF	Degree of freedom
E	Modulus of elasticity
f	Natural frequency
$f_{1,0}$	Natural frequency for the non-rotating blade
$f_{1,R}$	Natural frequency for the rotating blade
$F(t)$	Harmonic excitation force
$f(x,t)$	External force
$F(\omega)$	Fourier transform of a force $f(t)$
FRF	Frequency response function
F_t	Thrust load
G	Shear modulus
HAWT	Horizontal axis wind turbine
H_{ij}	Transfer function
I	Moment of inertia
KE	Kinetic energy
L	Length of beams

L_f	Resultant lift force
M	Mass matrices
$M(x,t)$	Bending moment
$\mathrm{N_b}$	Number of rotor blades
P	Power
PE	Potential energy
Pr	Rated output of the turbine
r	Radius
S	Stiffness matrices
$S_i(x)$	Shape function
T	Thickness of beams
U	Motion of the cross section
U_P	Axial component of wind
U_T	Rotational component of wind
U_x	Edge-wise deflection
U_y	Flap-wise deflection
V	Wind speed
VAWT	Vertical axis wind turbine
Vc	Cut in speed
Vf	Furling speed
Vr	Rated speed
V_0	Upstream undisturbed wind speed
V_{tip}	Tip speed
V_w	Relative wind vector
$V(x,t)$	Shear force
W	Width of beams

Wh	Wall thickness
$w(x,t)$	Transverse vibrations
$X(\omega)$	Fourier transform of the response $x\ (t)$
α	Angle of attack
v	Poisson's ratio
$v_1,\ v_2$	Displacements of the endpoints of the beam element
v_k	Eigenvectors
$\theta_1,\ \theta_2$	Rotational displacements at the end of the beam element
θ	Section pitch angle
θ_t	Torsional deflection
ϕ	Angle of relative wind velocity
ρ	Air density
τ	Torque
η_P	Power train efficiency
Ω	Rotating speed of the rotor
ω_r	Rotor angular velocity
λ_k	Eigenvalues
σ_k	Damping factor
δ_k	Logarithmic decrements

CHAPTER 1
INTRODUCTION

1.1 Thesis Structure

The research described in this thesis is directed towards a better understanding of the structural dynamic characteristics of a variable length blade for wind turbines. Three basic shapes representing the wind turbine blade have been investigated:

- A uniform beam;
- a stepped beam and,
- a variable length blade (variblade).

Chapter 1 includes background on wind turbines in general, partly for the purpose of contextualising the problem and making the thesis accessible to non-specialists. This chapter leads to the concept of a variable length blade for wind turbines and to the goal of the research.

In Chapter 2, a literature survey is given.

In Chapter 3, structural dynamic considerations related to wind turbine blade are presented. Excitations and resonances have been described. Moreover, the frequency equation and mode shapes for an uniform Euler-Bernoulli beam has been investigated.

Chapter 4 describes experimental modal analysis performed on a uniform beam and stepped beam for three purposes:

- To gain insight into experimental verification;
- to measure flap-wise natural frequencies and,
- to validate numerical results.

In Chapter 5, finite element analysis is discussed:

- To gain insight into the numerical simulation by developing a MATLAB program for a one-dimensional model and three-dimensional model in NX5;
- to calculate natural frequencies of a uniform beam and a stepped beam and,
- to calculate natural frequencies of a composite variblade.

Chapter 6 presents, compares and discusses the results.

Chapter 7 summarises the contribution of this thesis. The chapter also includes recommendations for further research.

Appendices present instruments specifications, the purpose written MATLAB codes and numerical results.

1.2 Wind turbine technology and design concepts

1.2.1 Wind energy

"A wind turbine is a machine which converts the wind's kinetic energy into mechanical energy. If the mechanical energy is used directly by machinery, such as a pump or grinding stones, the machine is usually called a windmill. If the mechanical energy is converted to electricity, the machine is described as wind generator, or more commonly a wind turbine (wind energy converter WEC)" (Burton et al., 2008). Wind turbines are classified according to their size and power output. Small wind turbines supply energy for battery charging systems and large wind turbines, grouped on wind farms supply electricity to a grid. Whatever the size or output, the basic arrangement of electricity generating turbines remains identical.

Wind energy has been used for centuries. The first field of application was to propel boats along the River Nile around 5000 BC (United States Department of Energy, 2005). By comparison, wind turbines are a more modern invention. The first simple windmills were used in Persia as early as the seventh century for irrigation purposes and for milling grain (Edinger & Kaul, 2000). The modern concept of windmills began around the time of the industrial revolution. However, as the industrial revolution proceeded, industrialisation sparked the development of larger wind turbines to generate electricity. The first electricity generating wind turbine was developed by Poul la Cour in 1897 (Danish Wind Turbine Manufacturers Association, 2003). "Today, wind energy is the world's fastest growing energy technology". Wind energy installations have surged from a capacity of less than 2 GW in 1990 to about 94 MW (October 2008) (Wind Power Monthly, 2008).

An abundance of wind energy resources, vast tracts of open land and electricity distribution infrastructure give South Africa a potential to become a "wind powerhouse" (Kowalik & Coetzee, 2005). According to wind power revolution pioneers in South Africa, "the Western Cape has prevailing winds from the south-east and north-west and they often blow during peak electricity consumption periods. These winds have a potential to generate 10 times the official national wind energy estimates" (Kowalik & Coetzee, 2005). There are two pilot wind power projects in South Africa: At Klipheuwel and Darling, both in the Western Cape (Kowalik & Coetzee, 2005).

1.2.2 Types of wind turbines

The most common turbine design is the horizontal axis wind turbine (HAWT). There are also vertical axis wind turbines (VAWT). The HAWT is more practical than the VAWT and is the focus of remainder of the discussion here for the following reasons (Manwell et al, 2004):

- Horizontal axis wind turbines are more efficient, since the blades always move perpendicularly to the wind, receiving power through the entire rotation. In contrast, all vertical axis wind turbines require aerofoil surfaces to backtrack against the wind for part of the cycle. Backtracking against the wind leads to inherently lower efficiency.
- Vertical axis wind turbines use guy wires to keep them in place and put stress on the bottom bearing as all the weight of the rotor is on the bearing. Guy wires attached to the top bearing increase downward thrust during wind gusts. Solving this problem requires a superstructure to hold a top bearing in place to eliminate the downward thrusts of gusts in guy wired models.

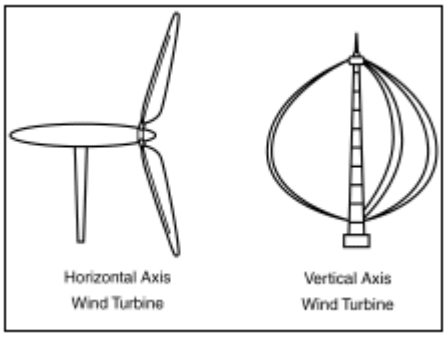

Figure 1.1: Two basic wind turbines, horizontal axis and vertical axis

(Adapted from Ontario Ministry of Energy, 2008)

1.2.3 Components of wind energy systems

The principal subsystems of a typical horizontal axis wind turbine are shown in Figure 1.2. These include: rotor; drive train, nacelle and main frame, including wind turbine housing and bedplate, yawing system, tower and foundation, machine controls, alternator and balance of the electrical system (Manwell et al, 2004).

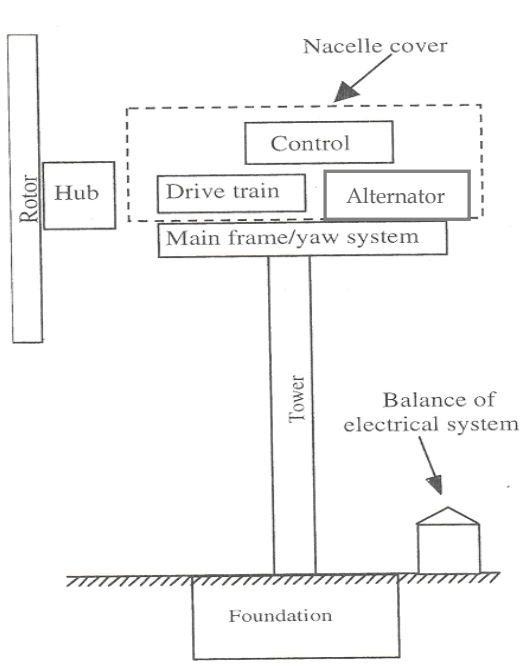

Figure 1.2: **Major components of a horizontal axis wind turbine**

(Adapted from Manwell et al, 2004)

The rotor

The rotor (the hub and blades of a wind turbine) is often considered to be the most important component from performance and overall cost standpoints. The rotor assembly may be placed in the following two directions (Manwell et al, 2004):

- Upwind of the tower and nacelle, therefore, it receives unperturbed wind and must be actively yawed by an electrical motor.
- Downwind of the tower, this enables self-alignment of the rotor with the wind direction (yawing), but the tower causes deflection and turbulence before the wind arrives at the rotor (tower shadow).

Some rotors include a pitch drive. This system controls the pitch of the blades to achieve an optimum angle to handle the wind speed and the desired rotation speed. For lower wind speed, an almost perpendicular pitch increases the energy harnessed by the blades; at high wind speed, a parallel pitch minimizes the blade surface area and prevents over speeding the rotor. Typically one motor controls each blade.

Many types of materials are used in wind turbines construction. The following list provides materials in general use for blade manufacture (Burton et al, 2004):

- Wood (including laminated wood composites)

- Synthetic composites (usually a polyester or epoxy matrix reinforced by glass fibres)
- Metals (predominantly steel or aluminium alloys)

The drive train

The drive train consists of the rotating parts of the wind turbine (exclusive of the rotor). These, typically, include shafts, gearbox, bearings, a mechanical brake and an alternator. Blades are connected to the main shaft and ultimately the rest of the drive train by the hub. There are three basic types of hub design which have been applied in modern horizontal wind turbines (Figure 1.3):

- Rigid hubs;
- teetering hubs and,
- hinged hubs.

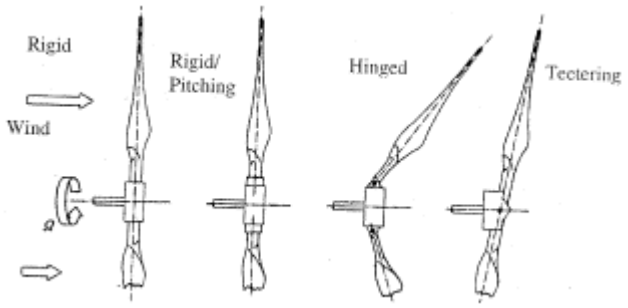

Figure 1.3: Hub options

(Adapted from Manwell et al, 2004)

The nacelle and yaw system

This category includes the wind housing, machine bedplate or mainframe and the yaw orientation system. The main frame provides for the mounting and proper alignment of the drive train components. A yaw orientation system for upwind turbines is required to ensure the rotor shaft remains parallel with the wind.

Tower and the foundation

This includes the tower structure and supporting foundation. The tower of a wind turbine supports the nacelle assembly and elevates the rotor to a height at which the wind velocity is significantly greater and less perturbed than at ground level.

Controls and Balance of electrical system

A wind turbine control system includes the following components: Sensors, controllers, power amplifiers and actuators. In addition to the alternator, the wind turbine utilises a number of other electrical components such as cables, switchgear, transformers and possibly electronic power converters, power factor correction capacitors, yaw and pitch motors.

Alternator

The most common types encountered in wind turbines are induction and synchronous alternators. In addition, some smaller turbines use DC machines (generators).

1.2.4 Working principle of a wind turbine

Modern wind turbines work on an aerodynamic lift principle, just as do the wings of an aeroplane. The wind does not "push" the turbine blades, but instead, as wind flows across and passes a turbine blade, the difference in pressure on either side of the blade produces a lifting force, causing the rotor to rotate and cut across the wind as illustrated in Figure 1.4.

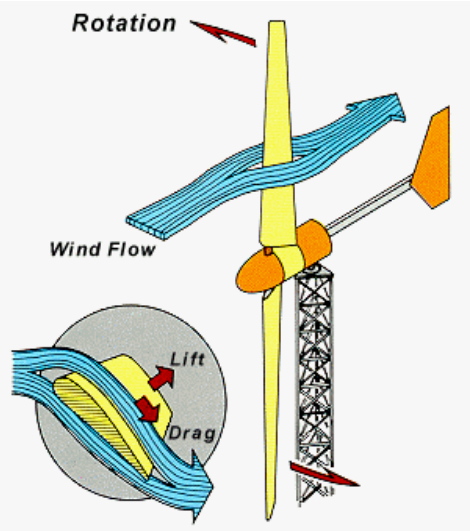

Figure 1.4: **Lift and drag on the rotor of a wind turbine**

(Adapted from Aerowind Systems, n.d.)

A section of a blade at radius *r* is illustrated in Figure 1.5, with the associated velocities, forces and angles indicated.

- The relative wind velocity vector at radius *r*, denoted by V_w, is the resultant of the axial component U_P and the rotational component U_T
- The axial velocity U_P is reduced by a component $V_0 a$, because of the wake effect or retardation imposed by the blades, where V_0 is the upstream undisturbed wind speed.
- The rotational component is the sum of the velocity from to the blade's motion, $r\Omega$, and the swirl velocity of the air, $r\Omega a'$.

The *a'* and *a* terms represent rotational and axial interference factors respectively.

θ = Section pitch angle

α = Angle of attack

$\phi = \theta + \alpha$ = Angle of relative wind velocity

L_f = Resultant lift force

D = Resultant drag force

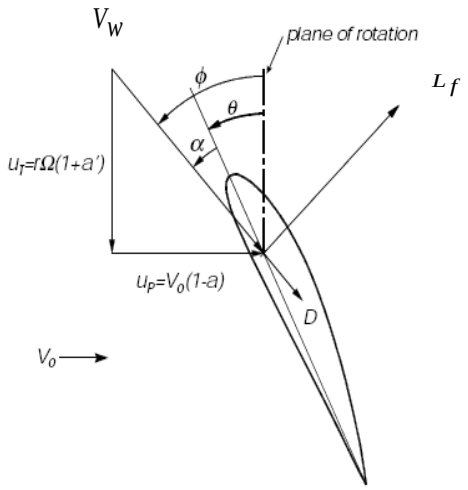

Figure 1.5: Blade element force-velocity diagram

(Adapted from Lee & Flay, 2000)

Wind turbines are designed to work between certain wind speeds. When the wind speed increases above a certain velocity, known as the "cut in" speed (typically about 3 to 4 m/s) the turbine will begin to generate electricity and continue to do so until the wind speed reaches "cut out" speed (about 25 m/s). At this point the turbine shuts down, rotates the blades out of the wind and waits for the wind speed to drop to a suitable speed which will allow the turbine to restart. The "cut out" speed is

determined by any particular machine's ability to withstand high wind (Research Institute for Sustainable Energy, 2006). The turbine will have an optimum operating wind speed ("rated speed") at which maximum output will be achieved; typically about 13 to 16 m/s. The "rated speed" is the wind speed at which a particular machine achieves its design output power. Above this speed it may have mechanisms to maintain the output at a constant value with increasing wind speed (see Figure 1.6).

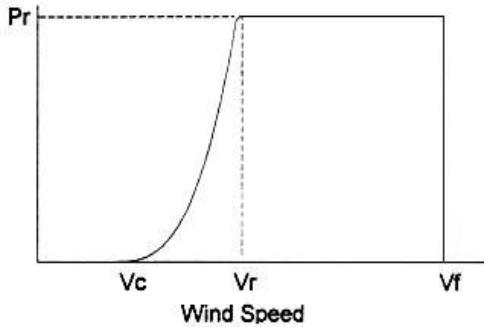

Figure 1.6: Power output from a wind turbine as a function of wind speed

(Adapted from Research Institute for Sustainable Energy, 2006)

Figure 1.6 details an ideal power curve for a small wind turbine with a furling mechanism. The machine starts to produce power at Vc (cut in speed), it reaches its rated power at Vr (rated speed) and shuts down to avoid damage at Vf (the furling speed). Pr is the rated output of the turbine. This curve is typical of a horizontal-axis two- or three-bladed machine. The curve is ideal, as the machine follows the peak power available from the wind until it reaches alternator capacity, then regulates to maintain a steady output until shut down.

1.3 Wind turbine power output and variable length blade concept

The power *P* of the wind that flows at speed *V* through an area *A* is given by the expression (Ackermann, 2000):

$$P = \frac{1}{2}\rho A V^3 \qquad \textbf{Equation 1.1}$$

ρ = air density

A = area is the cross-sectional area of the flowing air

V = wind speed

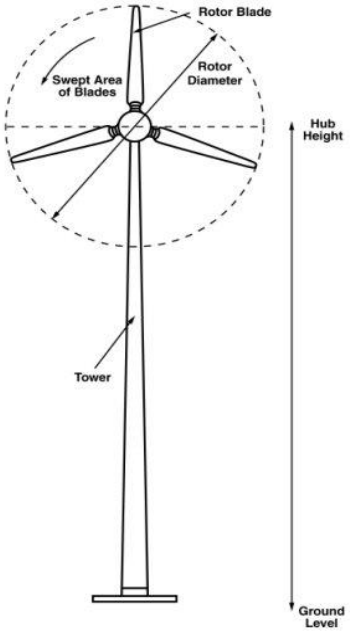

Figure 1.7: **Wind turbine schematic**

(Adapted from Ontario Ministry of Energy, 2008)

The power in the wind is the total available energy per unit time. This power is converted into the mechanical-rotational energy of the wind turbine rotor, resulting in a reduced speed of the air mass.

There are three basic physical laws governing the amount of energy available from the wind (Research Institute for Sustainable Energy, 2006).

- Firstly, the power generated by a turbine is proportional to the cube of wind speed. For example if the wind speed doubles, the power available increases by a factor of eight; if the wind speed triples then 27 times more power is available. Conversely, there is little power in the wind at low speed;
- secondly, power available is directly proportional to the swept area of the blades. Hence, the power is proportional to the square of the blade length. For example, doubling the blade length will increase the potential for power generation four times; tripling blade length increases the potential for power generation nine times and,
- finally, power in the wind cannot be extracted completely by a wind turbine. The theoretical optimum for utilizing the power by reducing its velocity was first discovered by Betz in 1926. He argued the theoretically maximum power to be extracted from the wind is given by (Ackermann, 2000):

$$P_{Betz} = \frac{1}{2}\rho A V^3 C_{P.Betz} = \frac{1}{2}\rho A V^3 0.59$$ **Equation 1.2**

Hence, even if power extraction without any loss was possible, only 59% of the power in the wind could be utilized by a wind turbine (Ackermann, 2000).

The energy capture at low wind speed (below Vc in Figure 1.6) is proportional to the rotor's swept area, which in turn is proportional to the rotor diameter squared. From Equation 1.2, it can be seen that significant increases in the output power can be achieved only by increasing the swept area of the rotor, or locating the wind turbines on sites with higher wind speeds. If a large rotor relative to the size of the alternator is suddenly acted upon by high winds, it might produce more electricity than the alternator can absorb and additionally overstress the structure. Conversely, in time of low winds, if a rotor is too small for the alternator, wind turbine efficiency may be low and the system only achieves a small proportion of its energy producing potential.

What is required is a wind turbine able to adjust to handling varying wind speed conditions efficiently, while attempting to maximise energy capture for a given support structure. This constitutes the basic concept of the variable length blade for wind turbine. The variable length blade considered here:

- Allows the rotor to yield significant increases in power capture through increase of its swept area and,
- provides a method of controllably limiting mechanical loads, such as torque, thrust, blade lead-lag (in-plane), blade flap (out-of-plane), or tower top bending loads, delivered by the rotor to the power train below a threshold value. Achieving this goal enables a single extended rotor blade configuration to operate within an adjustable load limit.

The torque (τ) delivered by the rotor to the power train is given by (U.S. Patent No 6,726,439 B2, 2004)

$$\tau = \frac{P}{\omega_r}$$ **Equation 1.3**

where P is power and ω_r is rotor angular velocity. When the angular velocity is limited by tip speed (V_{tip}), the torque can be shown to be related to the rotor radius, r, as

$$\tau = \frac{P}{V_{tip}} r$$ **Equation 1.4**

To hold torque below a set design limit, $\tau_{\lim}$, the maximum power the rotor can produce, while remaining within the tip speed and torque limit, can be seen to be inversely proportional to the rotor radius, as given by (U.S. Patent No 6,726,439 B2, 2004)

$$P_{\max} = \frac{\tau_{\lim} V_{tip}}{r} \qquad \textbf{Equation 1.5}$$

Then, if we observe that power for a given wind speed V and density ρ is given as (U.S. Patent No 6,726,439 B2, 2004)

$$P = \frac{1}{2}\rho\pi r^2 V^3 C_P \qquad \textbf{Equation 1.6}$$

where C_P is the power capture efficiency of a given rotor geometry at a specified rotor angular velocity and wind speed. The relationship between rotor radius and wind velocity can be shown to be

$$r = \frac{1}{V}\sqrt[3]{\frac{2\tau_{\lim} V_{tip}}{\rho\pi C_P}} \qquad \textbf{Equation 1.7}$$

This means as wind speed increases, the rotor radius must decrease almost as much as the inverse of this increase (C_P may vary slightly as this occurs) to remain within torque limitations. However, in practice a wind turbine will measure its power output (via electrical current for instance) and rotor speed. Therefore, one may determine the appropriate radius by (U.S. Patent No 6,726,439 B2, 2004)

$$r = \frac{\tau_{\lim} V_{tip} \eta_P}{P} \qquad \textbf{Equation 1.8}$$

where η_P is the approximate power train efficiency at a given observed output power, P. The thrust load (F_t) is calculated as (U.S. Patent No 6,726,439 B2, 2004)

$$F_t = \frac{1}{2}\rho\pi r^2 V^2 C_t \qquad \textbf{Equation 1.9}$$

where C_t is the rotor thrust coefficient at a given flow velocity, rotor speed and blade pitch angle. If the thrust is held below the nominal limit ($F_{t,\lim}$), then the rotor radius can be seen to vary as

$$r = \frac{1}{V}\sqrt{\frac{2F_{t,\lim}}{\rho\pi C_t}} \qquad \textbf{Equation 1.10}$$

where the rotor radius must decrease nearly as much as the inverse of an increase in velocity, similar to Equation 1.7.

Variable length blade (variblade) is possible if there are two parts: an inboard portion and an outboard part. The outboard portion is mounted inside the inboard portion, guided to be telescoped relative to the inboard portion. An actuator system moves the outboard portion of the blade radially to adjust the wind turbine's rotor diameter. A controller will measure electrical power and retract the outboard portion of the blade when rated power is reached, or nearly reached (Pasupulati et al., 2005). However, the mechanism is beyond the scope of this research. Design manufacture and testing of variable length blade for wind turbine is being undertaken by another student.

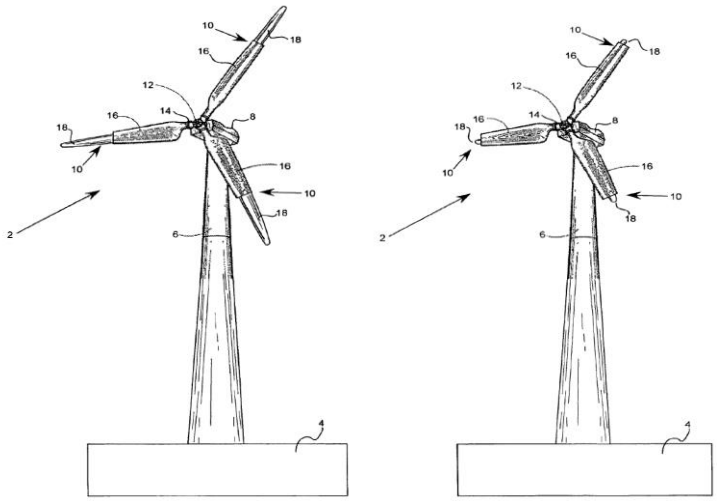

Figure 1.8: Wind turbine with variable length blades with the blades extended and retracted

(Adapted from Pasupulati et al., 2005)

1.4 Vibration and Resonance

The term vibration refers to the limited reciprocating motion of a particle or an object in an elastic system (Manwell et al, 2004). In most mechanical systems, vibrations are undesirable and dangerous if the vibratory motion becomes excessive. However, in a rotating system, such as in a wind turbine, vibrations are unavoidable. Wind turbines are partially elastic structures and operate in an unsteady environment that tends to result in vibrating response. Therefore, the interplay of the forces from the external environment, primarily because of the wind and the motion of the various components of the wind turbine, results not only in the desired energy production from the turbine, but also in stresses in its constituent materials. For the turbine designer these stresses are of primary concern, as they directly affect the strength of the turbine and how long it will last. In order to be viable for providing energy, a wind turbine must:

- Produce energy;
- survive and,

- be cost-effective.

That means that the turbine design must not only be functional in terms of extracting energy. It must also be structurally sound so that it can withstand the loads it experiences and the costs to make it structurally sound must be commensurate with the value of energy produced.

Hence, a key to good wind turbine design is to minimize vibrations by avoiding resonance. Resonance is a phenomenon occurring in a structure when an exciting or forcing frequency equals or nearly equals one of the natural frequencies of the system (Burton et al., 2004). It is characterized by a large increase in displacements and internal loads. Damping reduces these displacements and loads. That is why some turbines blades are partially filled with a foam material, which helps dampen the vibration of a blade in turbulent wind conditions (Composites world, 2008). This reduces the chances of the blade generating a resonant response.

In a rotating system the exciting frequencies are integer multiples of the rotational speed. The designer must ensure the resonant frequencies are not excited excessively. Although dynamic loads on the blades will, in general, also excite the tower dynamics, in this study, tower head motion is excluded from consideration, in order to focus exclusively on blade dynamic behaviour.

For a wind turbine blade, the deflections of interest are lateral translations (flap-wise, edge-wise) and cord rotation (about the blade's longitudinal axis) (Hau, 2000). Most directions and loads referred to are illustrated in Figure 1.9. The chordwise direction is often called edge-wise direction.

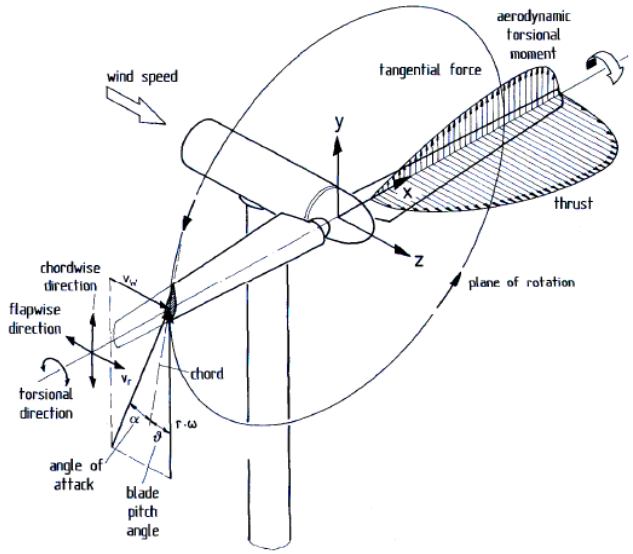

Figure 1.9: **Terms used for representing displacements, loads and stresses on the rotor.**

(Adapted from Hau, 2000)

The design of a wind turbine structure involves many considerations such as strength, stability, cost and vibration. Reduction of vibration is a good measure for a successful design in blade structure (Maalawi & Negm 2002). Dealing with vibration in an early phase of the design process avoids costly modification of a prototype after detection of a problem. Therefore, both experimental and theoretical methods are required for studying the structural characteristics of turbine blades in order to avoid vibration problems.

1.5 Problem statement

The amplitude of the generated vibrations of a wind turbine blade depends on its stiffness (Jureczko *et al*. 2005) which is a function of material, design and size. One issue a variable length blade design presents to blade designers is that of structural dynamics. A wind turbine blade has certain characteristic natural frequencies and mode shapes which can be excited by mechanical or aerodynamic forces. Variable length blade design presents additional challenges as stiffness and mass distribution change as the moveable blade portion slides in and out of the fixed blade portion.

This vibration analysis has the aim of verifying dynamic stability and the absence of resonance within the permissible operating range. Although material properties are an important factor, this analysis does not include the effect of material choice. However, it provides tools which enable wind turbine blade designers to investigate the effect of material choices.

1.6 Aims and objectives

The previous section indicated that vibration problems in a variable length blade results in two needs:

- To verify the dynamic stability and absence of resonance and
- to understand structural dynamic characteristics.

In engineering, there is a prerequisite for accurate numerical models. Computational fluid dynamics for new aircraft, the finite element method for structural analysis and finite difference programs for heat transfer are examples of numerical methods essential to a design process. In such applications, numerical models provide design performance prediction which facilitates making decisions early in the design process, thus saving money and ultimately delivering a better product. Numerical models allow

the comparison of design alternatives, normally prohibitively expensive to conduct using manufactured prototypes.

The goals of this project are:

- To develop computer models of a variblade. The model chosen is of a single blade fitted with a telescoping mechanism to vary length;
- to calculate the natural frequencies of the variblade with the computer models for the two main vibration directions (flap-wise and edge-wise);

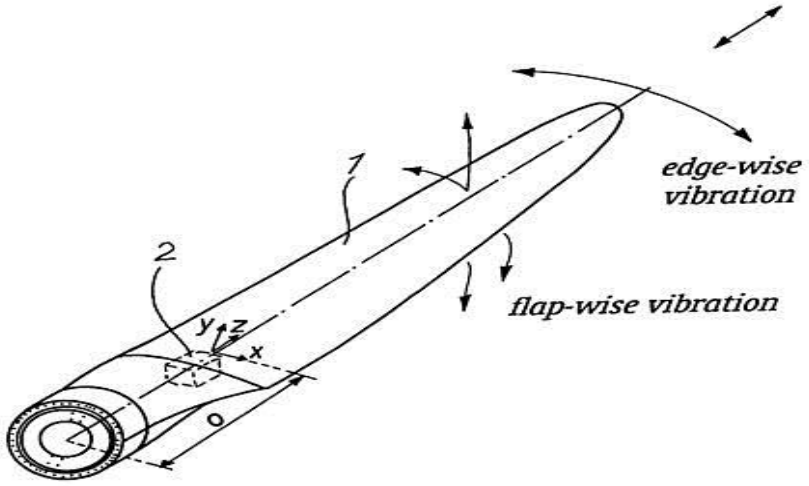

Figure 1.10: Edge-wise and flap-wise vibrations of the blade

(Adapted from Grabau & Petersensvej, 1999)

- to gain insight into experimental modal analysis, finite element analysis and analytical methods;
- to compare the output of a computer model with the experimental data and,
- to use the computer model to make recommendations on design and operation of variblades.

CHAPTER 2
LITERATURE REVIEW

2.1. Vibration

2.1.1 Classification of previous research

Vibration in wind turbines is a recognised phenomenon. As far back as the Middle Ages, the post windmill of that time was also called a “rocking mill”, as the mounting of the entire mill house on a trestle led to a rocking motion. This drawback then became the stimulus to continued development, from which evolved the more stable Dutch windmill which ran more smoothly (Hau, 2000).

Patil et al. classified the previous research on the structural dynamics of HAWTs into three groups:

- The first group of studies analyzed isolated blades;
- studies on rotor/tower or rotor/yaw coupling problems form the second group and,
- a third group of studies considers the complete system dynamics of HAWTs.

An isolated variable length blade constitutes the focus of this research and this study fits quite well in the first group of studies.

2.1.2 Presenting natural frequency data

Historically, the most basic requirement of structural dynamics analysis was to identify structural resonances and ensure they were not close to the frequency or harmonics of main rotor excitation forces (Thresher, 1982). In wind turbines, as with other rotating structures, exciting forces are generated by the rotating structure before being transmitted to the fixed structure at the frequencies which are integer multiples of the rotation rate.

A common way to present natural frequency data and to look for possible resonances is to plot a Campbell Diagram. Figure 2.1 taken from Sullivan (Sullivan, 1981), is a Campbell Diagram for a hypothetical wind turbine. It consists of:

- A plot of natural frequencies of a system versus the rotor speed and
- a set of star-like straight lines which pass through the origin and express the relationship between the possible exciting frequencies and the rotor speed.

Because it is expected that excitation frequencies will always be integer multiples of the rotor speed, the intersection of one of the straight lines with one of the natural frequency curves indicates a potential for resonant vibration near the rotor speed of the intersection point.

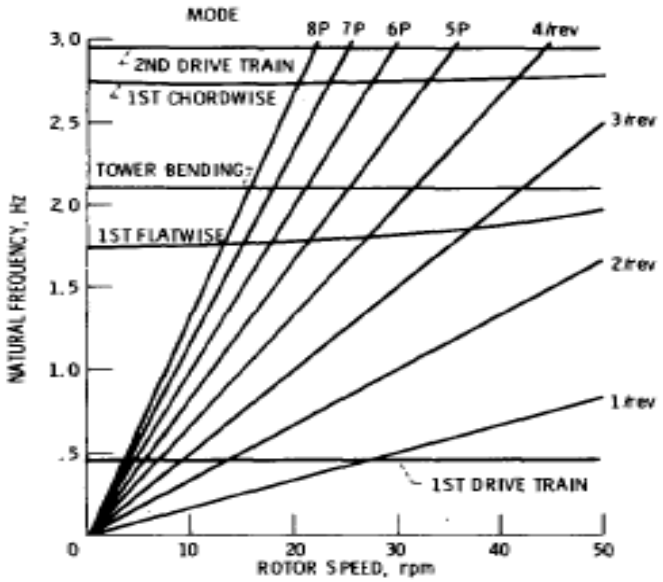

Figure 2.1: Campbell Diagram for a hypothetical wind turbine

(Adapted from Sullivan, 1981)

Another way to present this same information is to make a tabulation as shown in Figure 2.2. In this presentation of the Mod-1 (a horizontal axis wind turbine) system natural frequencies, also from Sullivan, the per revolution frequencies of various important motions are tabulated in columns. Regions of possible resonance near integer multiples of the rotational speed have been designated as regions to be avoided.

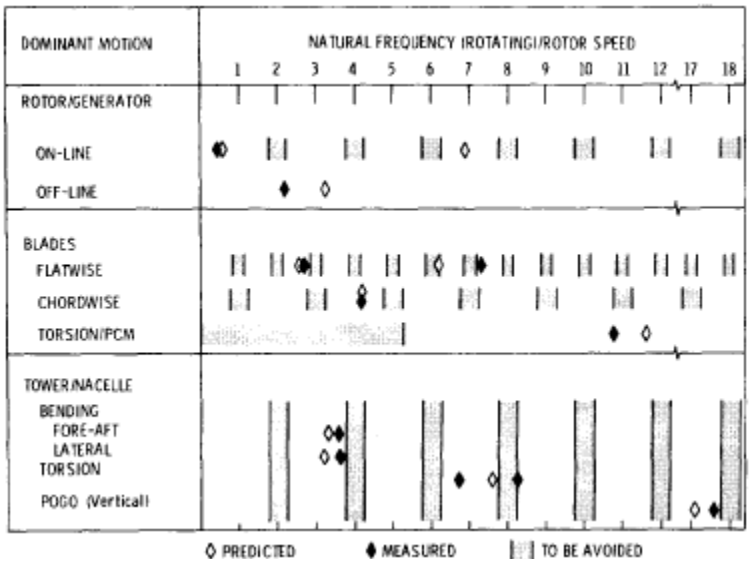

Figure 2.2: Mod-1 system natural frequencies

(Adapted from Sullivan, 1981)

2.2 Beam models

The blades of a wind turbine rotor are generally regarded as the most critical component of the wind turbine system (Kong et al, 2000). A concentrated study was made by Zhiquan et al. (Zhiquan et al., 2001). They used both experimental and theoretical methods to study the structural dynamic characteristics of rotor blades to avoid sympathetic vibration. Experimental and theoretical modal analyses were performed on a blade from a 300 W machine. In the experiments, to extract modal parameters, a DAS (dynamic signal analysis and fault diagnosis system) was used by measuring vibrations at various locations along the blade's surface. For the theoretical modal analysis a finite element analysis method was used. The effects of different constraint conditions of the finite element model were discussed. The results calculated using "*Bladed for Windows*" of Garrad Hassan and Partners Ltd. (UK) are compared with those found previously and satisfactory agreement between them obtained. The test indicated the natural frequencies of flap-wise vibrations as being lower than the torsional vibrations; flap-wise vibration being the main vibration mode of the rotor blade.

From a modelling viewpoint, properties such as mass and stiffness distributions are of great importance for the dynamic behaviour of the wind turbine blade (Mckittrick et al., 2001). The spar (Figure 2.3) is the most important part for structural analysis and acts

as a main beam. The blade can, therefore, be treated as a beam structure and a classical beam element is often used (Spera, 1994). There are several beam element types available. The most common types are based on the Euler-Bernoulli or the Timoshenko beam theories. The Euler-Bernoulli beam can be chosen because of the slender nature of the structure, which makes shear effects small. The blade is modelled as a cantilever, therefore, it is fully constrained where attached to the turbine shaft/hub.

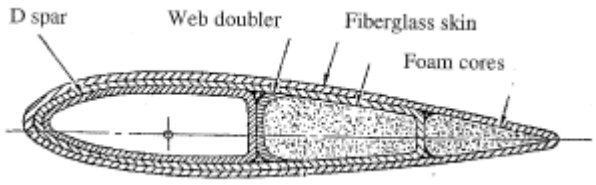

Figure 2.3: Typical fibreglass blade cross-section

(Adapted from Manwell et al., 2004)

2.3 Rotating beams/ blades

A detailed analysis of the blade undertaken by Bechly and Clausent (Bechly & Clausent, 1997) indicates the natural frequencies of a rotating blade are higher than those of its non-rotating counterpart, because of stress-stiffening. Therefore, mechanical systems, such as helicopter or turbine blades, robotic arms and satellite appendages, will often be represented by an Euler-Bernoulli cantilever beam attached to a rotating body. A well-known result from a free vibration analysis is that as the rotation speed increases, the natural frequencies of the beam also increase (Bazoune, 2001). In fact, this “stiffening" effect has been measured on rotor blades in the helicopter and engine industries. Since significant variations of dynamics characteristics result from rotational motion of such structures, they have been investigated for many years.

Southwell and Gough suggested an analytical model to calculate natural frequencies of a rotating cantilever beam (Southwell & Gough, 1921). They established a simple equation, relating the natural frequency to the rotating frequency of a beam based on the Raleigh Energy Theorem. This equation is known as the Southwell Equation. The stiffening effect due to centrifugal forces could be estimated by using the Southwell Equation, (Southwell & Gough, 1921)

$$f_{1,R} = \sqrt{f_{1,0}^2 + \phi_1 \Omega^2}$$ **Equation 2.1**

in which $f_{1,0}$ is the corresponding frequency for the non-rotating blade and Ω the rotating speed of the rotor. The ϕ_1 value is dependent on the mass and stiffness distribution and is typically set to 1.73 (Madsen, 1984). With knowledge of:

- The speed of rotation;
- the out-of-plane frequencies for the non-rotating blade;
- the in-plane frequencies the non-rotating blade and,
- the Southwell Equation.

the in-plane or out-of-plane frequency of the rotating blade is easily investigated without recourse to further extensive calculations. Therefore, the Southwell Equation provides a suitable tool for natural frequency estimates of rotating beams at a preliminary design stage.

2.4 Extendable blades

Extendable rotor blades have been recognised since the 1930's (U.S. Patent No 2,163,482, 1939). Numerous specific mechanical designs have been shown:

- The torque tube and spar assembly for a screw-driven extendable rotor blade (U.S. Patent No 5,636,969, 1997);
- The mounting arrangement for variable diameter rotor assemblies (U.S. No Patent 5,655,879, 1997);
- The variable diameter rotor blade actuation with system retention straps wound around a centrally actuated drum (U.S. Patent No 5,642,982, 1997);
- A locking mechanism and safety stop against over extension for a variable diameter rotor (U.S. No Patent 4,080,097, 1978);
- A variable diameter rotor with offset twist (U.S. No Patent 5,253,979, 1993) and,
- A drive system for changing the diameter of a variable rotor using right angle gears to interface with screw-driven retraction mechanism (U.S. Patent No 5,299,912, 1994).

U.S. Patent No 6,902,370, to Dawson and Wallace, granted in June 2005, entitled "*Telescoping wind turbine blade*" disclosed a wind turbine blade made of a fixed section attached to a wind turbine hub. A moveable blade section is attached to the fixed section so that it is free to move in a longitudinal direction relative to the fixed blade section. A positioning device allows the rotor diameter to be increased to provide high power output in low wind conditions. Diameter can be decreased in

order to minimize loads in high wind conditions. U.S. Patent No 6,972,498, to Jamieson, Jones, Moroz and Blakemore, granted in December 2003, entitled "*Variable diameter wind turbine rotor blades*", discloses a system and method for changing wind turbine rotor diameters to meet changing speeds and control system loads. U.S. Patent No 6,726,439, to Mikhail and Deane, granted in March 2003, entitled "*Retractable rotor blades for power generating wind and ocean current turbines and means for operating below set rotor torque limits*" discloses a method of controlling wind or ocean current turbines in a manner that increases energy production, while constraining torque, thrust, or other loads below a threshold value. An advantage of the invention is it enables an extended rotor blade configuration to operate within adjustable torque and thrust load limits

2.5 Summary and Conclusion

Based on the Campbell diagram (see Figure 2.1), regions of possible resonance may be determined and avoided. Through the use of experimental, numerical and theoretical methods, natural frequencies can be determined. A cantilever beam can be used to approximate the blade. Once properties such as mass and stiffness distribution are available from the design process, they can be used as input data in a computer simulation for calculating natural frequencies. Using the Southwell equation (Equation 2.1), the effects of rotation on natural frequencies can be understood. When all this is accomplished, knowledge of the structural behaviour of a wind turbine blade can be gained.

An area that has not been widely considered is the structural dynamics of a variable length blade for wind turbines. Such study could assist wind turbine designers to optimise many aspects of wind turbine design. Stiffness and mass distribution change when the moveable portion of the blade slides in and out of the fixed portion. Moreover, since the natural frequencies are functions of the geometry of the structure and the variable length blade will have different configurations (position of the outboard portion of the blade), its natural frequencies will also vary. Numerical modelling is an efficient way to determine the natural frequencies for each configuration.

CHAPTER 3

STRUCTURAL DYNAMIC CONSIDERATIONS IN WIND TURBINE DESIGN

3.1. Introduction

Problems of structural dynamics can be subdivided into two broad classifications (Knight, 1993):

- The first deals with the determination of natural frequencies of vibration and corresponding mode shapes. Usually, these natural frequencies of the structure are compared to frequencies of excitation. In design, it is usually desirable to assure these frequencies are well separated.
- A second investigates how the structure moves with time under prescribed loads and/or motions of its supports; in other words, a time history analysis has to be performed.

In this study, the focus is on determining natural frequencies.

3.2. Fundamentals of vibration analysis

The importance of proper modelling of the structural dynamics can be most conveniently illustrated by considering a single degree of freedom mass-spring-damper system as shown in Figure 3.1.

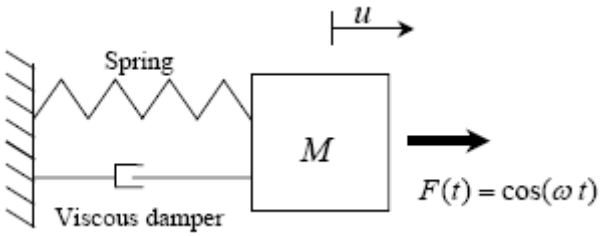

Figure 3.1: **Single degree of freedom mass-spring-damper system**

(Adapted from Van Der Tempel & Molenaar, 2002)

When a harmonic excitation force (i.e. a sinusoid) $F(t)$ is applied to a mass, the magnitude and phase of the resulting displacement u strongly depends on the frequency of excitation ω. Three response regions can be distinguished:

- Quasi-static (or stiff);
- resonance and,
- inertia dominated (or soft).

For frequencies of excitation well below the natural frequency of the system, the response will be quasi-static as illustrated in Figure 3.2: the displacement of the mass follows the time-varying force almost instantaneously (i.e. with a small phase lag) as if it had been excited by a static force.

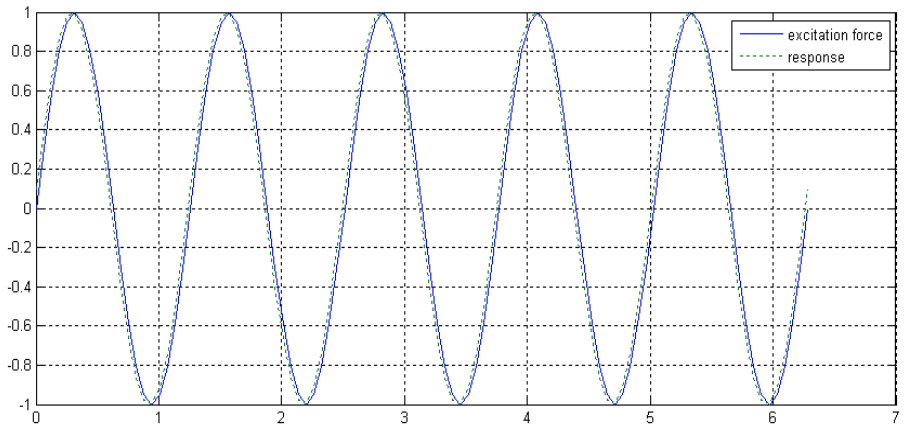

Figure 3.2: **Quasi-static response. Solid line: excitation force, and dashed line: simulated response.**

Figure 3.3 presents a typical response for frequencies of excitation within a narrow region around the system's natural frequency. In this region the spring force and inertia force (almost) cancel, producing a response a number of times larger than it would be statically (the resulting amplitude is governed by the damping present in the system).

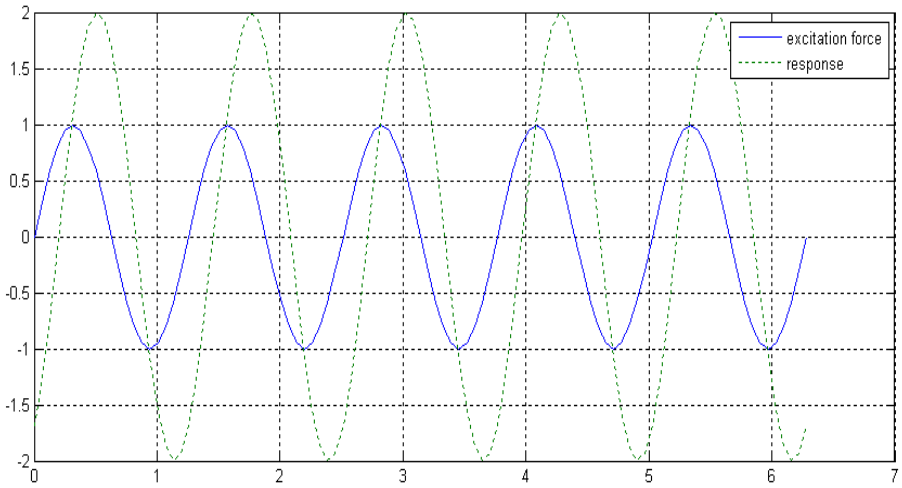

Figure 3.3: **Resonant response. Solid line: excitation force, and dashed line: simulated response.**

For frequencies of excitation well above the natural frequency, the mass can no longer “follow” the movement. Consequently, the response level is low and almost in counter-phase as illustrated in Figure 3.4. In this case the inertia of the system dominates the response and is, therefore, classified as “soft”.

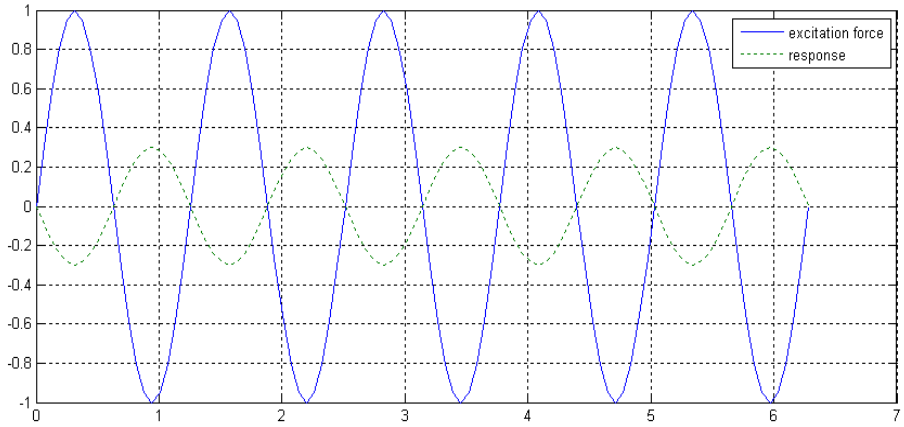

Figure 3.4: **Inertia dominated response. Solid line: excitation force, and dashed line: simulated response.**

In all three figures the magnitude of the excitation force $F(t)$ is identical, but it is applied at different excitation frequencies. The normalised ratios of the amplitude of the Figures 3.2-3.4 illustrate that:

- In steady state, sinusoidal inputs applied to a linear system generate sinusoidal outputs of the same frequency and,
- the magnitude and phase (i.e. shift between the sinusoidal input and output) are different.

The magnitude and phase modifying property of linear systems can be conveniently summarised by plotting the frequency response function (FRF). This depicts the ratio of output to input amplitudes, as well as the corresponding phase shift as functions of the frequency of excitation. Figure 3.5 shows the FRF of the single degree of freedom system depicted in Figure 3.1.

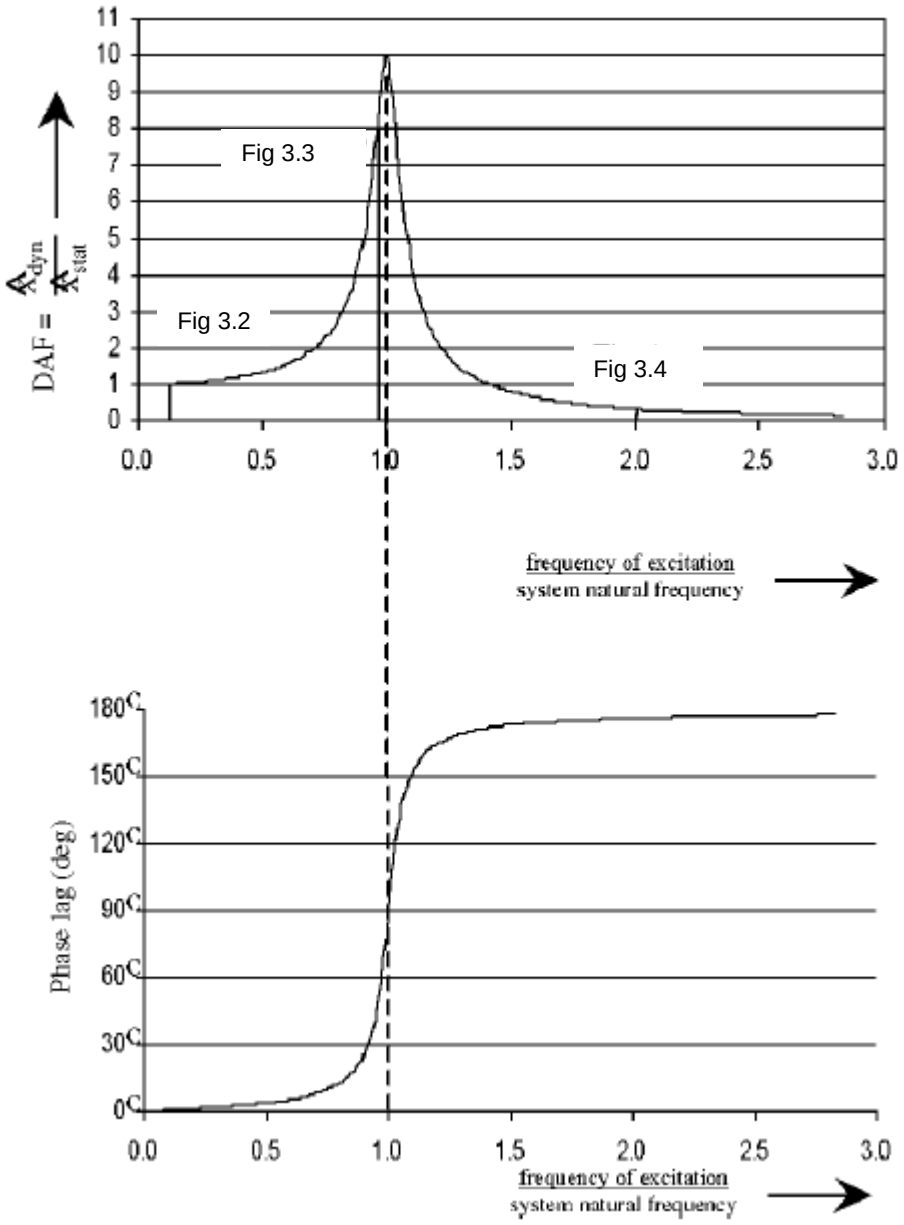

Figure 3.5: **Frequency response function. Upper figure: magnitude versus frequency, and lower figure: phase lag versus frequency.**

(Adapted from Van Der Tempel & Molenaar, 2002)

The peak in Figure 3.5 corresponds to the system's natural frequency. The height of the peak is determined by damping. In structural dynamics, the frequency of the excitation force is at least as important as its magnitude. Resonant behaviour can result in severe load cases, even failure; but it is most feared for fatigue problems (Hau, 2000). Fatigue of materials occurs due to time varying external loads, when cracks develop causing internal damage. Wind turbines are subject to fluctuating loads, which can cause such material failure. The lifetime of a wind turbine blade

depends, among other factors, on the intensity and frequency of these loads. For structures subject to dynamics loads, detailed knowledge of the expected frequencies of the excitation forces and the natural frequencies of the structure and its substructures becomes vital.

Strictly speaking, the vibrational behaviour of a system with several degrees of freedom can be treated only as a total system. This is true above all, when the dynamic coupling of the excited degrees of freedom is so strong that complex vibrational coupling modes produce natural frequencies which deviate distinctly from the separate natural frequencies of the components involved. This is basically the situation found in wind turbines (Hau, 2000). In addition, aerodynamic forces, gravitational forces, structural and aerodynamic damping and control characteristics must also be included in the calculation.

Before beginning with a mathematical simulation of such an overall system, it is helpful to discover as much as possible about the basic vibrational character of the turbine so that critical vibration modes can be recognised. In most cases, isolated mathematical treatment of the components of a specific subsystem of the turbine is feasible. For this purpose, the first and some higher natural frequencies of the variblade are calculated.

3.3. Turbine loadings and their origins

In this section, the term “load” refers to forces or moments that may act upon the turbine. Wind turbines are, by necessity, installed in areas with relatively consistent and often strong winds. As a result, wind loads are one of the dominant concerns in regard to the structural behaviour and life of a wind turbine blade. The load on a wind turbine during operation is complex. The multitude of loads of varying frequencies and amplitudes can result in potentially dangerous dynamic structural responses.

During design and operation of a wind turbine, it is necessary:

- To understand turbine loads and,
- to understand the response of the turbine due to these loads.

Wind turbine loads can be considered in five categories (Manwell et al., 2004):

- ***Steady loads*** include those because of mean wind speed, centrifugal forces in the blades due to the rotation, weight of the machine on the tower, etc;
- ***cyclic loads*** are those which arise due to the rotation of the rotor. The most basic periodic load is that experienced at the blade roots (of a HAWT) from

gravity. Other periodic loads arise from wind shear, cross wind (yaw error), vertical wind, yaw velocity and tower shadow. Mass imbalances or pitch imbalances can also give rise to periodic loads;

- ***stochastic loads*** are from turbulence or short-term variations in wind speed, both in time and space across the rotor. These can cause rapidly varying aerodynamic forces on the blades. The variations appear random, but may be described in statistical terms;
- ***transient loads*** are those which occur occasionally and, because of events of limited duration. The most common transient loads are associated with starting and stopping. Other transient loads arise from sudden wind gusts, change in wind direction, blade pitching motions or teetering. However, wind turbines are seldom erected in areas where gusts are frequent and,
- ***resonance-induced loads*** arise as a result of some part of the structure being excited at one of its natural frequencies. The designer tries to avoid the possibility of that taking place, but response to turbulence often inevitably excites some resonant response.

These loads and their origins are summarised and illustrated in Figures 3.6 and 3.7.

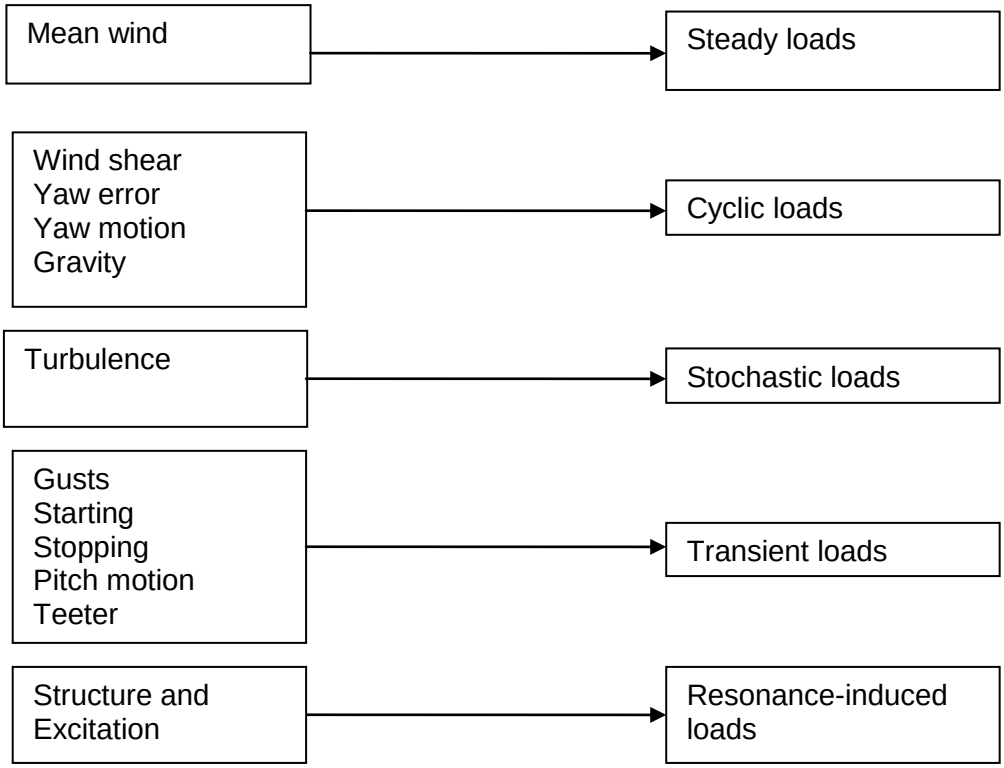

Figure 3.6: Sources of wind turbine loads

(Adapted from Manwell et al., 2004)

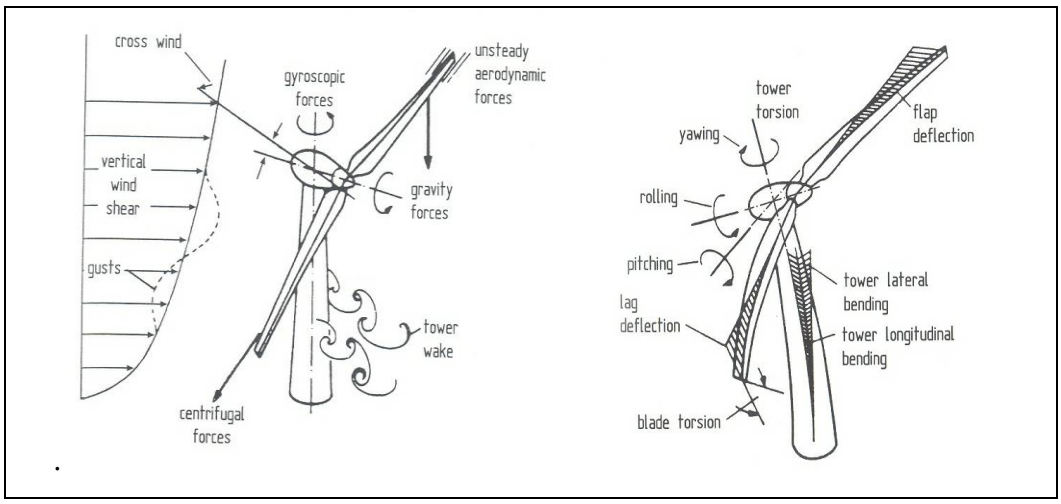

Figure 3.7: Exciting forces and degrees of vibrational freedom of a wind turbine

(Adapted from Hau, 2000)

3.4. Rotor excitations and resonances

In this section, the dynamic approach presented in Section 3.2 is applied to a wind turbine system. To translate the basic model to a wind turbine system, first excitation frequencies are examined.

The most visible source of excitation in a wind turbine system is the rotor. In this example a constant speed turbine will be investigated. The constant rotational speed is the first excitation frequency, mostly referred to as 1P. The second excitation frequency is the rotor blade passing frequency emanating from the wake generated by the tower when the rotor revolves downwind of the support: N_bP in which N_b is the number of rotor blades (2P for a turbine equipped with two rotor blades, 3P for a three-bladed rotor). To avoid resonance, the structure should be designed so its first natural frequency does not coincide with either 1P or N_bP (Van Der Tempel & Molenaar, 2002). This leaves three possible intervals of safe operation. Using a three-bladed turbine as an example, a very stiff structure, with a high natural frequency, above 3P (stiff-stiff), a natural frequency between 1P and 3P: soft-stiff and a very soft structure below 1P: soft-soft (Figure 3.8).

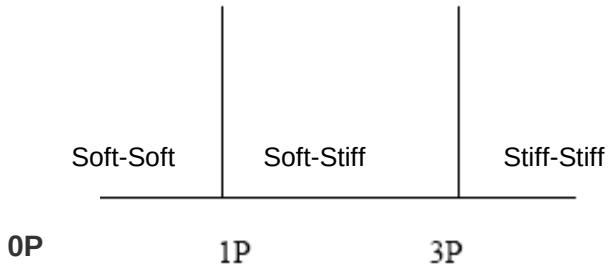

Figure 3.8: **Soft to stiff frequency intervals of a three-bladed, constant rotational speed wind turbine**

(Adapted from Van Der Tempel & Molenaar, 2002)

Most large wind turbines have three blades; smaller turbines may use two blades for ease of construction and installation. Vibration intensity decreases with increasing number of blades (Van Der Tempel & Molenaar, 2002). Noise and wear generally diminish, but efficiency improves when using three instead of two blades. Turbines with larger numbers of smaller blades operate at a lower Reynolds number and so are less efficient. Small turbines, with four or more blades, suffer further losses as each blade operates partly in the wake of other blades. Also, as the number of blades increases, usually cost also increases (Van Der Tempel & Molenaar, 2002).

3.5. Beam: theory and background

In order to determine the dynamic behaviour of a mechanical system, one needs to develop an appropriate mathematical model. This section deals with vibration of beams. The equation of motion for a beam is described and a free vibration solution derived. Investigation is made in terms of natural frequencies and modes shapes by considering the case of a cantilever. [The source of most of the material presented in Sections 3.5.2 and 3.5.3 is Rao, 2004].

3.5.1 Equation of motion for a uniform beam

Consider a free-body diagram of an element of a beam shown in Figure 3.9(a). The transverse vibrations are denoted as $w(x,t)$. The cross-sectional area is $A(x)$, the modulus of elasticity is $E(x)$, the density is $\rho(x)$ and the moment of inertia is $I(x)$. The external force applied to the beam per unit length is denoted by $f(x,t)$. The bending moment $M(x,t)$ is related to the beam deflection $w(x,t)$ by

$$M(x,t) = E(x)I(x)\frac{\partial^2 w(x,t)}{\partial x^2}$$ **Equation 3.1**

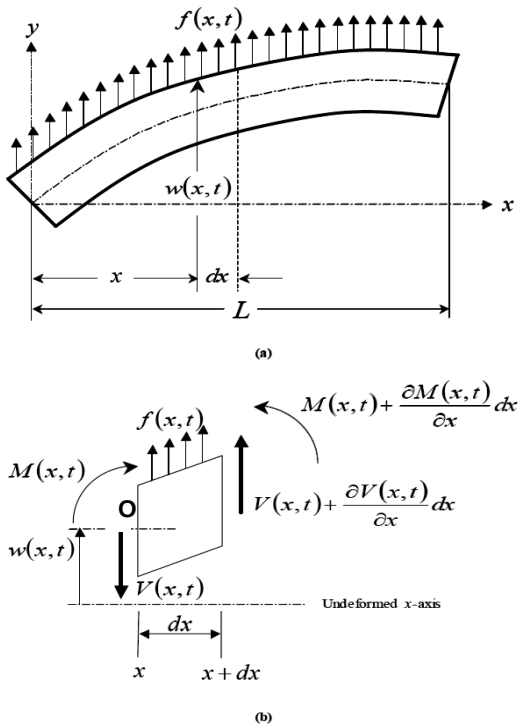

Figure 3.9: A beam in bending

(Adapted from Rao, 2004)

$V(x,t)$ is the shear force at the left end of the element dx and $V(x,t)+\frac{\partial V(x,t)}{\partial x}dx$ is the shear force at the right end of the element. One can consider an infinitesimal element of the beam, shown in Figure 3.9(b) and determine the model of transverse vibrations. It is assumed the deformation is small enough such that the shear deformation is far smaller than $w(x,t)$. The force equation of motion in the *y* direction gives

$$\left[V(x,t)+\frac{\partial V(x,t)}{\partial x}dx\right]-V(x,t)+f(x,t)dx=\rho(x)A(x)dx\frac{\partial^2 w(x,t)}{\partial t^2}$$ **Equation 3.2**

And the equation simplifies to

$$\frac{\partial V(x,t)}{\partial x}+f(x,t)=\rho(x)A(x)\frac{\partial^2 w(x,t)}{\partial t^2}$$ **Equation 3.3**

The term on the right hand side of the equation is the inertia force of the element.

The moment equation of motion about the z axis passing through point O in Figure 3.9(b) leads to

$$\left[M(x,t)+\frac{\partial M(x,t)}{\partial x}dx\right]-M(x,t)+\left[V(x,t)+\frac{\partial V(x,t)}{\partial x}dx\right]dx+\left[f(x,t)dx\right]\frac{dx}{2}=0$$ **Equation 3.4**

Assuming that the rotary inertia of the element dx is negligible; the right hand side of Equation 3.4 is zero. Simplification of this expression leads to

$$\left[\frac{\partial M(x,t)}{\partial x}+V(x,t)\right]dx+\left[\frac{\partial V(x,t)}{\partial x}+\frac{f(x,t)}{2}\right](dx)^2=0 \qquad \textbf{Equation 3.5}$$

Since dx is small, it is assumed that $(dx)^2$ is negligible and the above expression takes the form

$$V(x,t)=-\frac{\partial M(x,t)}{\partial x} \qquad \textbf{Equation 3.6}$$

This expression relates shear force and the bending moment. Substituting Equation 3.6 in Equation 3.3 leads to

$$-\frac{\partial^2}{\partial x^2}\left[M(x,t)\right]+f(x,t)=\rho(x)A(x)\frac{\partial^2 w(x,t)}{\partial t^2} \qquad \textbf{Equation 3.7}$$

Substituting Equation 3.1 in Equation 3.7 leads to

$$\rho(x)A(x)\frac{\partial^2 w(x,t)}{\partial t^2}+\frac{\partial^2}{\partial x^2}\left[E(x)I(x)\frac{\partial^2 w(x,t)}{\partial x^2}\right]=f(x,t) \qquad \textbf{Equation 3.8}$$

If no external force is applied $f(x,t)=0$. The equation of motion for free vibration of the beam (*0< x < L , t>0)* is then given as

$$\rho(x)A(x)\frac{\partial^2 w(x,t)}{\partial t^2}+\frac{\partial^2}{\partial x^2}\left[E(x)I(x)\frac{\partial^2 w(x,t)}{\partial x^2}\right]=0 \qquad \textbf{Equation 3.9}$$

The above expression (Equation 3.9) is a fourth-order partial differential equation, which governs the free vibration of a non-uniform Euler-Bernoulli beam. If the parameters $E(x)$, $A(x)$, $I(x)$ and $\rho(x)$ are constant then Equation 3.9 can be further simplified to give

$$\frac{\partial^2 w(x,t)}{\partial t^2}+c^2\frac{\partial^4 w(x,t)}{\partial x^4}=0, \qquad \textbf{Equation 3.10}$$

Where

$$c=\sqrt{\frac{EI}{\rho A}} \qquad \textbf{Equation 3.11}$$

3.5.2 Natural frequencies and modes shapes

The equation of motion (Equation 3.10) contains a fourth-order derivative with respect to position x and a second-order derivative with respect to time t. Hence, in order to determine a unique solution for $w(x,t)$, four boundary conditions and two initial conditions are required. Usually, the values of displacement and velocity are specified at time t=0, and so the initial conditions can be given as,

$w(x,0) = 0,$ and $\dot{w}(x,0) = 0,$ **Equation 3.12**

where dots denote derivates with respect to time. The method of separation of variables is used to determine the free vibration solution,

$$w(x,t) = V(x)T(t) \quad \textbf{Equation 3.13}$$

Substituting Equation 3.2 in Equation 3.10 and rearranging leads to

$$\frac{c^2}{V(x)}\frac{d^4V(x)}{dx^4} = -\frac{1}{T(t)}\frac{d^2T(t)}{dt^2} = \omega^2 \quad \textbf{Equation 3.14}$$

Here ω^2 is a positive constant. The above equation can now be written as two ordinary differential equations as shown below.

$$\frac{d^4V(x)}{dx^4} - \beta^4 V(x) = 0, \quad \textbf{Equation 3.15}$$

$$\frac{d^2T(t)}{dt^2} + \omega^2 T(t) = 0, \quad \textbf{Equation 3.16}$$

Where

$$\beta^4 = \frac{\omega^2}{c^2} = \frac{\rho A \omega^2}{EI} \quad \textbf{Equation 3.17}$$

The solution to Equation 3.15 is assumed as to be of the form

$$V(x) = \Phi e^{sx} \quad \textbf{Equation 3.18}$$

Where Φ and s are constants and we derive the auxiliary equation

$$s^4 - \beta^4 = 0$$

The roots of this equation are

$$s_{1,2} = \pm\beta, \qquad s_{3,4} = \pm i\beta, \quad \textbf{Equation 3.19}$$

Hence, the solution to Equation 3.15 can be given as

$$V(x) = \Phi_1 e^{\beta x} + \Phi_2 e^{\beta x} + \Phi_3 e^{i\beta x} + \Phi_4 e^{i\beta x} \quad \textbf{Equation 3.20}$$

Equation 3.20 can also be expressed as

$$V(x) = \Phi_1 \cos\beta x + \Phi_2 \sin\beta x + \Phi_3 \cosh\beta x + \Phi_4 \sinh\beta x$$

Or

$$V(x) = \Phi_1(\cos\beta x + \cosh\beta x) + \Phi_2(\cos\beta x - \cosh\beta x) + \Phi_3(\sin\beta x + \sinh\beta x) + \Phi_4(\sin\beta x - \sinh\beta x)$$

where Φ_1, Φ_2, Φ_3 and Φ_4 are arbitrary constants.

The function $V(x)$ is known as the normal mode or characteristic function of the beam. The frequency equation and the mode shapes for the transverse vibration of the cantilever is obtained by applying the four boundary conditions to $V(x)$. The natural frequency of the beam can therefore be computed from Equation 3.17. The

frequency equation and the mode shapes (normal functions) for cantilevered beams are given in Table 3.1. The natural frequency of the beam is obtained from

$$f = \frac{\omega}{2\pi} = \frac{(\beta L)^2}{2\pi}\sqrt{\frac{EI}{\rho A L^4}} \qquad \textbf{Equation 3.21}$$

The value of β in Equation 3.21 can be determined from the third column in Table 3.1.

Table 3.1: **Frequency equation and mode shape for the transverse vibration of a cantilever**

Frequency equation	Mode shape (normal function)	Value for $\beta_n L$
$\cos\beta_n L \cosh\beta_n L = -1$	$V_n(x) = \Phi_n[\sin\beta_n x - \sinh\beta_n x - \alpha_n(\cos\beta_n x - \cosh\beta_n x)]$ Where $\alpha_n = \left(\frac{\sin\beta_n L + \sinh\beta_n L}{\cos\beta_n L + \cosh\beta_n L}\right)$	$\beta_1 L$ =1.875104 $\beta_2 L$ =4.694091 $\beta_3 L$ =7.854757 $\beta_4 L$ =10.995541 $\beta_5 L$ =14.137168

3.6 Summary

Structural dynamic considerations related to the wind turbine blade have been presented; Excitations and resonances described.

The wind turbine blade can be approximated by an Euler-Bernoulli beam. For this purpose, the five first natural frequencies and the vibration modes of the beam are presented for a non-rotating condition. To validate numerical and modal testing results, those natural frequencies will be compared to these available solutions.

CHAPTER 4
EXPERIMENTAL VERIFICATION

4.1. Introduction

This chapter examines the experimental modal analysis techniques applied in experiments using a uniform and a stepped beam. These simplified shapes are representative of the non-extendable blades. The aims are:

- To gain an insight into experimental modal analysis;
- to provide an overview of this theory and,
- to explain some of the experimental tasks related to that theory.

In Chapter 6, comparison will be made between those experimental results and numerical results. Therefore, the simplified shapes shown on Page 40 (Figure 4.3 and Figure 4.4) were chosen.

4.2 Theory of experimental modal analysis

Modal analysis provides information on the dynamic characteristics of structural elements at resonance, and thus helps in understanding the detailed dynamic behaviour of these (Ewins, 2000). Modal analysis can be accomplished through experimental techniques. It is the most common method for characterising the dynamic properties of a mechanical system. The modal parameters are:

- The modal frequency;
- the damping factor and,
- the mode shape.

The free dynamic response of the wind turbine blade can be reduced to these discrete set of modes. It should be noted that determination of the damping properties is usually considered to be somewhat uncertain, which relates to the small quantities of the damping characteristics (Larsen et al., 2002).

4.2.1 Discrete blade motion

Real structures have an infinite number of degrees of freedom (DOFs) and an infinite number of modes. They can be sampled spatially at as many DOFs as is desired from a testing point of view. There is no limit to the number of unique DOFs between which FRF (frequency response function) measurements can be made. However, time and cost

constraints, result in only a small subset of the FRFs being measured on a structure. The modes that are within the frequency range of the measurements can be accurately defined, from this small subset of FRFs. The more the surface of the structure is spatially sampled by taking more measurements, the more definition is given to its mode shapes.

Because a wind turbine blade is generally a large structure (length >20m) it is necessary to treat it in successive cross-sections. The modal analysis of the wind turbine blade is performed by exciting it at a fixed point during the test. This excitation represents the input signal to the system. The output signal consists of accelerations measured in cross sections along the blade. A finite number of degrees of freedom are used to describe blade motion. The mode shapes of the blade are assumed to be described by deflection in the flap-wise and edge-wise directions as well as by rotation of the chord about the pitch axis (torsion). The rigid body motion can be described by three DOFs in each cross-section. Two flap-wise DOFs describe the flap-wise deflection and torsion (denoted U_y and θ_t) and one edge-wise DOF describes the edge-wise deflection (denoted U_x). The rigid body motion (response) can be derived as a function of the three amplitudes of the DOFs in the following form:

$$U = Ax \qquad \textbf{Equation 4.1}$$

where *U* is the motion of the cross-section and x (excitation) is the corresponding amplitudes in the three DOFs of the cross-section.

$$U = \begin{Bmatrix} U_x \\ U_y \\ \theta_t \end{Bmatrix} \text{ and } x = \begin{Bmatrix} x_i \\ x_{i+1} \\ x_{i+2} \end{Bmatrix}$$

and A (the FRFs) is a three by three matrix given by the positions of the three DOFs.

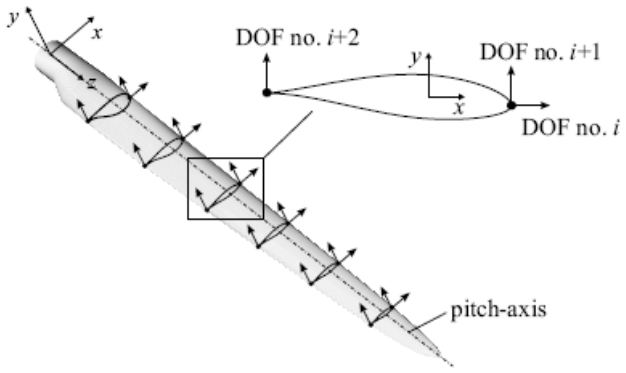

Figure 4.1: The degrees of freedom for a wind turbine blade

(Adapted from Larsen et al., 2002)

Using Equation 4.1 a mode shape of the blade can be estimated in a number of cross-sections, presuming the corresponding modal amplitudes *(U* and x*)* have been measured in the three DOFs of each cross-section.

4.2.2 Extraction of modal properties

a. Modal properties from an eigenvalue problem

To introduce this mathematical concept the linear equation of free motion for the blade is considered. The motion of the blade is described by *N* DOFs as shown in Figure 4.1. The deflection in DOF i is denoted x_i, and the vector x describes the discretized motion of the blade. Assuming small deflections and moderate rotation of the blade cross-sections, the linear equation of motion can be written as (Larsen et al., 2002):

$$M\ddot{x} + C\dot{x} + Sx = 0, \qquad \textbf{Equation 4.2}$$

where dots denote derivates with respect to time, and the matrices M , C and S are the mass, damping and stiffness matrices. Inserting the solution $x = ve^{\lambda t}$ into Equation 4.2 yields

$$(\lambda^2 M + \lambda C + S)v = 0, \qquad \textbf{Equation 4.3}$$

which is an eigenvalue problem. The solution to this problem is the eigenvalues λ_k and the corresponding eigenvectors v_k for *k* = 1*, 2, . . ., N*. The eigenvalues of a damped blade are complex and given by:

$$\lambda_k = \sigma_k + i\omega_k$$

where σ_k and ω_k are respectively the damping factor and the modal frequency for mode k. The relationship between natural frequencies (f_k), logarithmic decrements (δ_k) and the eigenvalues are:

$$f_k = \frac{\omega_k}{2\pi} \text{ and } \delta_k = -\sigma_k / f_k \qquad \textbf{Equation 4.4}$$

The natural frequencies and logarithmic decrements are obtained from the eigenvalues, and mode shapes are obtained from the eigenvectors of the eigenvalue problem. The above eigenvalue problem indicates that the problem of determining natural frequencies, logarithmic decrements, and mode shapes of a blade could be solved if one had a way to measure mass, damping, and stiffness matrices. Such measurements are, however,

impossible. Instead one can measure transfer functions in the frequency domain which hold enough information to extract the modal properties.

b. From transfer functions to modal properties

A transfer function describes in the frequency domain what the response is in one DOF due to a unity forcing function in another DOF. It is defined as (Larsen et al., 2002):

$$H_{ij}(\omega) \equiv X_i(\omega) / F_j(\omega) \qquad \textbf{Equation 4.5}$$

where,

ω is the frequency of excitation

$X_i(\omega)$ is the Fourier transform of the response $x_i(t)$ in DOF i

$F_j(\omega)$ is the Fourier transform of a force $f_j(t)$ acting in DOF number *j*.

By measuring the response x_i and the forcing function f_j, and performing the Fourier transformations, the transfer function H_{ij} can be calculated from Equation 4.5. This transfer function is one of *N* × *N* transfer functions which can be measured for the blade with *N* DOFs. The complete set of functions is referred to as the transfer matrix H. To understand this basic principle of modal analysis, consider the linear equation of motion (Equation 4.2) for the blade with external excitation.

$$M\ddot{x} + C\dot{x} + Sx = f(t) \qquad \textbf{Equation 4.6}$$

Where the vector *f* is a forcing vector containing the external forces $f_j(t)$ which may be acting in the DOFs j = 1, 2, . . ., *N.*

The transfer matrix can be derived as (Larsen et al., 2002):

$$H(\omega) = \sum_{k=1}^{N} H_k(\omega) = \sum_{k=1}^{N} \frac{v_k v_k^T}{(i\omega - \sigma_k - i\omega_k)(i\omega - \sigma_k + i\omega_k)} \qquad \textbf{Equation 4.7}$$

This relation is the basis of modal analysis. It relates the measurable transfer functions to the modal properties ω_k, σ_k, and v_k. Each mode k contributes a modal transfer matrix H_k to the complete transfer matrix. Hence, a measured transfer function can be approximated by a sum of modal transfer functions (Larsen et al., 2002):

$$H_{ij}(\omega) \approx \sum_{k=1}^{N} H_{k,ij}(\omega), \qquad \textbf{Equation 4.8}$$

where the modal transfer functions $H_{k,ij}(\omega)$ by decomposition can be written as (Larsen et al., 2002)

$$H_{k,ij}(\omega) = \frac{r_{k,ij}}{i\omega - p_k} + \frac{\overline{r_{k,ij}}}{i\omega - \overline{p_k}} \qquad \textbf{Equation 4.9}$$

where the bar denotes the complex conjugate. $p_k = \sigma_k + i\omega_k$ is called the pole of mode k and $r_{k,ij} = v_{k,i} v_{k,j}$ is called the residue of mode k at DOF i with reference to DOF j. Thus, a pole is a complex quantity describing the natural frequency and damping of the mode. A residue is a complex quantity describing the product of two complex modal amplitudes. The modal properties are extracted from measured transfer functions by curve fitting functions derived from Equation 4.8 and Equation 4.9, with poles and residues as fitting parameters.

4.3 Experimental setup

4.3.1 Measurement method

There are several methods available to measure the frequency response functions needed to perform a modal analysis. The most important differences between these methods are in the number of inputs and outputs and in the excitation method used:

- The single input single output (SISO) methods and,
- the multiple input multiple output (MIMO) methods.

The two most common excitation methods are

- Excitation using an impact hammer and,
- excitation using an electrodynamical shaker.

Each of these methods has specific advantages and disadvantages which determine the most suitable measurement in a specific case. The advantages and disadvantages of each method are discussed by Ewins (Ewins, 2000). In order to measure the frequency response functions of the turbine blade model a single input, single output impact test with fixed boundary conditions is performed. The reasons behind the choice for this type of test are:

- The test has been performed to extract only the natural frequencies;
- all the test equipment needed for an impact test were readily available making an impact test cheaper than alternative methods for which most of the equipment required is not available and,
- the extra sensors and data processing capability needed to implement an alternative testing method were also unavailable.

4.3.2 Exciting modes with impact testing

Impact testing is a quick, convenient way of finding the modes of machines and structures. Impact testing is shown in Figure 4.2. The equipment required to perform an impact test in one direction are:

1. An ***impact hammer*** with a load cell attached to its head to measure the input force.
2. An ***accelerometer*** to measure the response acceleration at a fixed point and in a fixed direction.
3. A two channel ***FFT analyser*** to compute frequency response function (FRFs).
4. ***Post-processing modal software*** for identifying modal parameters and displaying the mode shapes in animation.

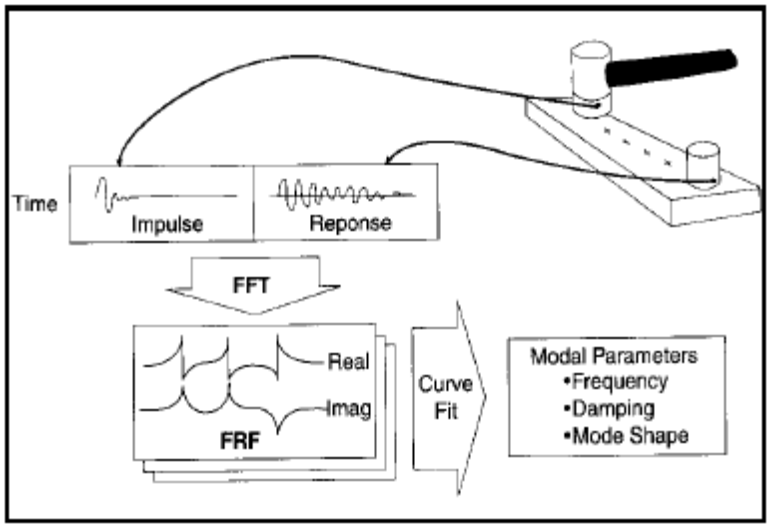

Figure 4.2: Impact testing

(Adapted from Schwarz & Richardson, 1999)

4.3.3 Determination of natural frequencies

Experimental modal analysis has been performed successively on uniform and stepped beams, to extract natural frequencies. The uniform beam was chosen as a starting point because the analytical solution is available (Chapter 3). The stepped beam is an approximation for a tapered wind turbine blade.

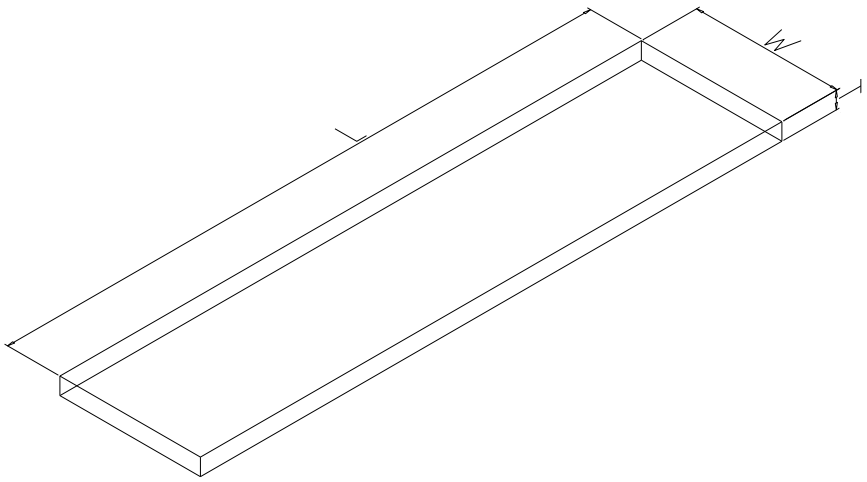

Figure 4.3: Dimensions of the uniform beam used in the experiment

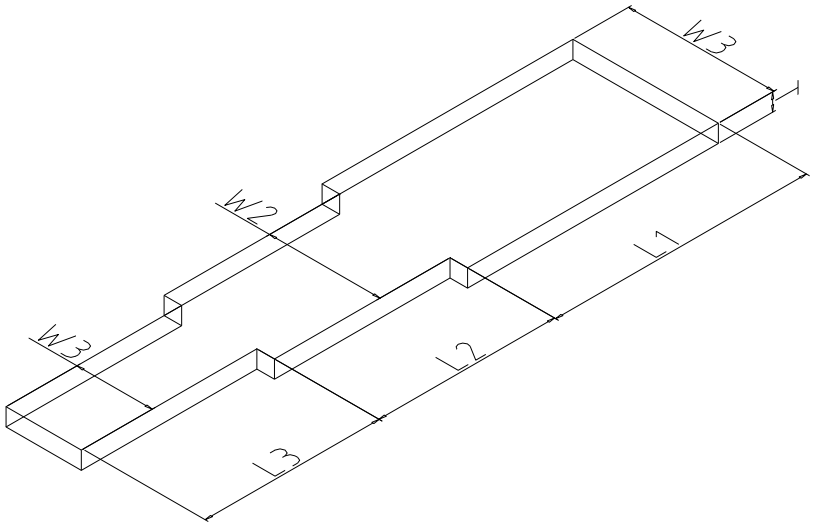

Figure 4.4: Dimensions of the uniform and stepped beam used in the experiment

Modal testing has been performed in order to extract the natural frequencies of the test beam. The following material gives a brief description of the set-up, necessary equipment and procedure for performing the test

(i) Test Beam

A test beam is fastened to a table with a clamp at one location. Clamping details are shown in Figure 4.5.

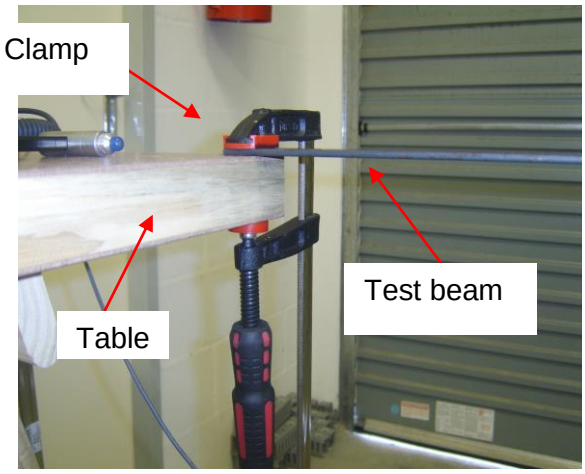

Figure 4.5: Clamping details

(ii) Impact Hammer

Model 086C02 from PCB Piezotronics is used to cause an impact. It consists of an integral ICP quartz force sensor mounted on the striking end of the hammerhead. The hammer range is about $\pm 440\ N$. Its resonant frequency is near *22 kHz*. Figure 4.6 shows a picture of the hammer and the beam. Some relevant properties of this impact hammer are presented in Appendix A.

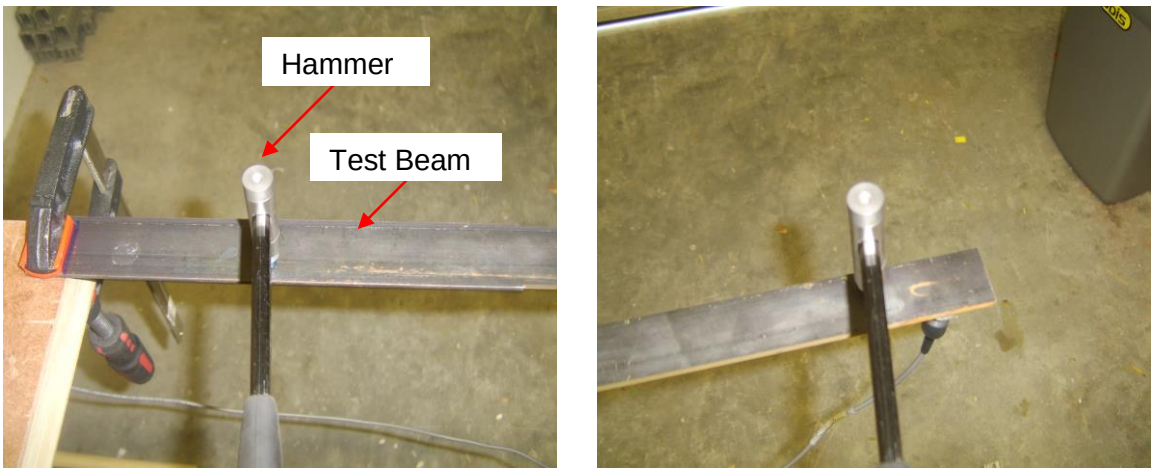

Figure 4.6: Impact hammer

(iii) Accelerometer

IEPE Accelerometer, Model IA11T, from IDEAS SOLUTION is used in the test. The range of frequencies is from *0.32 Hz* to *10 kHz* and voltage sensitivity is *10.2* $mV/(m/s^2)$**.** The relevant properties of this accelerometer are presented in Appendix A.

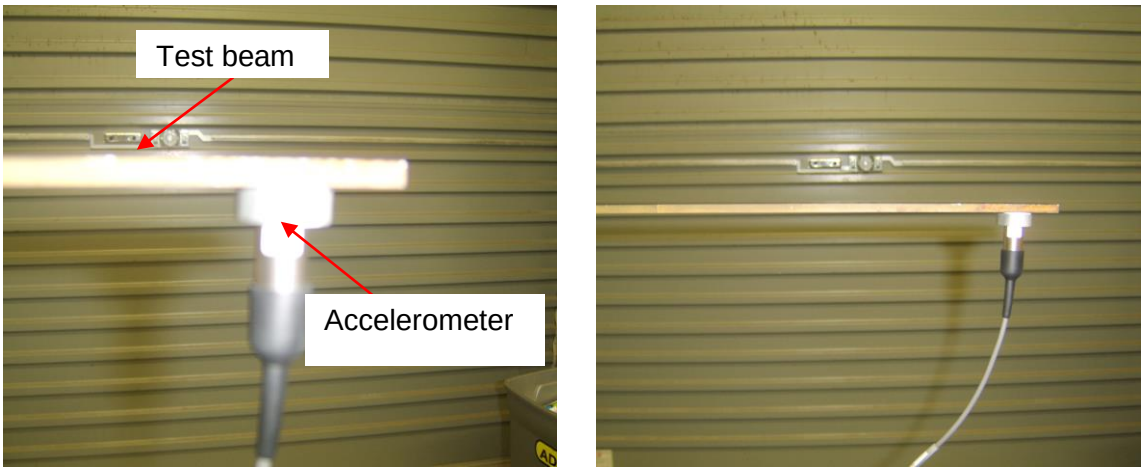

Figure 4.7: Accelerometer

(iv) *Dynamic Signal Analyser*

Measurement of the force and acceleration signals is performed using a "OneproD MVP-2C" 2-channel dynamic signal analyser. Some properties of this dynamic signal analyser are shown in Appendix A. The dynamic signal analyser samples the voltage signals emanating from the impact hammer and accelerometer. The sensitivity information of the sensors is used to convert the voltages to equivalent force and acceleration values. The dynamic signal analyser also performs the transformations and calculations necessary to convert the two measured time domain signals into a frequency response function. Measurement data may be processed on a computer using Vib-Graph software.

Figure 4.8: Dynamic signal analyser

4.4 Modal analysis technique

The idea of exciting a structure with an impact hammer is actually simple:

- One strikes a structure at a particular location and in a particular direction with an impact hammer. The uniform and stepped beams are successively excited in flap-wise direction;
- the force transducer in the tip of the impact hammer measures the force used to excite the structure;
- responses are measured by means of accelerometers mounted successively at the tip of the uniform and stepped beams;
- the force input and corresponding responses are then used to compute the FRFs (frequency response functions) and,
- desktop or laptop computer with suitable software collects the data, estimates the modal parameters and displays results.

For this work a program named Vib-Graph was used. It is special software for the measurement of frequency response functions of structures. Using the transfer function measurements, it determines the dynamic parameters of a system.

4.5 Summary

This chapter describes the theory and laboratory setup of the experimental modal analysis that was performed on a uniform and a stepped beam. The purpose is to gain insight in modal testing and to use experimental results to validate finite element results.

CHAPTER 5
NUMERICAL SIMULATION

5.1 Introduction

There are two main approaches to wind turbine blade dynamics analysis. For existing blades, dynamics can be measured using experimental techniques as discussed in Chapter 4. Although this is considered a rapid approach, it requires the experimental set-up to be available. Prediction of the blade dynamics during the design is critical where dynamics analysis is required. Obviously, testing is not a possible technique in this case. Finite element analysis (and similar methods) constitutes the second approach. It can be used to predict the dynamics.

5.2 Modelling theory

The goal of this analysis is to determine at what frequencies a structure vibrates if it is excited by a load applied suddenly, then removed. As mentioned in section 1.2, these frequencies are described as natural frequencies and are dependent on the fundamental characteristics of the structure, such as geometry, density and stiffness. These same characteristics may be included in a finite element model of a structural component. The finite element model can be used to determine the natural modes of vibration and corresponding frequencies. Once the geometry, density, and elastic material models have been defined for the finite element model, in the absence of damping, the dynamic character of the model can be expressed in matrix form as (Mckittrick et al., 2001):

$$KV = \omega^2 MV \qquad \textbf{Equation 5.1}$$

Here K is the stiffness matrix, M is the mass matrix, ω is the angular frequency of vibration for a given mode and V is the mode vector that expresses the corresponding mode shape. A finite element program uses iterative techniques to determine a set of frequencies and shapes that satisfy the finite element matrix equation.

5.3 Euler-Bernoulli beam element

The beam element is shown in Figure 5.1

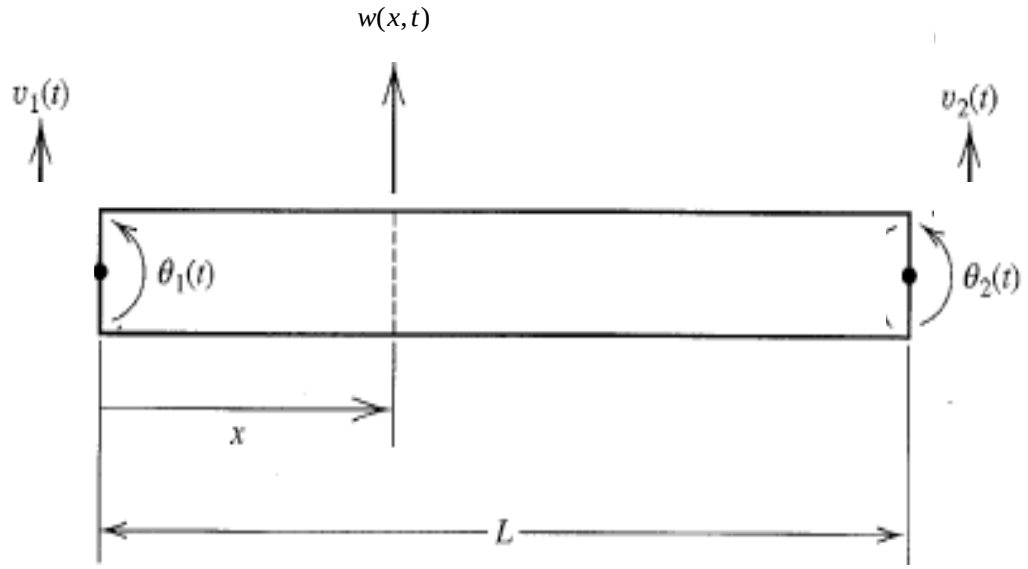

Figure 5.1: Euler-Bernoulli beam element

(Adapted from Palm, 2007)

The variables v_1 and v_2 are the displacements of the endpoints. The variables θ_1 and θ_2 are the rotational displacements at the end of the beam element. Thus we defined the displacement vector of the beam element to be

$$V = \begin{bmatrix} v_1 \\ \theta_1 \\ v_2 \\ \theta_2 \end{bmatrix}$$ **Equation 5.2**

This displacement vector is linked to the solution $w(x,t)$ of the Euler-Bernoulli beam Equation 3.9 by the conditions

$$w(0,t) = v_1(t)$$

$$\frac{\partial w(0,t)}{\partial x} = \theta_1(t)$$

$$w(L,t) = v_2(t)$$

$$\frac{\partial w(L,t)}{\partial x} = \theta_2(t)$$

It is assumed that $w(x,t)$, the solution of the distributed-parameter model, is approximated by

$$w(x,t) \approx a(t) + b(t)x + c(t)x^2 + d(t)x^3$$

Applying the boundary conditions, we find that

$$a(t) = v_1(t)$$

$$b(t) = \theta_1(t)$$

$$c(t) = \frac{1}{L^2}[-3v_1(t) - 2L\theta_1(t) + 3v_2(t) - L\theta_2(t)]$$

$$d(t) = \frac{1}{L^3}[2v_1(t) + L\theta_1(t) - 2v_2(t) + L\theta_2(t)]$$

Thus $w(x,t)$ has the form

$$w(x,t) \approx S_1(x)v_1(t) + S_2(x)\theta_1(t) + S_3(x)v_2(t) + S_4(x)\theta_2(t) \qquad \textbf{Equation 5.3}$$

where the $S_i(x)$ terms are the following shape functions:

$$S_1(x) = 1 - 3\left(\frac{x}{L}\right)^2 + 2\left(\frac{x}{L}\right)^3 \qquad \textbf{Equation 5.4}$$

$$S_2(x) = x - 2L\left(\frac{x}{L}\right)^2 + L\left(\frac{x}{L}\right)^3 \qquad \textbf{Equation 5.5}$$

$$S_3(x) = 3\left(\frac{x}{L}\right)^2 - 2\left(\frac{x}{L}\right)^3 \qquad \textbf{Equation 5.6}$$

$$S_4(x) = -L\left(\frac{x}{L}\right)^2 + L\left(\frac{x}{L}\right)^3 \qquad \textbf{Equation 5.7}$$

With the assumed mode shape, the kinetic energy of the beam can be expressed as follows: $KE = \int_0^L \frac{1}{2}\rho A\left(\frac{\partial w}{\partial t}\right)^2 dx = \frac{1}{2}\rho A \int_0^L \left[S_1(x)\dot{v}_1(t) + S_2(x)\dot{\theta}_1(t) + S_3(x)\dot{v}_2(t) + S_4(x)\dot{\theta}_2(t)\right]^2 dx$

Evaluation of the integrals gives

$$KE = \frac{\rho AL}{420}\dot{v}^T M \dot{v}$$

where $\dot{v} = \begin{bmatrix} \dot{v}_1 \\ \dot{\theta}_1 \\ \dot{v}_2 \\ \dot{\theta}_2 \end{bmatrix}$

The mass matrix of the beam element is (Rao, 2004)

$$M = \frac{\rho AL}{420}\begin{bmatrix} 156 & 22L & 54 & -13L \\ 22L & 4L^2 & 13L & -3L^2 \\ 54 & 13L & 156 & -22L \\ -13L & -3L^2 & -22L & 4L^2 \end{bmatrix}$$ **Equation 5.8**

The stiffness matrix K can be derived from the potential energy expression for the beam element, as follows:

$$PE = \frac{1}{2} EI \int_0^L \left(\frac{\partial^2 v}{\partial x^2} \right)^2 dx = v^T K v$$

Using Equation 5.3 and calculating the integrals gives (Rao, 2004)

$$K = \frac{EI}{L^3}\begin{bmatrix} 12 & 6L & -12 & 6L \\ 6L & 4L^2 & -6L & 2L^2 \\ -12 & -6L & 12 & -6L \\ 6L & 2L^2 & -6L & 4L^2 \end{bmatrix}$$ **Equation 5.9**

5.4 One-dimensional models: MATLAB

Although many commercial finite element codes exist which are capable of modelling the beam structure, it was decided that a code would be written within MATLAB to do all the modelling. This provides the benefit of being able to run the code on any computer using MATLAB. The basis for the MATLAB code was the one-dimensional Euler-Bernoulli beam element. Two different programs (BEAMANALYSYS.m and VARIBLADEANALYSIS.m) were developed. The natural frequencies are provided by the solution of the resulting eigenvalue problem.

The purpose of this study is to predict the dynamic properties of a variable length blade. Before building a computer model of a variable length blade, a uniform beam and a stepped beam were investigated. The first MATLAB program (BEAMANALYSIS.m) was written for the purpose of:

- Validate and update the computer model, by comparing it to the experimental result obtained after performing modal testing on a stepped beam and a uniform beam (Figure 4.3) and,
- adapt changes (geometries and materials properties) to the blade being designed.

The program requires the following input data, supplied in an m-file (Appendix B):

- Beam dimensions (length , width and thickness);
- material properties (Young's modulus, density);
- global degree of freedom;
- vibration direction (flap-wise or edge-wise) and,
- element definition (number of elements).

BEAMANALYSIS.m uses this input data and constructs element stiffness and mass matrices according to the formulas for the Euler-Bernoulli element in Section 5.3. These element stiffness and mass matrices are transformed into global coordinates and added to appropriate locations in the global stiffness and mass matrices. A detailed program explanation is given in Appendix C.

A wind turbine blade can be seen as beam of finite length with airofoil profiles as cross sections. A rectangular cross section representing a cross section of the blade can give qualitatively appropriate results in a simpler way. Therefore, such a model has been adopted for this analysis. The fixed portion and the moveable portion of the variable length blade have been approximated respectively by a hollow beam and a solid beam which can be slid in and out as shown in Figure 2.

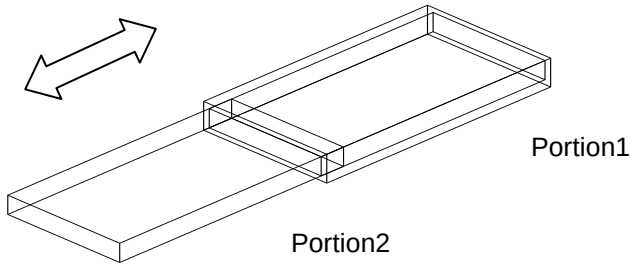

Figure 5. 2: Variblade

The second MATLAB program (VARIBLADEANALYSIS.m) has been developed for a one- dimensional model for the variblade. The geometry, material properties, vibration modes (flap-wise or edge-wise), number of elements and configuration of the variblade have been made as selectable parameters which allow analysis of blades with different sizes and properties. The program requires the following input data, supplied in an m-file (Appendix D):

- Beam dimensions (length of beam portions, width of hollow and solid beam, thickness of hollow and solid beam),
- material properties sets: Young's modulus, density;
- global degree of freedom;
- vibration direction (flap-wise or edge-wise);
- element definition (number of element) and,
- beam configuration (position of moveable portion).

Both flap-wise and edge-wise natural frequencies have been calculated for ten different configurations. The ten different configurations depending on the position of the second portion of the variblade are represented below. These configurations change from zero extension to full extension in ten equal steps.

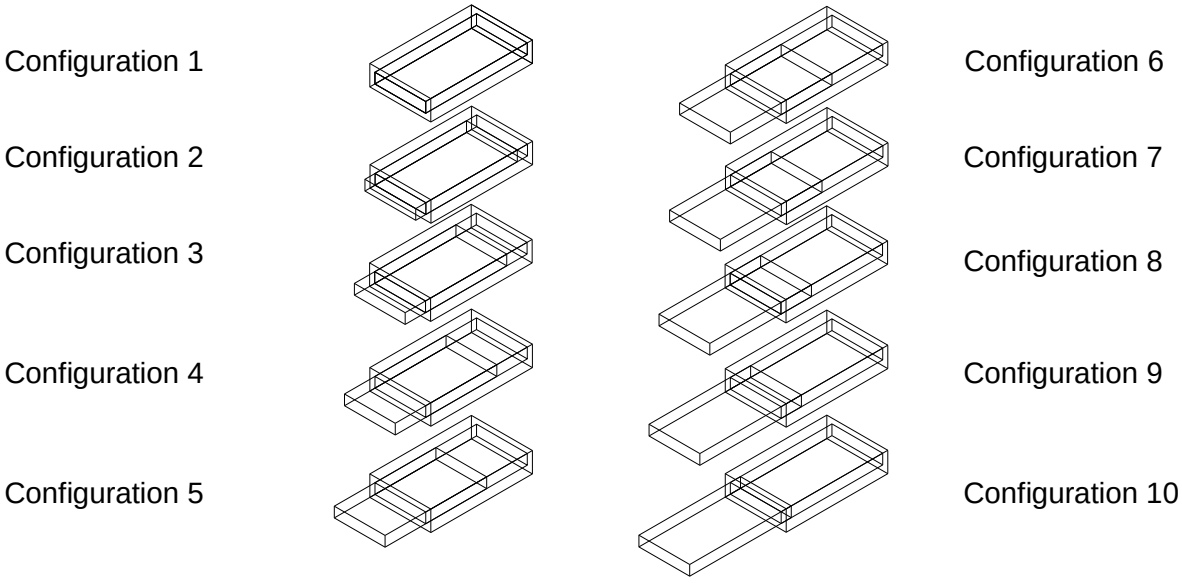

Figure 5.3: Ten configurations of variblade

5.4 Three-dimensional model: NX5

Three-dimensional models of all the different previous beams have been developed in the commercial finite element analysis program Unigraphics NX5. Those models are designed to capture three-dimensional behaviour. The blade has been modelled as a cantilever, therefore, is fully constrained at the end of the inboard portion (where it is attached to the turbine shaft/hub). The outputs of the simulation are the natural frequencies of vibration: flap-wise, edge-wise and torsional natural frequencies as well as their mode shapes.

One end in each model has been fully constrained. The geometrical model of the beams is meshed by using a tetrahedral mesh. Nastran-SEMODES103 has been used as solver for modal analysis. Normal modes and natural frequencies have been evaluated. Damping is not considered and loads are irrelevant (Figure 5.4). The mode shapes were identified by examining the deformation plot (flap-wise, edge-wise and torsional deformation) and by the animated mode shape display.

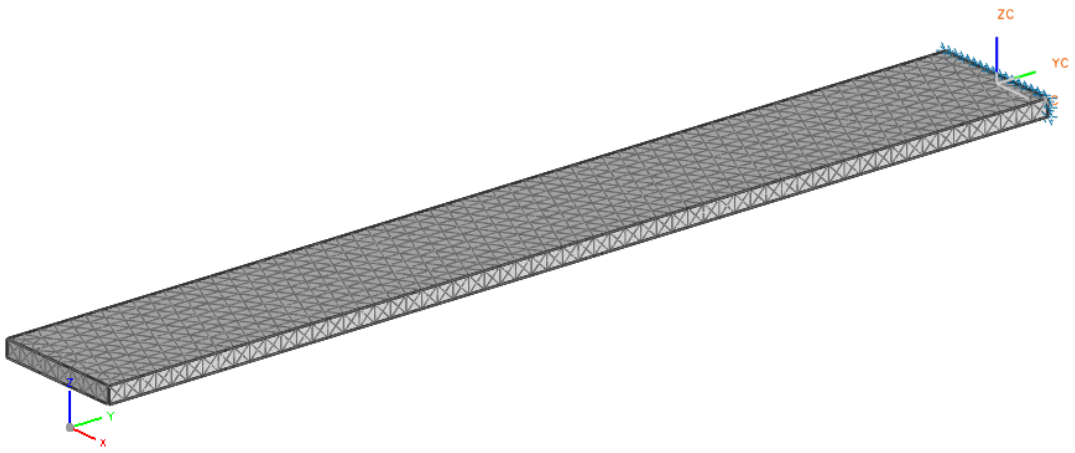

Figure 5.4: Simulation part with constraint

5.5 Summary

A one-dimensional model and a three-dimensional model of a uniform beam and stepped beam have been investigated, to gain insight into finite element modelling. A MATLAB program for a one dimensional model (BEAMANALYSIS.m) has been used, the results (natural frequencies) found will be compared to those of a three-dimensional model built in NX5.

Subsequently, to gain insight into the nature of the vibration problem for the variblade, a rectangular cross-section model with two portions have been used to approximate the blade. That model has been chosen in this analysis for reason of simplicity. A MATLAB program for a one-dimensional model (VARIBLADEANALYSIS.m) has been developed to predict natural frequencies of a variblade.

In Chapter 6, the results found will be compared to those found using a three-dimensional model in NX5.

CHAPTER 6
RESULTS AND DISCUSSION

6.1 Introduction

In this study the natural frequencies of three different beams have been investigated:

- A uniform beam (Figure 4.3);
- a stepped beam (Figure 4.4) and,
- a variblade (Figure 4.5).

The main objective of this work is to calculate natural frequencies of the variblade using commercial software. A secondary aim is to gain insight in experimental modal analysis, finite element modelling and analytical methods. Therefore, a uniform beam and a stepped beam have been investigated.

Four different methods are used for obtaining the natural frequencies:

- Exact solution of Euler-Bernoulli beam equations;
- MATLAB program for one-dimensional finite element models;
- NX5 three dimensional models and,
- experimental modal analysis.

To validate results, the outputs from different methods are evaluated and compared.

Finally, the effect of varying blade length is examined. Some suggestions concerning blade design conclude the chapter.

6.2 Convergence test for finite element models

The number of elements used in finite element analysis affects the quality of the solution. As the number of elements increases, natural frequencies converge to values independent of the mesh size. However, a finer mesh with more elements places greater demands on the computing resources than does a coarse mesh. A good compromise is to select the coarsest mesh for which natural frequencies are independent of mesh size. Such a mesh can be found by using finer meshes to model the structure until the results converge; the coarsest mesh for which results are adequate can then be selected and used in future simulations. Convergence tests on the finite element models have been conducted to confirm a fine enough discretisation has been used. Several models with different mesh sizes have been

created and the resulting natural frequencies compared. Values of the material and geometric properties of the uniform beam under investigation are given in Table 6.1.

Table 6.1: Material and geometric properties of the beam

Geometric properties			Material properties (mild steel) (Southern Africa Institute of Steel Construction, n.d)		
$L(mm)$	$W(mm)$	$T(mm)$	$E(mN/mm^2)$	$\rho\ (kg/mm^3)$	v
1000	40	5	206×10^6	7.85×10^{-6}	0.3
L: length			E: Young's modulus		
W: width			ρ : density		
T: thickness			v : Poisson's ratio		

The one-dimensional model (MATLAB) developed has been divided successively into 3, 6, 12, and 24 elements. The first five frequencies associated with the modes are presented in Figure 6.1.

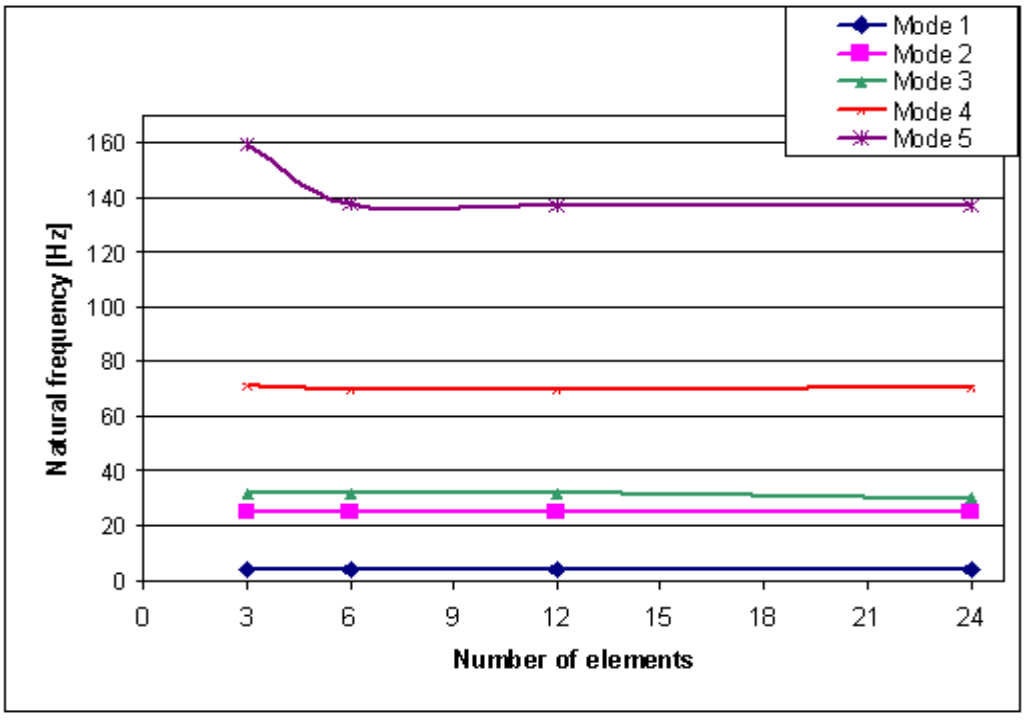

Figure 6.1: MATLAB program convergence test results

The same procedure has been applied to the three-dimensional model (NX5). Successively the following overall element size has been chosen: 25.4, 20, 15, 10, 5 and 2 mm. The first five frequencies are presented in Figure 6.2.

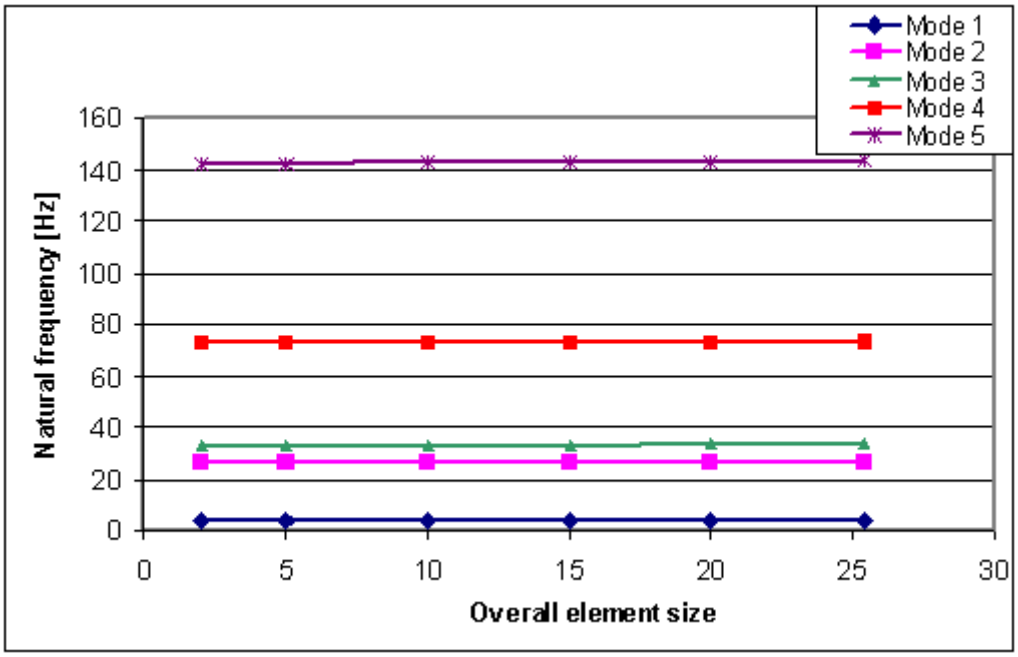

Figure 6.2: NX convergence test results

The two previous tests indicated the predicted frequencies are not influenced significantly by mesh size in the range chosen for investigation. Therefore, for the simulations presented here, a minimum of 12 elements and overall element size of 10 mm were chosen respectively for the one-dimensional and the three-dimensional models.

6.3 Results for uniform beam

The uniform beam had a rectangular cross-section with width *W* and thickness *T*. The length of the beam was *L*. The values of these dimensions are shown in Table 6.2.

Table 6.2: Material and geometric properties of the uniform beam

Geometric properties			Material properties (mild steel) (Southern Africa Institute of Steel Construction, n.d)		
$L(mm)$	$W(mm)$	$T(mm)$	$E(mN/mm^2)$	$\rho\ (Kg/mm^3)$	ν
795	40	4.45	206×10^6	7.85×10^{-6}	0.3
L: length *W*: width *T*: thickness			*E*: Young's modulus ρ : density ν : Poisson's ratio		

6.3.1 Exact solution

The exact solution was established in Section 3.5. The natural frequency of the beam can be calculated from Equation 3.21 as follows

$$f = \frac{\beta^2}{2\pi}\sqrt{\frac{EI}{\rho A}} = \frac{(\beta L)^2}{2\pi}\sqrt{\frac{EI}{\rho A L^4}}$$

Values of βL are shown in Table 3.1

$\beta_1 L = 1.875104$

$\beta_2 L = 4.6940914$

$\beta_3 L = 7.8547577$

$\beta_4 L = 10.995541$

$\beta_5 L = 14.137168$

Values of β can be obtained by dividing those previous values by length *L* = 795 mm, as follows:

$$\beta_1 = \frac{1.875104}{795} = 0.00235862$$

The cross-section A and the area moment of inertia I are given as follow

$$A = W \times T$$
$$= 40 \times 4.45$$
$$= 178\ mm^2$$

For flap-wise modes,

$$I = \frac{1}{12}(W \times T^3)$$
$$= \frac{1}{12}(40 \times 4.45^3)$$
$$= 293.74\ mm^4$$

The natural frequencies can be calculated as follows:

$$f_1 = \frac{(\beta_1 L)^2}{2\pi}\sqrt{\frac{EI}{\rho A L^4}}$$
$$= \frac{(0.00235862)^2}{2\pi}\sqrt{\frac{206\times10^6 \times 293.74}{7.85\times10^{-6}\times178\times795^4}}$$
$$= 5.83 \text{ Hz}$$

Similarly

$f_2 = 36.5$ Hz

$f_3 = 102$ Hz

$f_4 = 200$ Hz

$f_5 = 331$ Hz

For edge-wise modes,

$$I = \frac{1}{12}(W^3 \times T)$$

$$= \frac{1}{12}(40^3 \times 4.45)$$

$$= 23733.33\ mm^4$$

Hence,

$$f_1 = \frac{(\beta_1 L)^2}{2\pi}\sqrt{\frac{EI}{\rho A L^4}}$$

$$= \frac{(0.00235862)^2}{2\pi}\sqrt{\frac{206\times10^6 \times 2373333}{7.85\times10^{-6}\times178\times795^4}}$$

$$= 52.4 \text{ Hz}$$

Similarly

$f_2 = 328$ Hz

$f_3 = 919$ Hz

$f_4 = 1800$ Hz

$f_5 = 2977$ Hz

The frequencies of torsional modes of a rectangular cantilever with a width to thickness ratio greater than six may be approximated by (Harris, 1988):

$$f_n = \frac{(2n-1)}{4L}\frac{2T}{W}\sqrt{\frac{G}{\rho}}$$

Where the shear modulus *G* is given by:

$$G = \frac{E}{2(1+v)}$$

$$= \frac{206\times10^6}{2(1+0.3)}$$

$$= 79230769.23$$

Therefore, the torsional modes become:

$$f_1 = \frac{(2\times1-1)}{(4\times795)}\frac{(2\times4.45)}{40}\sqrt{\frac{79230769.23}{7.85\times10^{-6}}}$$

$$= 224.79 \text{ Hz}$$

Similarly

$f_2 = 449.57$ Hz

$f_3 = 674.36$ Hz

$f_4 = 899.14$ Hz

$f_5 = 1123.93$Hz

6.3.2 MATLAB program

The MATLAB program (BEAMANALYSIS) found in Appendix C is used to compute successively flap-wise and edge-wise natural frequencies. Material and geometric properties used as input data are given in Table 6.2. As mentioned before, this program is based on the Euler-Bernoulli model. The following first five flap-wise and edge-wise natural frequencies have been found:

Table 6.3: MATLAB natural frequencies

Natural frequencies (Hz)	
Flap-wise	Edge-wise
5.89	52.52
36.92	327.86
103.45	919.92
202.76	1801.63
335.34	2980.97

6.3.3 NX5 model

The three dimensional model shown in Figure 5.4 is designed to capture three dimensional behaviour. Therefore flap-wise, edge-wise and additionally torsional natural frequencies have been found. As previously, material and geometric properties are given in Table 6.2. The mode shape associated with a specific frequency indicates whether it is a flap-wise, edge-wise or torsional frequency. Some examples of mode shapes are given in Figure 6.3.

Flap-wise deflection (Mode 2)

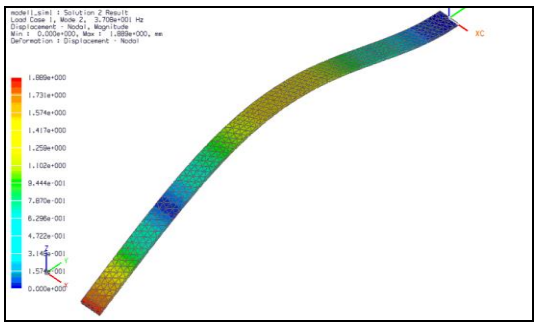

Edge-wise deflection (Mode 7)

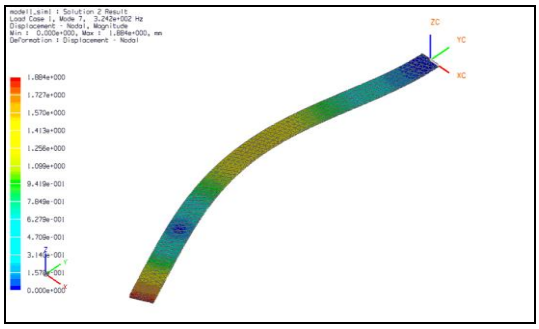

Torsional deflection (Mode 6)

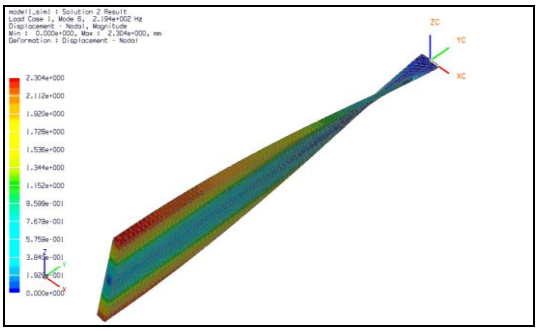

Figure 6.3: Uniform beam deflections

The first five flap-wise, edge-wise and torsional natural frequencies are:

Table 6.4: NX5 natural frequencies

Natural frequencies (Hz)		
Flap-wise	Edge-wise	Torsional
5.918	52.34	219.4
37.08	324.2	659.1
103.8	891.6	1102
203.5	1704	1549
336.6	2734	2005

6.3.4 Experimental modal analysis results

The performed modal analysis gives estimates of only flap-wise natural frequencies. The results are based on the measurements performed on uniform beam as described in Chapter 4. Figure 6.4 shows a screenshot of Vib-Graph after measured transfer functions are imported. Crosses (**+**) indicate natural frequencies. The natural frequencies, obtained from the modal analysis, are presented in Table 6.5.

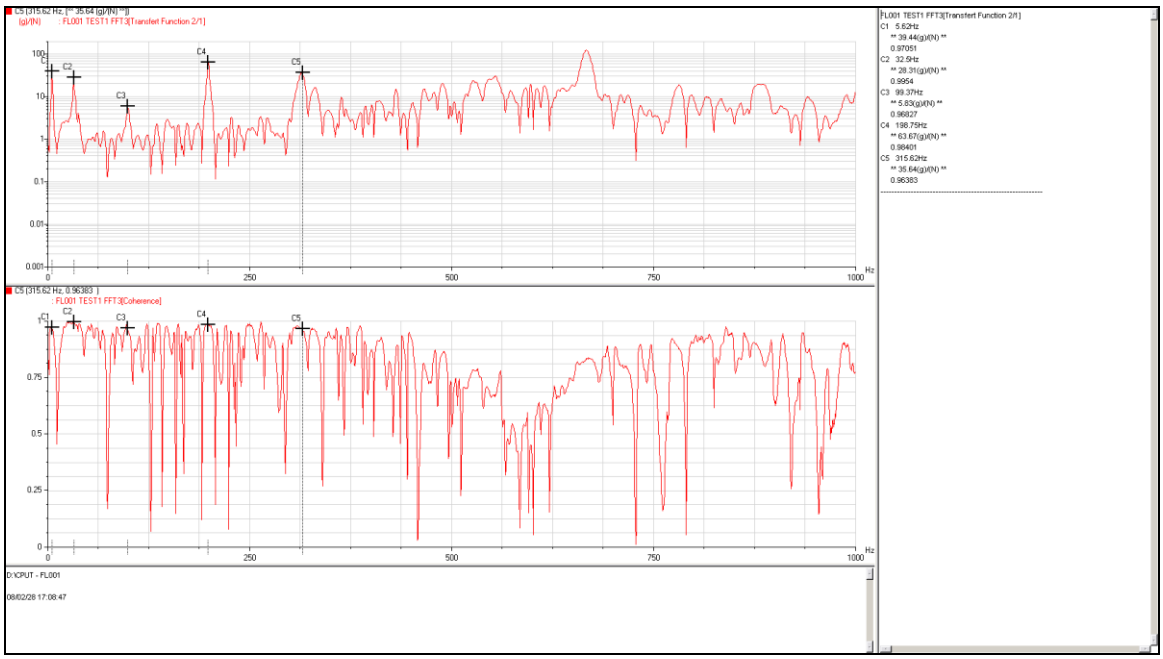

Figure 6.4: Measured transfer functions imported into Vib-Graph

6.3.5 Comparison of natural frequencies

The results found using the four different methods have been compared. It should be noted that:

- The experimental modal analysis provides only the first five flap-wise natural frequencies and,
- The MATLAB program provides only flap-wise and edge-wise natural frequencies.

Therefore, the comparison has been limited to the data available.

Table 6.5: Measured and computed natural frequencies

	Exact solution [Hz]	Measured frequencies [Hz]	Computed frequencies [Hz]	
			MATLAB	NX5
Flap-wise	5.83	5.62	5.89	5.918
	36.5	32.5	36.92	37.08
	102	99.3	103.45	103.8
	200	198.75	202.76	203.5
	331	315.62	335.34	336.6
Edge-wise	52.4		52.52	52.34
	328		327.86	324.2
	919		919.92	891.6
	1800		1801.63	1704
	2977		2980.97	2734
Torsional	224.79			219.4
	449.57			659.1
	674.36			1102
	899.14			1549
	1123.93			2005

Some conclusions can be drawn from the previous table:

- As expected, there are no significant discrepancies between the exact solution and MATLAB results;
- highest edge-wise frequencies introduce some discrepancies between MATLAB and NX5 results. This may be due to the limitation of the one dimensional model (MATLAB) compared to the three dimensional model (NX5) when it comes to computing higher natural frequencies;
- highest torsional frequencies produce also some discrepancies between exact solution and NX5 results for similar reason as above. Interestingly, Larsen et al. (Larsen et al., 2002) in their study compares the results from the modal analysis with the corresponding results from the finite element analysis. Better agreement has been found for the deflection components associated with low natural frequencies than for deflection components associated with higher natural frequencies. The same tendency was also observed in the estimation of natural frequencies. The bending torsion coupling has been identified as a reason for those discrepancies. It has been found that these deflections are difficult to resolve experimentally (due to small signal levels) as well as numerically (due to lack of sufficiently detailed information on the material properties). The numerical

model is seen to over-estimate the structural couplings. Although, torsional natural frequencies are not included in experimental results, this may also explain discrepancies at higher frequencies.

- the closeness between the experimental (for at least the first five flap-wise and edge-wise and the first torsional) results and the finite element analysis results means that finite element analysis can be used as a good computational tool and,
- the closeness between the analytical results, the measured frequencies and the computed frequencies means that natural frequencies can be predicted accurately by either of those methods.

6.4 Results for stepped beam

The stepped beam (Figure 4.4) had a rectangular cross-section with width *W*1*, W*2*, W*3 and thickness *T*. The length of each portion was given by *L*1*, L*2*, L*3. The values of these dimensions are shown in Table 6.6.

Table 6.6: Material and geometric properties of the stepped beam

	Geometric properties			Material properties (Southern Africa Institute of Steel Construction, n.d)		
	$L(mm)$	$W(mm)$	$T(mm)$	$E(mN/mm^2)$	$\rho\ (kg/mm^3)$	v
Portion1	295	40	4.5	206×10^6	7.85×10^{-6}	0.3
Portion2	250	36	4.5	206×10^6	7.85×10^{-6}	0.3
Portion3	250	30	4.5	206×10^6	7.85×10^{-6}	0.3
L: length *W*: width *T*: thickness				*E*: Young's modulus ρ : Density v : Poisson's ratio		

Hereafter the MATLAB, NX5 and experimental modal analysis results are presented. No exact solution is available for the stepped beam.

6.4.1 MATLAB program

The MATLAB program (BEAMANALYSIS) found in Appendix C is used to compute successively flap-wise and edge-wise natural frequencies. The following first five flap-wise and edge-wise natural frequencies have been found:

Table 6.7: MATLAB natural frequencies

Natural frequencies (Hz)	
Flap-wise	Edge-wise
6.61	57.62
37.88	305.41
103.55	807.10
202.72	1587.27
335.28	2628.71

6.4.2 NX5 model

A three-dimensional stepped beam (Figure 4.4) has been built in the finite element program NX5. Flap-wise, edge-wise and additionally torsional natural frequencies have been found. The mode shapes corresponding to the natural frequencies are used to determine whether a particular frequency is flap-wise, edge-wise or torsional.

Flap-wise deflection (Mode 2)

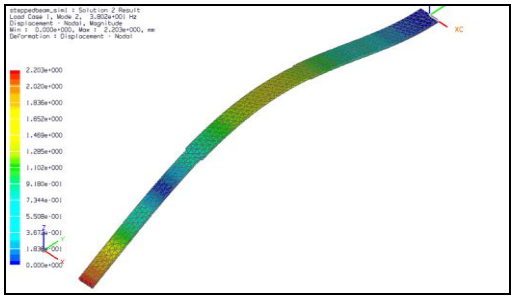

Edge-wise deflection (Mode 7)

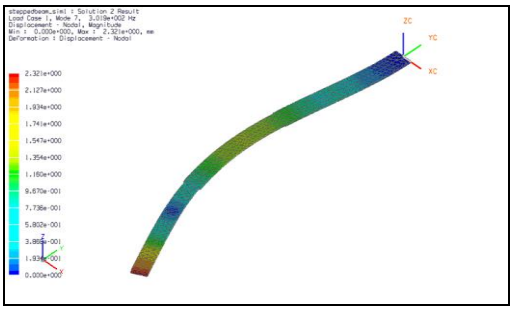

Torsional deflection (Mode 6)

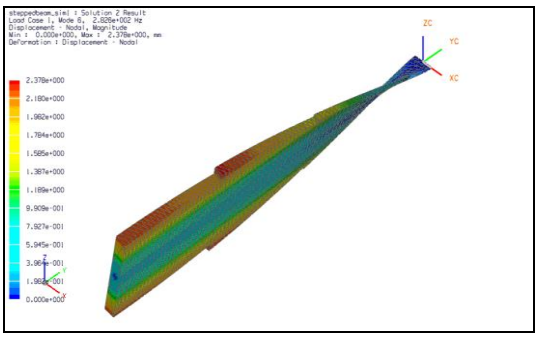

Figure 6.5: Stepped beam deflections

The first five flap-wise, edge-wise and torsional natural frequencies are:

Table 6.8: NX5 natural frequencies

Natural frequencies (Hz)		
Flap-wise	Edge-wise	Torsional
6.636	57.55	282.6
38.02	301.9	742.1
103.9	786	1202
203.5	1516	1733
336.2	2447	2249

6.4.3 Experimental modal analysis results

The performed modal analysis gives estimates of only flap-wise natural frequencies. The results are based the measurements performed on the stepped beam described in Chapter 4. Figure 6.6 shows a screenshot of Vib-Graph after measured transfer functions are imported. Crosses (**+**) indicates natural frequencies. The natural frequencies, obtained from the modal analysis, are presented in Table 6.9.

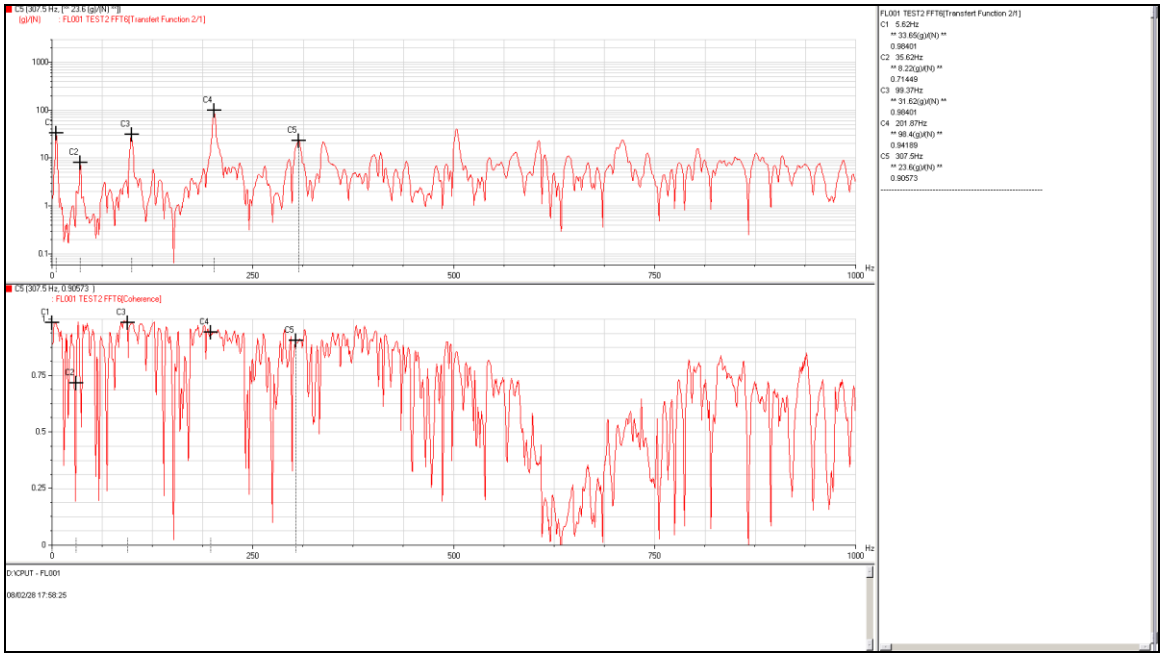

Figure 6.6: Measured transfer functions imported into Vib-Graph

6.4.4 Comparison of natural frequencies

The results found previously have been compared. This comparison has been limited to the data available.

Table 6.9: Measured and computed natural frequencies

	Measured frequencies [Hz]	Computed frequencies [Hz]	
		MATLAB	NX5
Flap-wise	5.62	6.61	6.636
	35.62	37.88	38.02
	99.37	103.55	103.9
	201.87	202.72	203.5
	307.5	335.28	336.2
Edge-wise		57.62	57.55
		305.41	301.9
		807.10	786
		1587.27	1516
		2628.71	2447

It can be seen that the measured frequencies results and the computed frequencies remain close. However, as previously, some discrepancies can be observed for highest frequencies. Interestingly, Jaworski and Dowell (Jaworski & Dowell, 2007) in their study predicted the three lowest natural frequencies of a multiple-stepped beam using:

- A classic Rayleigh–Ritz formulation;
- commercial finite element code ANSYS and,
- experimental results from impact testing data.

It has been shown that:

- Classical Rayleigh–Ritz provides more accurate results at the highest frequency for global parameters once sufficient degrees-of-freedom are introduced and,
- the disagreement between beam model and experimental results is attributed to non-beam effects present in the higher-dimensional elasticity models, but absent in Euler–Bernoulli and Timoshenko beam theories. This conclusion is corroborated by predictions from one-, two-, and three-dimensional finite element models.

It should be specified, however, that this study is not concerned with higher natural frequencies.

6.5 Results for variblade

6.5.1 NX5 and MATLAB results comparison for variblade

Since finite element analysis has been established as an important tool in vibration analysis and proven reliable in this study, it has been used to provide an approximation for the variblade being designed.

As explained before the variable length blade has been approximated to a variblade with two portions (Figure 5.2). Ten different configurations (Figure 5.3) depending of the position of the outboard portion are investigated. These configurations change from zero extension to full extension in ten equal steps of 100 mm. Values of the material and geometric properties of the two portion of the variblade under investigation are given in Table 6.10. No exact solution and experimental modal analysis results are available.

Table 6.10: Material and geometric properties of the variblade

	Geometric properties				Material properties (Carbon fiber composite) (Zweben et al., 1989)		
	$L(mm)$	$W(mm)$	$T(mm)$	$Wh(mm)$	$E(mN/mm^2)$	$\rho\ (kg/mm^3)$	v
Portion1	1000	60	20	5	230×10^{6}	1.8×10^{-6}	0.3
Portion2	1000	50	10	N/A	230×10^{6}	1.8×10^{-6}	0.3

L: length
W: width
T: thickness
Wh: wall thickness
E: Young's modulus
ρ : density
v : Poisson's ratio

This section contains examples of the results obtained with NX5 for three different configurations of the variblade. Flap-wise, edge-wise and torsional deflections are represented.

Mode 3 (Flap-wise)

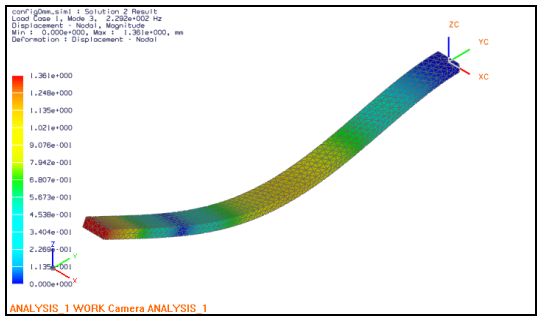

Mode 5 (Edge-wise)

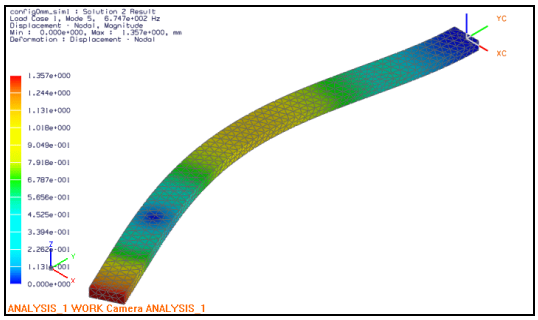

Mode 6 (Torsional)

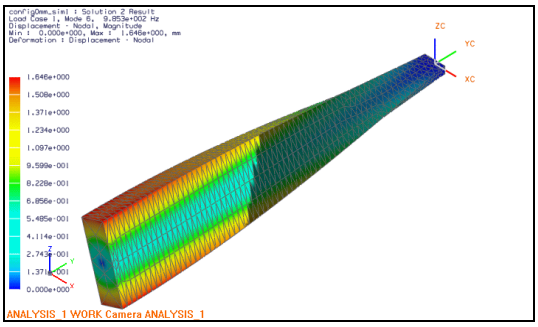

Figure 6.7: Flap-wise, edge-wise and torsional deflection for configuration 1

Mode 3 (Flap-wise)

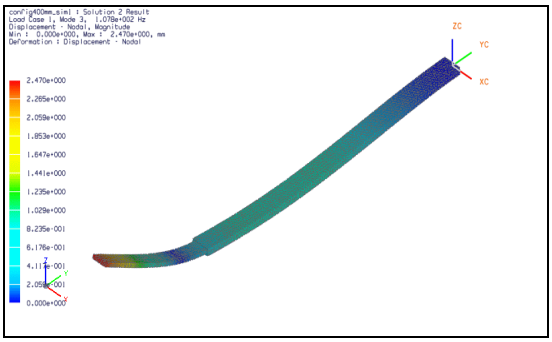

Mode 5 (Edge-wise)

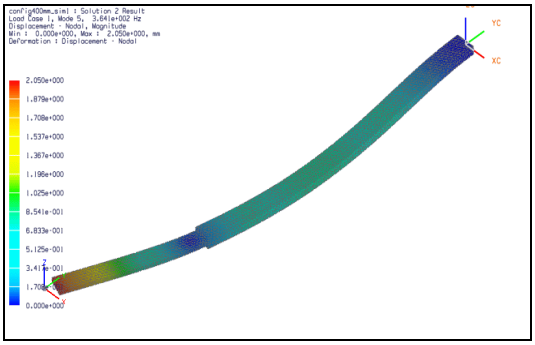

Mode 9 (Torsional)

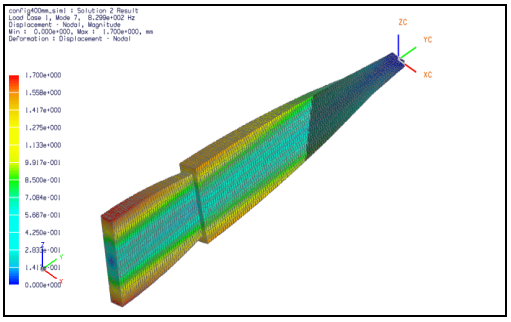

Figure 6.8: Flap-wise, edge-wise and torsional deflection for configuration 5

Mode 4 (Flap-wise)

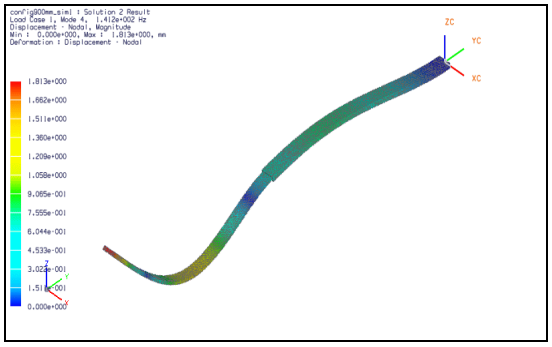

Mode 8 (Edge-wise)

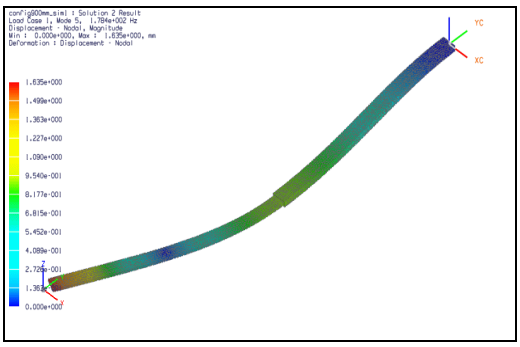

Mode 10 (Torsional)

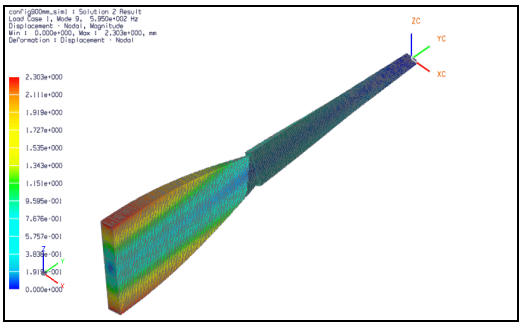

Figure 6.9: Flap-wise, edge-wise and torsional deflection for configuration 10

The complete set of NX5 results are presented in Appendix E.

The MATLAB program VARIBLADEANALYSIS.m (Appendix D) has been used to compute natural frequencies. The results found using this MATLAB program have been compared to those found using NX5. The first five natural frequencies (flap-wise and edge-wise) of the variblade are calculated successively for ten different configurations. Torsional natural frequencies obtained with NX5 have been ignored because the MATLAB program can calculate only flap-wise and edge-wise natural frequencies. Figure 6.10 represents the results obtained for configuration 1, configuration 5 and configuration 10. The complete results comparison for all configurations is presented in Appendix F.

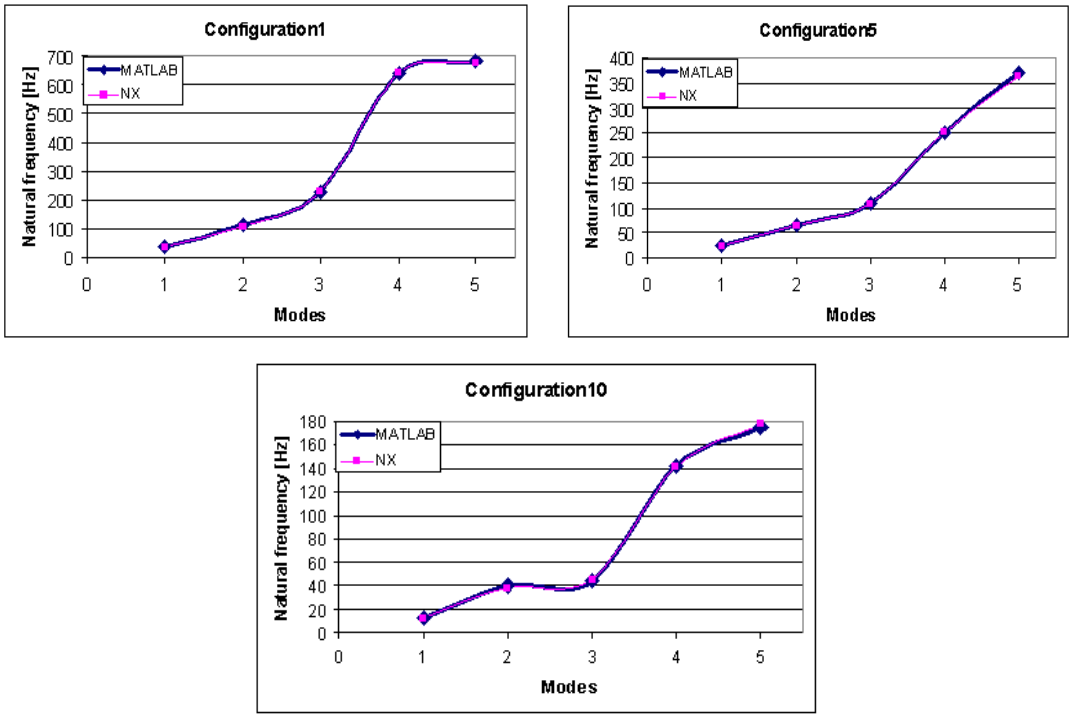

Figure 6.10: MATLAB and NX5 results comparison

6.5.2 Influence of blade length

The influence of varying the blade length has been studied and the results are shown in Figure 6.11 for the first five natural frequencies related to the configurations of the variblade. Table 6.11 and Table 6.12 provide values of these first five natural frequencies calculated for each configuration of the variblade shown in Figure 5.3.

Table 6.11: Computed natural frequencies (NX5)

Configuration number	Computed natural frequencies (Hz)				
	Mode1	Mode2	Mode3	Mode4	Mode5
1	36.6	109	229	640	675
2	33.1	94.6	205	560	589
3	29.5	82.2	174	422	509
4	26.4	72.7	140	302	434
5	23.6	64.7	108	250	364
6	21.0	57.8	83.8	225	305
7	18.7	51.8	67.8	205	259
8	16.5	46.5	57.2	184	224
9	14.5	41.9	50.0	162	198
10	12.7	37.8	45.2	141	178

Table 6.12: Computed natural frequencies (MATLAB)

Configuration number	Computed natural frequencies (Hz)				
	Mode1	Mode2	Mode3	Mode4	Mode5
1	36.6	111	229	641	684
2	33.4	95.5	204	562	589
3	30.2	79.6	175	426	525
4	27.1	73.2	142	304	441
5	23.9	65.3	108	251	369
6	20.7	63.7	84.4	226	302
7	19.1	47.8	68.4	205	255
8	15.9	47.8	57.3	184	223
9	14.3	47.8	49.3	162	206
10	12.7	40.0	44.6	142	175

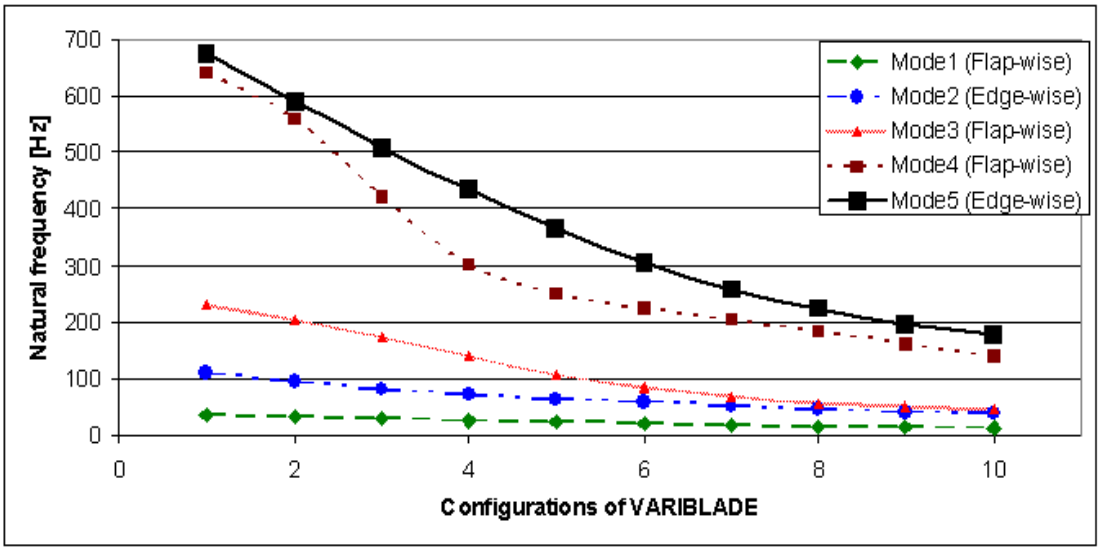

Figure 6.11: Natural frequencies

6.5.3 Effect of rotation

Referring to Equation 2.1, it has been shown that there is an increase of the first mode frequency due to centrifugal stiffening.

$$f_{1,R} = \sqrt{f_{1,0}^2 + \phi_1 \Omega^2}$$

The natural frequencies calculated (Table 6.7) correspond to $f_{1,0}$. The value of ϕ_1 depends on the blade mass and stiffness distribution, and Madsen and al. (Madsen and al., 1984) suggest the value of 1.73 for wind turbine blade flap-wise oscillations.

In the case of blade rotating at 30 r.p.m and for ϕ_1=1.73, the following natural frequencies will be obtained:

Table 6.13: Natural frequencies of the rotating variblade

Configuration number	$f_{1,0}$ [Hz]	$f_{1,R}$ [Hz]	Percentage increase [%]
1	36.6	36.606	0.016
2	33.1	33.107	0.020
3	29.5	29.507	0.025
4	26.4	26.408	0.031
5	23.6	23.609	0.039
6	21.0	21.010	0.049
7	18.7	18.712	0.062
8	16.5	16.513	0.079
9	14.5	14.515	0.103
10	12.7	12.717	0.134

6.6. Contextualization of the findings

During design of a wind turbine blade, the 1st flap-wise, 2nd flap-wise, 1st edge-wise and the 1st torsional natural frequencies shall be determined as a minimum (Larsen et al., 2002). It can be seen (Figure 6.10) there is good agreement between the MATLAB and NX5 results for the first five natural frequencies.

It should be noted that only the frequency range between 0.5 Hz and 30 Hz (Larsen et al., 2002) is of relevance to wind turbine blades. In that range, MATLAB and NX5 provide identical results. Torsional natural frequencies have been calculated using NX5. The lowest torsional natural frequency (configuration 10) determined is 595 Hz (Appendix E). It can be concluded that torsional natural frequencies are not a concern for this variblade model as they are out of the range of interest.

The study of the influence of blade length on natural frequencies represented in Figure 6.11 has shown that with increasing blade length, the natural frequencies decrease. This is probably because the blade becomes more flexible as its length increases. The excitation loads are concentrated in the interval 0.5 Hz-30 Hz. As shown in Table 6.11 and Table 6.12, mode 1 (included in the interval 12.7 Hz-36.6

Hz) may coincide with these excitation frequencies. Therefore the first mode may be subjected to excitation.

The relative effect of the centrifugal loads is small because of the small size of the model under investigation. In fact, the longer the length of the model, the lower the natural frequencies will be. The increase in the first mode frequency for edge-wise oscillations from centrifugal force is 0.134 % for configuration10; the largest expected increase; which is probably small enough to be ignored.

CHAPTER 7
CONCLUSIONS AND RECOMMENDATIONS FOR FUTURE WORK

7.1 Conclusions

A variblade can be seen as beam of finite length with aerofoils as cross sections. A rectangular cross-section model, representing the variblade, can give qualitatively appropriate results in a simpler way than considering a blade with aerofoil profiles. Therefore, such a model has been adopted for this analysis. The fixed and sliding portions of the blade have been approximated by a hollow beam and a solid beam. As the outboard portion of the blade can be slid in and out of the inboard portion, 10 different configurations have been investigated. A one-dimensional model and a three-dimensional model have been investigated

The following expected conclusions have been drawn:

- Good agreement between NX5 and MATLAB results has been confirmed for the frequency range of interest using a composite material variblade. Therefore both NX5 and the MATLAB program can be use to calculate natural frequencies for any other isotropic material. This means that an effective method to compute natural frequencies of a variblade was developed;
- natural frequencies are a function of configuration number and,
- increasing the blade length reduces natural frequencies.

More specifically for variblades, the following conclusions have been drawn:

- The range between 0.5 Hz and 30 Hz is of relevance to wind turbine blades. Although the first five natural frequencies have been calculated, only the first flap-wise natural frequency is of concern. Higher flap-wise natural frequencies, all edge-wise and all torsional natural frequencies are out of this range of concern.
- the first mode (included in the interval 12.7-36.6 Hz) (Table 6.11 and Table 6.12) may coincide with the excitation frequencies, therefore during operation this range of frequencies should be avoided;
- modal testing only needs to be performed to extract the first flap-wise natural frequency in each configuration of the variblade and,
- influence of rotation on natural frequencies is small enough to be ignored.

- Non-obvious advantages of the variblades is the following: The higher the rotor speed, the smaller the blade length becomes and, therefore the higher the natural frequency is. Similarly, as the rotor speed decreases, natural frequency decreases.
- For the variblade, it can be seen that a smaller blade size (Table 6.11 and Table 6.12) (configuration 1, configuration 2 and configuration 3) does not present a risk for the variblade, since those natural frequencies are out of the range of concern. Therefore, reducing the blade length reduces the chances of resonance. Although it is an obvious conclusion, it is an non-obvious benefit.
- Due to variation in blade length, natural frequency is not constant. Even if one found that the first flap-wise natural frequency is in the region of concern, that frequency is not constant, thus reducing chances of resonance.

7.2 Recommendations

7.2.1 Finite element analysis

- The models developed include some approximation. The results for these simplified models shows further research with a more accurate model is required since the first mode may be subjected to excitation. The blade profile needs to be taken into account for more accurate results;
- the MATLAB program was written to be applicable to different blade shapes and materials, therefore, the cross section can be taken into account for the variblade being designed;
- the two portions of the blade have been considered as one body in finite element analysis. Further studies can be undertaken to investigate the the effect of modelling the blade with the two portions joined in a more realistic way (e.g. with gap or contact elements) and,
- since discrepancies between results have been found for frequencies above 500 Hz, further research can be undertaken in order to assess the ability of finite element analysis software to compute higher natural frequencies.

7.2.2 Experimental modal analysis

- Experimental verification for the variblade is left for future studies to extend the work presented in this thesis;
- experimental modal analysis should be performed on the variblade being designed:
    - To verify the accuracy of the computed natural frequencies.
    - to verify the method considering the two portions of the blade as one portion in finite element analysis and,
- higher natural frequencies (edge-wise and torsional natural frequencies) should also be measured in order to assess the ability of the finite element software to accurately compute higher natural frequencies.

BIBLIOGRAPHY/REFERENCES

Ackermann, T. and Söder, L. 2000. Wind energy technology and current status: a review. *Renewable and sustainable energy reviews*, 4(4): 315-374. December.

Aerowind Systems. n.d. *Basic Aerodynamic Operating Principles of Wind Turbines.* http://www.aerowinds.co.uk/a11.html
[13 October 2008].

Bazoune, A. 2005. Relationship between softening and stiffening effects in terms of Southwell coefficients. *Journal of sound and vibration*, 287: (4-5). November.

Bechly, M.E. and Clausent, P.D. 1997. Technical note: Structural Design of a Composite Wind Turbine Blade using finite element analysis. *Computers & Structures.* 63(3): 639–646.

Bir, G. and Stol, C. 2000. *Modal Analysis of a Teetered-Rotor Wind Turbine Using the Floquet Approach*. In Proceedings of the ASME Wind Energy Symposium, Reno, Nevada. 23–33. January.

Bir, G. S. and Butterfield, C. P. 1997. *Modal Dynamics of a Next-Generation Flexible-Rotor Soft-Tower Wind Turbine.* In Proceedings of the 15th International Modal Conference, Orlando, Florida, 76–84.

Burton, T., Sharpe, D., Jenkins, N. & Bossanyi, E. 2004. *Wind Energy Handbook.* Chichester: Wiley.

Cameron, P. 1939. *Aircraft having rotative sustaining means*. U.S. Patent 2,163,482.

Chopra, I. and Dugundji, J. 1979. Non-Linear Dynamic Response of a Wind Turbine Blade. *Journal of Sound and Vibration*. 63(2): 265–286.

Composites world. 2008. *Getting To The Core Of Composite Laminates.* http://www.compositesworld.com/
[13 October 2008].

Danish Wind Turbine Manufacturers Association. 2003. *The Wind Energy Pioneer— Poul la Cour.* http://www.windpower.org/en/pictures/lacour.htm
[13 October 2008].

Edinger, R. and Kaul, S. 2000. *Renewable Resources for Electric Power: Prospects and challenges*. Quorum: Westport.

Ewins, D.J. 2000. *Modal Testing: Theory, Practice and Application*, Research Studies Press Ltd, Baldock, UK.

Fradenburgh, E. A. and Miller, G. G. 1994. *A drive system for changing the diameter of a variable rotor*. U.S. Patent 5,299,912.

Fradenburgh, E. A., Davis, J. S., Moffitt, R. C. and Visintainer, J. A. 1993. *Variable diameter rotor having an offset twist.* U.S. Patent 5,253,979.

Garrad, A. D. and Quarton, D. C. 1986. Symbolic Computing as a Tool in Wind Turbine Dynamics. *Journal of Sound and Vibration*. 109(1): 65–78.

Grabau**,** P**.** & Petersensvej, H.C. 1999. Wind turbine with stress indicator. *World International Property Organization*, WO 99/57435 A1: 1-26. November 11.

Hager, L. N., Fradenburgh, E. A. and Yarm, J. M. 1978. *Locking control and over travel safety stop system for variable length rotor blades.* U.S. Patent 4,080,097.

Hansen, A. C. 1992. *Yaw Dynamics of Horizontal Axis Wind Turbines*. Final Subcontract Report NICH Report No. TP- 442-4822, NREL, 1992.

Harris, C. M. 1988. *Shock & Vibration Handbook.* 3rd Ed. New York, NY: McGraw-Hill.

Hau, E. 2000. *Wind turbines: Fundamentals, Technologies, Application and Economics*. München: Springer.

Jamieson, P. M. 2005. *Variable diameter wind turbine rotor blades*. U.S. Patent 6,972,498 B2.

Jaworski, J. W. and Dowell, E. H. 2007. Free vibration of a cantilevered beam with multiple steps: Comparison of several theoretical methods with experiment. *Journal of Sound and Vibration* 312: 713–725.

Jureczko, M., Pawlak M. & Mężyk, A. 2005. Optimisation of wind turbine blades**.** *Materials Processing Technology*, 167(3-5): 463-471. August 30.

Kaza, K. R. V. and Hammond, C. E. 1976. *Investigation of Flap-lag Stability of Wind Turbine Rotors in the Presence of Velocity Gradients and Helicopters in Forward Flight.* In Proceedings of the Seventeenth Structures, Structural Dynamics, and Materials Conference, King of Prussia, Pennsylvania, May 5-7, 421–431.

Kiely, E. F. and Beatty, R. D. 1997**.** *The mounting arrangement for variable diameter rotor assemblies*. U.S. Patent 5,655,879.

Knight, C.E. 1993. *The Finite Element Method in Mechanical Design*. Boston: PWS-Kent publishing company.

Kong C., Kim H. and Kim J. A. 2000. *Study on structural and aerodynamic design of composite blade for large scale HAWT system*. Final report, Hankuk Fiber Ltd.

Kottapalli, S. B. R., Friedmann, P. and Rosen, A. 1978. *Aeroelastic Stability and Response of Horizontal Axis Wind Turbine Blades*. In Proceedings of the 2nd International Symposium on Wind Energy Systems, Amsterdam Netherlands, October.

Kowalik, P. and Coetzee, K. 2005. *The Scope of the Energy Industry in the Western Cape*. http://www.capegateway.gov.za/other/2005/11/final_first_paper_energy_printing.pdf [13 October 2008].

Larsen, G.C., Hansen, M.H., Baumgart, A., Carlen, I. 2002. *Modal Analysis of Wind Turbine Blades.* Risø National Laboratory.

Lee, A.T. and Flay, R. G. J. 2000. Compliant blades for passive power control of wind turbines. *Wind engineering*. 24(1): 3-11. January.

Maalawi, K.Y. & Negm, H.M. 2002. Optimal frequency design of wind turbine blades. *Wind Engineering and Industrial Aerodynamics*, 90(8): 961-986. August.

Madsen, P.H., Frandsen, S., Holley, W. E. and Hansen, J. C. 1984. *Dynamics and fatigue of wind turbine rotors during steady operation*. Riso National Laboratory, R-152. Riso National Laboratory, Roskilde, Denmark.

Manwell, J. F., McGowan, J. G. and Rogers. A. L. 2002. *Wind Energy Explained*. Chichester: John Wiley & Sons.

Matuska, D. G. and Gronenthal, E. W. 1997. *Retraction/extension mechanism for variable diameter rotors*. U.S. Patent 5,642,982.

Matuska, D. G., Gronenthal, E. W. and Jepson, D. W. 1997. *Torque tube/spar assembly for variable diameter helicopter rotors*. U.S. Patent 5,636,969.

Mckittrick, L.R., Cairns, D.S., MandelI, J., Combs, D.C., Rabem, D.A. & VanLuchene, R.D. 2001. *Analysis of a Composite Blade Design for the AOC 15/50 Wind Turbine Using a Finite Element Model.*

Mikhail, A. S. and Deane. G. F. 2004. *Retractable rotor blades for power generating wind and ocean current turbines and means for operating below set rotor torque limits*. U.S. Patent 6,726,439 B2.

Molenaarx, D. and Dijkstra, S. 1998. Modeling of Structural Dynamics of Lagerwey LW-50/750 Wind Turbine. *Wind Engineering.* 22(6): 253–264.

Oelsner, H. F. W. 2001. *Harvesting the wind in Southern Africa*. Darling, South African Wind Energy Association.

Olorunsola, O. 1986. On the Free Yaw Behaviour of Horizontal Axis Wind Turbine. *International Journal of Energy Research*. 10(4): 343–355.

Ontario Ministry of Energy. 2008**.** *Electricity Generation Using Small Wind Turbines At Your Home Or Farm.* http://www.omafra.gov.on.ca/english/engineer/facts/03-047.htm [13 October 2008].

Ormiston, R. A. 1975. *Dynamic Response of Wind Turbine Rotor Systems*. In Proceedings of the 31st Annual National Forum of the American Helicopter Society, Washington, D.C.
Palm, W. J. 2007. *Mechanical Vibration*. 1st Ed. John Wiley.

Pasupulati S., Wallace J. & Dawson M. 2005. Variable Length Blades Wind Turbine. *IEEE Power Engineering Society General Meeting*, Conference article (CA), Jun 12-16 2005, Pages 2097-2100.

Putter, S. and Manor, H. 1978. Natural frequencies of radial rotating beams. *Journal of Sound and Vibration*, 56 (2): 175-185.

Rao, S. S. 2004. *Mechanical Vibrations*. 4th Ed. New Jersey: Prentice Hall, Upper Saddle River.

Reference.com. 2008. *Wind power*.
http://www.reference.com/browse/wiki/Wind_power
[13 October 2008].

Research institute for sustainable energy. 2006. *Wind Electric.*
http://www.rise.org.au/info/Tech/wind/electric.html
[13 October 2008]

Schwarz, B. J. and Richardson, M. H. 1999. *Experimental modal analysis*. CSI Reliability Week, Orlando, FL.

Southern Africa Institute of Steel Construction. n.d. *Specification of weldable structural steel*.
http://www.saisc.co.za
[14 October 2008].

Southwell, R.V. and Gough, B. S. 1921. *On the free transverse vibrations of airscrew blades.* British A.R.C. Reports and Memoranda No. 766 (Ae. 26), 358–368.

Spera. D. A. 1994. *Wind turbine technology: fundamental concepts of wind turbine engineering*. ASME PRESS, New York.

Sullivan, T.L. 1981. *A Review of Resonance Response in Large Horizontal-Axis Wind Turbines*. Proceedings for the Wind Turbine Dynamics Workshop, NASA Conference Publications 2185/ DOE CONF-810226, 24-26.

Thresher RW. 1982. Structural dynamic analysis of wind turbine systems. J. *Solar Energy Engineering*. 104:89-95.

United States Department of Energy. 2005. *Wind Energy Program: History of Wind Energy Use*. http://www1.eere.energy.gov/windandhydro/wind_history.html
[13 October 2008].

Van Der Tempel, J. & Molenaar, D.P. 2002. Wind Turbine Structural Dynamics: A Review of the Principles for Modern Power Generation, Onshore and Offshore. *Wind Engineering*, 26(4): 211-220.

Warmbrodt, W. and Friedmann, P. P. 1979. *Formulation of the Aeroelastic Stability and Response Problem of Coupled Rotor/ tower Systems*. In Proceedings of the Twentieth Structures, Structural Dynamics and Materials Conference, St. Louis, Missouri. 39–52, AIAA Paper 79-0732. April.

Wind Power Monthly. 2008. *Wind energy facts and figures from Wind power Monthly*. http://windpower-monthly.com/spis/runisa.dll?WPM:WINDICATOR:910351.
[13 October 2008].

Zhiquan Y., Haomin M., Nengsheng B., Yan C. and Kang D. 2001. Structure dynamic analysis of a HAWT using a modal analysis method. *Wind Engineering.* 25(4): 237–248. July.

Zweben, C., Thomas, H. H. and Chou, T. W. 1989. *Mechanical behaviour and properties of composite materials.* Technomic Publishing Co., Inc. Vol. 1.

APPENDICES

Appendix A: Instrument specifications

This appendix presents a summary of the hardware used and evaluated in the experimental investigations performed. The product identification and product specifications are given.

- **ICP IMPACT HAMMER**

Model Number 086C02

PERFORMANCE	ENGLISH	SI
Sensitivity (±15 %)	50 mV/lb_f	11.2 mV/N
Measurement Range	±100 lb_f pk	±440 N pk
Resonant Frequency	≥22 kHz	≥22 kHz
Non-Linearity	≤1 %	≤1 %

- **ACCELEROMETER**

Model IA11T

DYNAMIC PERFORMANCE	ENGLISH	SI
Sensitivity (±10%)	100 mV/g	10.2 $mV/(m/s^2)$
Measurement Range	±50 g	±490 m/s^2
Frequency Range: (±3 dB)	20 – 600k cpm	0.32 – 10k Hz
Mounted Resonant Frequency	1320k cpm	22k Hz
Amplitude Linearity	±1%	±1%
Transverse Sensitivity	≤7%	≤7%

- **DYNAMIC SIGNAL ANALYSER**

The OneproD MVP-2C Portable Analyser is a modular, fully adaptable machinery analyser that can be configured at any time to be a two-channel vibration analyser, data collector, balancer, and data recorder to suit a wide variety of condition monitoring needs.

Specifications (Short Form)

- 1 or 2 channels;
- cross-channel functions with 2-channel configuration;
- resonance Analysis, bump test etc;
- running machine resonance/bump test;
- 128MB internal memory (-+ 20,000 Spectra @ 3200 lines);
- 12 800 lines of resolution;
- true zoom;
- USB/Ethernet communications;
- built-in laser tachometer;
- built-in pyrometer (infra-red thermometer) with laser sighting;
- 8 hours battery life (Li-On);
- remote route loading/unloading with E-route option;
- balancing option: 1 or 2 channels up to 4 planes;
- order analysis (run-up and run-down) and,
- long time-record acquisition for slow speed machines and event capture.

Appendix B: MATLAB program for uniform and stepped beam

% INPUT DATA

```
%*************************************************************************
%*************************************************************************
%************************ BEAMANALYSIS ***********************************
%*************************************************************************
%************************** Written by ***********************************
%*************************************************************************
%******************** TARTIBU KWANDA 2008 ********************************
%*************************************************************************
%*************************************************************************
%*************************************************************************
%Uniform beam and Stepped beam finite element program. Selectable number of step and %number of elements. Solves for eigenvalues and eigenvectors of a beam with user defined %dimensions. This program is able to calculate the natural frequencies of different uniform and %stepped beam geometries and material's properties.
%default values are included in the program for the purpose of showing how to input data.
   echo off
   clf;
   clear all;
   inp = input('Input "1" to enter beam dimensions, "Enter" to use default ... ');
   if (isempty(inp))
      inp = 0;
   else
   end
   if inp == 0
%   input size of beam and material
%   xl(i) = length of element (step)i
%   w(i) = width of element (step)i
%   t(i) = thickness of element (step)i
%   e = Young's modulus
%   bj = global degree of freedom number corresponding to the jth local degree
%   of freedom of element i
%   a(i) = area of cross section of element i
%   ne = number of elements
%   n = total number of degree of freedom
%   no = number of nodes
   format short
```

```
xl = [40 32 24];
xi = [1.333333 6.75 0.08333];
w = [4 6 2];
t = [2 3 1];
e = 206e+6;
rho = 7.85e-6;
bj = [1 2 3 4;3 4 5 6;5 6 7 8];
ne = 3;
n = 8;
else
```

% INPUT SIZE OF STEPPED BEAM AND MATERIAL

```
ne = input ('Input number of elements, default 3 ... ');
  if (isempty(ne))
     ne = 3;
  else
  end

  xl = input ('Input lengths of stepped beam, default [40 32 24], ... ');
  if (isempty(xl))
     xl = [40 32 24];
  else
  end

  w = input ('Input widths of stepped beam, default [4 6 2], ... ');
  if (isempty(w))
     w = [4 6 2];
  else
  end

  t = input ('Input thickness of stepped beam, default [2 3 1], ... ');
  if (isempty(t))
     t = [2 3 1];
  else
  end
```

```
    e = input('Input modulus of material, mN/mm^2, default mild steel 206e+6 ... ');
    if (isempty(e))
        e=206e+6;
    else
    end

    rho = input('Input density of material,kg/mm^3 , default mild steel 7.85e-6 ... ');
    if (isempty(rho))
        rho = 7.85e-6;
    else
    end

    bj = input('Input global degree of freedom, default global degree of freedom [1 2 3 4;3 4 5 6;5 6 7 8] ...
');
    if (isempty(bj))
        bj = [1 2 3 4;3 4 5 6;5 6 7 8];
    else
    end
    end
```

% CALCULATION

```
%   Calculate area (a), area moment of Inertia (xi) and mass per unit of length (xmas) of
%   the stepped beam
    a = w.*t;
%   Define area moment of inertia according to flap-wise or edge-wise
%   vibration of the stepped beam.
    vibrationdirection = input('enter "1" for edge-wise vibration, "enter" for flap-wise vibration ... ');
    if (isempty(vibrationdirection))
        vibrationdirection = 0;
    else
    end
    if vibrationdirection == 0
        xi=w.*t.^3/12;
    else
```

```
    xi=t.*w.^3/12;
  end

  for i=1:ne
    xmas(i)=a(i)*rho;
  end
```

% BUILDING OF MATRICES

```
% Size the stiffness and mass matrices
  no = ne+1;
  n = 2*no;
 bigm = zeros(n,n);
 bigk = zeros(n,n);
% Now build up the global stiffness and consistent mass matrices, element
% by element
  ai = zeros(4,n);
    i1=bj(ii,1);
    i2=bj(ii,2);
    i3=bj(ii,3);
    i4=bj(ii,4);
    ai(1,i1)=1;
    ai(2,i2)=1;
    ai(3,i3)=1;
    ai(4,i4)=1;
    xm(1,1)=156;
    xm(1,2)=22*xl(ii);
    xm(1,3)=54;
    xm(1,4)=-13*xl(ii);
    xm(2,2)=4*xl(ii)^2;
    xm(2,3)=13*xl(ii);
    xm(2,4)=-3*xl(ii)^2;
    xm(3,3)=156;
    xm(3,4)=-22*xl(ii);
    xm(4,4)=4*xl(ii)^2;
    xk(1,1)=12;
```

```
xk(1,2)=6*xl(ii);
xk(1,3)=-12;
xk(1,4)=6*xl(ii);
xk(2,2)=4*xl(ii)^2;
xk(2,3)=-6*xl(ii);
xk(2,4)=2*xl(ii)^2;
xk(3,3)=12;
xk(3,4)=-6*xl(ii);
xk(4,4)=4*xl(ii)^2;
for i=1:4
  for j=1:4
    xm(j,i)=xm(i,j);
    xk(j,i)=xk(i,j);
  end
end
for i=1:4
  for j=1:4
    xm(i,j)=(((xmas(ii)*xl(ii))/420))*xm(i,j);
    xk(i,j)=((e*xi(ii))/(xl(ii)^3))*xk(i,j);
  end
end
for i=1:n
  for j=1:4
    ait(i,j)=ai(j,i);
  end
end
xka=xk*ai;
xma=xm*ai;
aka=ait*xka;
ama=ait*xma;
for i=1:n
  for j=1:n
    bigm(i,j)=bigm(i,j)+ama(i,j);
    bigk(i,j)=bigk(i,j)+aka(i,j);
  end
end
```

```
end
% Application of boundary conditions
% Rows and columns corresponding to zero displacements are deleted

bigk(1:2,:) = [];
bigk(:,1:2) = [];

bigm(1:2,:) = [];
bigm(:,1:2) = [];
```

% CALCULATION OF NATURAL FREQUENCY

```
% Calculation of eigenvector and eigenvalue

[L, V] = eig (bigk,bigm)

% Natural frequency
V1 = V.^(1/2)
W = diag(V1)
f =W/(2*pi)
```

Appendix C: MATLAB Program explanation: 3 elements mesh

%: MATLAB treats all the information after the % on that line as a comment. MATLAB ignores this comment line when you run the M-file.
echo off: Turns off the echoing of commands in all script files
clf: deletes from the current figure all graphics objects whose handles are not hidden
clear all: removes all variables, functions, and MEX-files from memory, leaving the workspace empty
format long: scaled fixed point format with 14 to 15 digits after the decimal point for double; and 7 digits after the decimal point for single.
xl = [xl1 xl2 xl3] xl1 = length of step 1 (ii = 1) xl2 = length of step 2 (ii = 2) xl3 = length of step 3 (ii = 3)
xi = [xi1 xi2 xi3] xi1 = area moment of inertia step 1 xi2 = area moment of inertia step 2 xi3 = area moment of inertia step 3
w = [w1 w2 w3] w1 = width of step 1 w2 = width of step 2 w3 = width of step 3
t = [t1 t2 t3] t1 = thickness of step 1 t2 = thickness of step 2 t3 = thickness of step 3
bj = [1 2 3 4;3 4 5 6;5 6 7 8] = $\begin{bmatrix} 1 & 2 & 3 & 4 \\ 3 & 4 & 5 & 6 \\ 5 & 6 & 7 & 8 \end{bmatrix}$
a = w.*t = [w1 w2 w3].* [t1 t2 t3] = [w1*t1 w2*t2 w3*t3] = [a1 a2 a3]
xi = w.*t.^3/12 = [w1 w2 w3].* [t1 t2 t3].^3/12 = [w1*t1^3 w2*t2^3 w3*t3^3]/12
xmas1 = a1*rho for i = 1 xmas2 = a2*rho for i = 2 xmas3 = a3*rho for i = 3

bigm = $\begin{bmatrix} 0 & 0 & 0 & 0 & 0 & 0 & 0 & 0 \\ 0 & 0 & 0 & 0 & 0 & 0 & 0 & 0 \\ 0 & 0 & 0 & 0 & 0 & 0 & 0 & 0 \\ 0 & 0 & 0 & 0 & 0 & 0 & 0 & 0 \\ 0 & 0 & 0 & 0 & 0 & 0 & 0 & 0 \\ 0 & 0 & 0 & 0 & 0 & 0 & 0 & 0 \\ 0 & 0 & 0 & 0 & 0 & 0 & 0 & 0 \\ 0 & 0 & 0 & 0 & 0 & 0 & 0 & 0 \end{bmatrix}$

bigk = $\begin{bmatrix} 0 & 0 & 0 & 0 & 0 & 0 & 0 & 0 \\ 0 & 0 & 0 & 0 & 0 & 0 & 0 & 0 \\ 0 & 0 & 0 & 0 & 0 & 0 & 0 & 0 \\ 0 & 0 & 0 & 0 & 0 & 0 & 0 & 0 \\ 0 & 0 & 0 & 0 & 0 & 0 & 0 & 0 \\ 0 & 0 & 0 & 0 & 0 & 0 & 0 & 0 \\ 0 & 0 & 0 & 0 & 0 & 0 & 0 & 0 \\ 0 & 0 & 0 & 0 & 0 & 0 & 0 & 0 \end{bmatrix}$

ai(i,j) = $\begin{bmatrix} 0 & 0 & 0 & 0 & 0 & 0 & 0 & 0 \\ 0 & 0 & 0 & 0 & 0 & 0 & 0 & 0 \\ 0 & 0 & 0 & 0 & 0 & 0 & 0 & 0 \\ 0 & 0 & 0 & 0 & 0 & 0 & 0 & 0 \end{bmatrix}$

i1 = bj(1,1) = 1 for ii = 1 or bj(2,1) = 1 for ii = 2 or bj(3,1) = 1 for ii = 3

i2 = bj(1,2) = 1 for ii = 1 or bj(2,2) = 1 for ii = 2 or bj(3,2) = 1 for ii = 3

i1 = bj(1,3) = 1 for ii = 1 or bj(2,3) = 1 for ii = 2 or bj(3,3) = 1 for ii = 3

i1 = bj(1,4) = 1 for ii = 1 or bj(2,4) = 1 for ii = 2 or bj(3,4) = 1 for ii = 3

For ii = 1 ai(i,j) = $\begin{bmatrix} 1 & 0 & 0 & 0 & 0 & 0 & 0 & 0 \\ 0 & 1 & 0 & 0 & 0 & 0 & 0 & 0 \\ 0 & 0 & 1 & 0 & 0 & 0 & 0 & 0 \\ 0 & 0 & 0 & 1 & 0 & 0 & 0 & 0 \end{bmatrix}$

For ii = 2 ai(i,j) = $\begin{bmatrix} 0 & 0 & 1 & 0 & 0 & 0 & 0 & 0 \\ 0 & 0 & 0 & 1 & 0 & 0 & 0 & 0 \\ 0 & 0 & 0 & 0 & 1 & 0 & 0 & 0 \\ 0 & 0 & 0 & 0 & 0 & 1 & 0 & 0 \end{bmatrix}$

For ii = 3 ai(i,j) = $\begin{bmatrix} 0 & 0 & 0 & 0 & 1 & 0 & 0 & 0 \\ 0 & 0 & 0 & 0 & 0 & 1 & 0 & 0 \\ 0 & 0 & 0 & 0 & 0 & 0 & 1 & 0 \\ 0 & 0 & 0 & 0 & 0 & 0 & 0 & 1 \end{bmatrix}$

xm = $\begin{bmatrix} 156 & 22*xl(ii) & 54 & -13*xl(ii) \\ 22*xl(ii) & 4*xl(ii)\text{^}2 & 13*xl(ii) & -3*xl(ii)\text{^}2 \\ 54 & 13*xl(ii) & 156 & -22*xl(ii) \\ -13*xl(ii) & -3*xl(ii) & -22*xl(ii) & 4*xl(ii)\text{^}2 \end{bmatrix}$ for ii = 1:3

xk = $\begin{bmatrix} 12 & 6*xl(ii) & -12 & 6*xl(ii) \\ 22*xl(ii) & 4*xl(ii)\text{^}2 & -6*xl(ii) & 2*xl(ii)\text{^}2 \\ 6 & -6*xl(ii) & 12 & -6*xl(ii) \\ 6*xl(ii) & 2*xl(ii) & -6*xl(ii) & 4*xl(ii)\text{^}2 \end{bmatrix}$ for ii = 1:3

xm(i,j) = (xmas(ii)*xl(ii)/420)* $\begin{bmatrix} 156 & 22*xl(ii) & 54 & -13*xl(ii) \\ 22*xl(ii) & 4*xl(ii)\text{^}2 & 13*xl(ii) & -3*xl(ii)\text{^}2 \\ 54 & 13*xl(ii) & 156 & -22*xl(ii) \\ -13*xl(ii) & -3*xl(ii) & -22*xl(ii) & 4*xl(ii)\text{^}2 \end{bmatrix}$

- xm(i,j) = $\begin{bmatrix} xm11a & xm12a & xm13a & xm14a \\ xm21a & xm22a & xm23a & xm24a \\ xm31a & xm32a & xm33a & xm34a \\ xm41a & xm42a & xm43a & xm44a \end{bmatrix}$ for ii = 1
- xm(i,j) = $\begin{bmatrix} xm11b & xm12b & xm13b & xm14b \\ xm21b & xm22b & xm23b & xm24b \\ xm31b & xm32b & xm33b & xm34b \\ xm41b & xm42b & xm43b & xm44b \end{bmatrix}$ for ii = 2
- xm(i,j) = $\begin{bmatrix} xm11c & xm12c & xm13c & xm14c \\ xm21c & xm22c & xm23c & xm24c \\ xm31c & xm32c & xm33c & xm34c \\ xm41c & xm42c & xm43c & xm44c \end{bmatrix}$ for ii = 3

xk(i,j) = (e*xi(ii)/(xl(ii)^3))* $\begin{bmatrix} 12 & 6*xl(ii) & -12 & 6*xl(ii) \\ 22*xl(ii) & 4*xl(ii)\text{^}2 & -6*xl(ii) & 2*xl(ii)\text{^}2 \\ 6 & -6*xl(ii) & 12 & -6*xl(ii) \\ 6*xl(ii) & 2*xl(ii) & -6*xl(ii) & 4*xl(ii)\text{^}2 \end{bmatrix}$

- xk(i,j) = $\begin{bmatrix} xk11a & xk12a & xk13a & xk14a \\ xk21a & xk22a & xk23a & xk24a \\ xk31a & xk32a & xk33a & xk34a \\ xk41a & xk42a & xk43a & xk44a \end{bmatrix}$ for ii = 1

- xk(i,j) = $\begin{bmatrix} xk11b & xk12b & xk13b & xk14b \\ xk21b & xk22b & xk23b & xk24b \\ xk31b & xk32b & xk33b & xk34b \\ xk41b & xk42b & xk43b & xk44b \end{bmatrix}$ for ii = 2

- xk(i,j) = $\begin{bmatrix} xk11c & xk12c & xk13c & xk14c \\ xk21c & xk22c & xk23c & xk24c \\ xk31c & xk32c & xk33c & xk34c \\ xk41c & xk42c & xk43c & xk44c \end{bmatrix}$ for ii = 3

For ii = 1 ait(i,j) = ai(j,i) = $\begin{bmatrix} 1 & 0 & 0 & 0 \\ 0 & 1 & 0 & 0 \\ 0 & 0 & 1 & 0 \\ 0 & 0 & 0 & 1 \\ 0 & 0 & 0 & 0 \\ 0 & 0 & 0 & 0 \\ 0 & 0 & 0 & 0 \\ 0 & 0 & 0 & 0 \end{bmatrix}$

For ii = 2 ait(i,j) = $\begin{bmatrix} 0 & 0 & 0 & 0 \\ 0 & 0 & 0 & 0 \\ 1 & 0 & 0 & 0 \\ 0 & 1 & 0 & 0 \\ 0 & 0 & 1 & 0 \\ 0 & 0 & 0 & 1 \\ 0 & 0 & 0 & 0 \\ 0 & 0 & 0 & 0 \end{bmatrix}$

For ii = 3 ait(i,j) = $\begin{bmatrix} 0 & 0 & 0 & 0 \\ 0 & 0 & 0 & 0 \\ 0 & 0 & 0 & 0 \\ 0 & 0 & 0 & 0 \\ 1 & 0 & 0 & 0 \\ 0 & 1 & 0 & 0 \\ 0 & 0 & 1 & 0 \\ 0 & 0 & 0 & 1 \end{bmatrix}$

- For ii = 1

xka= $\begin{bmatrix} xk11a & xk12a & xk13a & xk14a \\ xk21a & xk22a & xk23a & xk24a \\ xk31a & xk32a & xk33a & xk34a \\ xk41a & xk42a & xk43a & xk44a \end{bmatrix} * \begin{bmatrix} 1 & 0 & 0 & 0 & 0 & 0 & 0 & 0 \\ 0 & 1 & 0 & 0 & 0 & 0 & 0 & 0 \\ 0 & 0 & 1 & 0 & 0 & 0 & 0 & 0 \\ 0 & 0 & 0 & 1 & 0 & 0 & 0 & 0 \end{bmatrix} =$

$\begin{bmatrix} xk11a & xk12a & xk13a & xk14a & 0 & 0 & 0 & 0 \\ xk21a & xk22a & xk23a & xk24a & 0 & 0 & 0 & 0 \\ xk31a & xk32a & xk33a & xk34a & 0 & 0 & 0 & 0 \\ xk41a & xk42a & xk43a & xk44a & 0 & 0 & 0 & 0 \end{bmatrix}$

xma= $\begin{bmatrix} xm11a & xm12a & xm13a & xm14a \\ xm21a & xm22a & xm23a & xm24a \\ xm31a & xm32a & xm33a & xm34a \\ xm41a & xm42a & xm43a & xm44a \end{bmatrix} * \begin{bmatrix} 1 & 0 & 0 & 0 & 0 & 0 & 0 & 0 \\ 0 & 1 & 0 & 0 & 0 & 0 & 0 & 0 \\ 0 & 0 & 1 & 0 & 0 & 0 & 0 & 0 \\ 0 & 0 & 0 & 1 & 0 & 0 & 0 & 0 \end{bmatrix} =$

$\begin{bmatrix} xm11a & xm12a & xm13a & xm14a & 0 & 0 & 0 & 0 \\ xm21a & xm22a & xm23a & xm24a & 0 & 0 & 0 & 0 \\ xm31a & xm32a & xm33a & xm34a & 0 & 0 & 0 & 0 \\ xm41a & xm42a & xm43a & xm44a & 0 & 0 & 0 & 0 \end{bmatrix}$

- For ii = 2

xka= $\begin{bmatrix} xk11b & xk12b & xk13b & xk14b \\ xk21b & xk22b & xk23b & xk24b \\ xk31b & xk32b & xk33b & xk34b \\ xk41b & xk42b & xk43b & xk44b \end{bmatrix} * \begin{bmatrix} 0 & 0 & 1 & 0 & 0 & 0 & 0 & 0 \\ 0 & 0 & 0 & 1 & 0 & 0 & 0 & 0 \\ 0 & 0 & 0 & 0 & 1 & 0 & 0 & 0 \\ 0 & 0 & 0 & 0 & 0 & 1 & 0 & 0 \end{bmatrix} =$

$$\begin{bmatrix} 0 & 0 & xk11b & xk12b & xk13b & xk14b & 0 & 0 \\ 0 & 0 & xk21b & xk22b & xk23b & xk24b & 0 & 0 \\ 0 & 0 & xk31b & xk32b & xk33b & xk34b & 0 & 0 \\ 0 & 0 & xk41b & xk42b & xk43b & xk44b & 0 & 0 \end{bmatrix}$$

$$\text{xma}=\begin{bmatrix} xm11b & xm12b & xm13b & xm14b \\ xm21b & xm22b & xm23b & xm24b \\ xm31b & xm32b & xm33b & xm34b \\ xm41b & xm42b & xm43b & xm44b \end{bmatrix} * \begin{bmatrix} 0 & 0 & 1 & 0 & 0 & 0 & 0 & 0 \\ 0 & 0 & 0 & 1 & 0 & 0 & 0 & 0 \\ 0 & 0 & 0 & 0 & 1 & 0 & 0 & 0 \\ 0 & 0 & 0 & 0 & 0 & 1 & 0 & 0 \end{bmatrix} =$$

$$\begin{bmatrix} 0 & 0 & xm11b & xm12b & xm13b & xm14b & 0 & 0 \\ 0 & 0 & xm21b & xm22b & xm23b & xm24b & 0 & 0 \\ 0 & 0 & xm31b & xm32b & xm33b & xm34b & 0 & 0 \\ 0 & 0 & xm41b & xm42b & xm43b & xm44b & 0 & 0 \end{bmatrix}$$

- For ii = 3

$$\text{xka}=\begin{bmatrix} xk11c & xk12c & xk13c & xk14c \\ xk21c & xk22c & xk23c & xk24c \\ xk31c & xk32c & xk33c & xk34c \\ xk41c & xk42c & xk43c & xk44c \end{bmatrix} * \begin{bmatrix} 0 & 0 & 0 & 0 & 1 & 0 & 0 & 0 \\ 0 & 0 & 0 & 0 & 0 & 1 & 0 & 0 \\ 0 & 0 & 0 & 0 & 0 & 0 & 1 & 0 \\ 0 & 0 & 0 & 0 & 0 & 0 & 0 & 1 \end{bmatrix} =$$

$$\begin{bmatrix} 0 & 0 & 0 & 0 & xk11c & xk12c & xk13c & xk14c \\ 0 & 0 & 0 & 0 & xk21c & xk22c & xk23c & xk24c \\ 0 & 0 & 0 & 0 & xk31c & xk32c & xk33c & xk34c \\ 0 & 0 & 0 & 0 & xk41c & xk42c & xk43c & xk44c \end{bmatrix}$$

$$\text{xma}=\begin{bmatrix} xm11c & xm12c & xm13c & xm14c \\ xm21c & xm22c & xm23c & xm24c \\ xm31c & xm32c & xm33c & xm34c \\ xm41c & xm42c & xm43c & xm44c \end{bmatrix} * \begin{bmatrix} 0 & 0 & 0 & 0 & 1 & 0 & 0 & 0 \\ 0 & 0 & 0 & 0 & 0 & 1 & 0 & 0 \\ 0 & 0 & 0 & 0 & 0 & 0 & 1 & 0 \\ 0 & 0 & 0 & 0 & 0 & 0 & 0 & 1 \end{bmatrix} =$$

$$\begin{bmatrix} 0 & 0 & 0 & 0 & xm11c & xm12c & xm13c & xm14c \\ 0 & 0 & 0 & 0 & xm21c & xm22c & xm23c & xm24c \\ 0 & 0 & 0 & 0 & xm31c & xm32c & xm33c & xm34c \\ 0 & 0 & 0 & 0 & xm41c & xm42c & xm43c & xm44c \end{bmatrix}$$

- For ii = 1

$$\text{aka} = \begin{bmatrix} 1 & 0 & 0 & 0 \\ 0 & 1 & 0 & 0 \\ 0 & 0 & 1 & 0 \\ 0 & 0 & 0 & 1 \\ 0 & 0 & 0 & 0 \\ 0 & 0 & 0 & 0 \\ 0 & 0 & 0 & 0 \\ 0 & 0 & 0 & 0 \end{bmatrix} * \begin{bmatrix} xk11a & xk12a & xk13a & xk14a & 0 & 0 & 0 & 0 \\ xk21a & xk22a & xk23a & xk24a & 0 & 0 & 0 & 0 \\ xk31a & xk32a & xk33a & xk34a & 0 & 0 & 0 & 0 \\ xk41a & xk42a & xk43a & xk44a & 0 & 0 & 0 & 0 \end{bmatrix} =$$

$$\begin{bmatrix} xk11a & xk12a & xk13a & xk14a & 0 & 0 & 0 & 0 \\ xk21a & xk22a & xk23a & xk24a & 0 & 0 & 0 & 0 \\ xk31a & xk32a & xk33a & xk34a & 0 & 0 & 0 & 0 \\ xk41a & xk42a & xk43a & xk44a & 0 & 0 & 0 & 0 \\ 0 & 0 & 0 & 0 & 0 & 0 & 0 & 0 \\ 0 & 0 & 0 & 0 & 0 & 0 & 0 & 0 \\ 0 & 0 & 0 & 0 & 0 & 0 & 0 & 0 \\ 0 & 0 & 0 & 0 & 0 & 0 & 0 & 0 \end{bmatrix}$$

$$\text{ama} = \begin{bmatrix} 1 & 0 & 0 & 0 \\ 0 & 1 & 0 & 0 \\ 0 & 0 & 1 & 0 \\ 0 & 0 & 0 & 1 \\ 0 & 0 & 0 & 0 \\ 0 & 0 & 0 & 0 \\ 0 & 0 & 0 & 0 \\ 0 & 0 & 0 & 0 \end{bmatrix} * \begin{bmatrix} xm11a & xm12a & xm13a & xm14a & 0 & 0 & 0 & 0 \\ xm21a & xm22a & xm23a & xm24a & 0 & 0 & 0 & 0 \\ xm31a & xm32a & xm33a & xm34a & 0 & 0 & 0 & 0 \\ xm41a & xm42a & xm43a & xm44a & 0 & 0 & 0 & 0 \end{bmatrix} =$$

$$\begin{bmatrix} xm11a & xm12a & xm13a & xm14a & 0 & 0 & 0 & 0 \\ xm21a & xm22a & xm23a & xm24a & 0 & 0 & 0 & 0 \\ xm31a & xm32a & xm33a & xm34a & 0 & 0 & 0 & 0 \\ xm41a & xm42a & xm43a & xm44a & 0 & 0 & 0 & 0 \\ 0 & 0 & 0 & 0 & 0 & 0 & 0 & 0 \\ 0 & 0 & 0 & 0 & 0 & 0 & 0 & 0 \\ 0 & 0 & 0 & 0 & 0 & 0 & 0 & 0 \\ 0 & 0 & 0 & 0 & 0 & 0 & 0 & 0 \end{bmatrix}$$

- For ii = 2

$$aka = \begin{bmatrix} 0 & 0 & 0 & 0 \\ 0 & 0 & 0 & 0 \\ 1 & 0 & 0 & 0 \\ 0 & 1 & 0 & 0 \\ 0 & 0 & 1 & 0 \\ 0 & 0 & 0 & 1 \\ 0 & 0 & 0 & 0 \\ 0 & 0 & 0 & 0 \end{bmatrix} * \begin{bmatrix} 0 & 0 & xk11b & xk12b & xk13b & xk14b & 0 & 0 \\ 0 & 0 & xk21b & xk22b & xk23b & xk24b & 0 & 0 \\ 0 & 0 & xk31b & xk32b & xk33b & xk34b & 0 & 0 \\ 0 & 0 & xk41b & xk42b & xk43b & xk44b & 0 & 0 \end{bmatrix} =$$

$$\begin{bmatrix} 0 & 0 & 0 & 0 & 0 & 0 & 0 & 0 \\ 0 & 0 & 0 & 0 & 0 & 0 & 0 & 0 \\ 0 & 0 & xk11b & xk12b & xk13b & xk14b & 0 & 0 \\ 0 & 0 & xk21b & xk22b & xk23b & xk24b & 0 & 0 \\ 0 & 0 & xk31b & xk32b & xk33b & xk34b & 0 & 0 \\ 0 & 0 & xk41b & xk42b & xk43b & xk44b & 0 & 0 \\ 0 & 0 & 0 & 0 & 0 & 0 & 0 & 0 \\ 0 & 0 & 0 & 0 & 0 & 0 & 0 & 0 \end{bmatrix}$$

$$ama = \begin{bmatrix} 0 & 0 & 0 & 0 \\ 0 & 0 & 0 & 0 \\ 1 & 0 & 0 & 0 \\ 0 & 1 & 0 & 0 \\ 0 & 0 & 1 & 0 \\ 0 & 0 & 0 & 1 \\ 0 & 0 & 0 & 0 \\ 0 & 0 & 0 & 0 \end{bmatrix} * \begin{bmatrix} 0 & 0 & xm11b & xm12b & xm13b & xm14b & 0 & 0 \\ 0 & 0 & xm21b & xm22b & xm23b & xm24b & 0 & 0 \\ 0 & 0 & xm31b & xm32b & xm33b & xm34b & 0 & 0 \\ 0 & 0 & xm41b & xm42b & xm43b & xm44b & 0 & 0 \end{bmatrix} =$$

$$\begin{bmatrix} 0 & 0 & 0 & 0 & 0 & 0 & 0 & 0 \\ 0 & 0 & 0 & 0 & 0 & 0 & 0 & 0 \\ 0 & 0 & xm11b & xm12b & xm13b & xm14b & 0 & 0 \\ 0 & 0 & xm21b & xm22b & xm23b & xm24b & 0 & 0 \\ 0 & 0 & xm31b & xm32b & xm33b & xm34b & 0 & 0 \\ 0 & 0 & xm41b & xm42b & xm43b & xm44b & 0 & 0 \\ 0 & 0 & 0 & 0 & 0 & 0 & 0 & 0 \\ 0 & 0 & 0 & 0 & 0 & 0 & 0 & 0 \end{bmatrix}$$

- For ii = 3

$$aka = \begin{bmatrix} 0 & 0 & 0 & 0 \\ 0 & 0 & 0 & 0 \\ 0 & 0 & 0 & 0 \\ 0 & 0 & 0 & 0 \\ 1 & 0 & 0 & 0 \\ 0 & 1 & 0 & 0 \\ 0 & 0 & 1 & 0 \\ 0 & 0 & 0 & 1 \end{bmatrix} * \begin{bmatrix} 0 & 0 & 0 & 0 & xk11c & xk12c & xk13c & xk14c \\ 0 & 0 & 0 & 0 & xk21c & xk22c & xk23c & xk24c \\ 0 & 0 & 0 & 0 & xk31c & xk32c & xk33c & xk34c \\ 0 & 0 & 0 & 0 & xk41c & xk42c & xk43c & xk44c \end{bmatrix} =$$

$$\begin{bmatrix} 0 & 0 & 0 & 0 & 0 & 0 & 0 & 0 \\ 0 & 0 & 0 & 0 & 0 & 0 & 0 & 0 \\ 0 & 0 & 0 & 0 & 0 & 0 & 0 & 0 \\ 0 & 0 & 0 & 0 & 0 & 0 & 0 & 0 \\ 0 & 0 & 0 & 0 & xk11c & xk12c & xk13c & xk14c \\ 0 & 0 & 0 & 0 & xk21c & xk22c & xk23c & xk24c \\ 0 & 0 & 0 & 0 & xk31c & xk32c & xk33c & xk34c \\ 0 & 0 & 0 & 0 & xk41c & xk42c & xk43c & xk44c \end{bmatrix}$$

$$ama = \begin{bmatrix} 0 & 0 & 0 & 0 \\ 0 & 0 & 0 & 0 \\ 0 & 0 & 0 & 0 \\ 0 & 0 & 0 & 0 \\ 1 & 0 & 0 & 0 \\ 0 & 1 & 0 & 0 \\ 0 & 0 & 1 & 0 \\ 0 & 0 & 0 & 1 \end{bmatrix} * \begin{bmatrix} 0 & 0 & 0 & 0 & xm11c & xm12c & xm13c & xm14c \\ 0 & 0 & 0 & 0 & xm21c & xm22c & xm23c & xm24c \\ 0 & 0 & 0 & 0 & xm31c & xm32c & xm33c & xm34c \\ 0 & 0 & 0 & 0 & xm41c & xm42c & xm43c & xm44c \end{bmatrix} =$$

$$\begin{bmatrix} 0 & 0 & 0 & 0 & 0 & 0 & 0 & 0 \\ 0 & 0 & 0 & 0 & 0 & 0 & 0 & 0 \\ 0 & 0 & 0 & 0 & 0 & 0 & 0 & 0 \\ 0 & 0 & 0 & 0 & 0 & 0 & 0 & 0 \\ 0 & 0 & 0 & 0 & xm11c & xm12c & xm13c & xm14c \\ 0 & 0 & 0 & 0 & xm21c & xm22c & xm23c & xm24c \\ 0 & 0 & 0 & 0 & xm31c & xm32c & xm33c & xm34c \\ 0 & 0 & 0 & 0 & xm41c & xm42c & xm43c & xm44c \end{bmatrix}$$

$$
\text{bigm}=\begin{bmatrix}
xm11a & xm12a & xm13a & xm14a & 0 & 0 & 0 & 0\\
xm21a & xm22a & xm23a & xm24a & 0 & 0 & 0 & 0\\
xm31a & xm32a & xm33a & xm34a & 0 & 0 & 0 & 0\\
xm41a & xm42a & xm43a & xm44a & 0 & 0 & 0 & 0\\
0 & 0 & 0 & 0 & 0 & 0 & 0 & 0\\
0 & 0 & 0 & 0 & 0 & 0 & 0 & 0\\
0 & 0 & 0 & 0 & 0 & 0 & 0 & 0\\
0 & 0 & 0 & 0 & 0 & 0 & 0 & 0
\end{bmatrix}+
$$

$$
\begin{bmatrix}
0 & 0 & 0 & 0 & 0 & 0 & 0 & 0\\
0 & 0 & 0 & 0 & 0 & 0 & 0 & 0\\
0 & 0 & xm11b & xm12b & xm13b & xm14b & 0 & 0\\
0 & 0 & xm21b & xm22b & xm23b & xm24b & 0 & 0\\
0 & 0 & xm31b & xm32b & xm33b & xm34b & 0 & 0\\
0 & 0 & xm41b & xm42b & xm43b & xm44b & 0 & 0\\
0 & 0 & 0 & 0 & 0 & 0 & 0 & 0\\
0 & 0 & 0 & 0 & 0 & 0 & 0 & 0
\end{bmatrix}+
$$

$$
\begin{bmatrix}
0 & 0 & 0 & 0 & 0 & 0 & 0 & 0\\
0 & 0 & 0 & 0 & 0 & 0 & 0 & 0\\
0 & 0 & 0 & 0 & 0 & 0 & 0 & 0\\
0 & 0 & 0 & 0 & 0 & 0 & 0 & 0\\
0 & 0 & 0 & 0 & xm11c & xm12c & xm13c & xm14c\\
0 & 0 & 0 & 0 & xm21c & xm22c & xm23c & xm24c\\
0 & 0 & 0 & 0 & xm31c & xm32c & xm33c & xm34c\\
0 & 0 & 0 & 0 & xm41c & xm42c & xm43c & xm44c
\end{bmatrix}
$$

$$
\text{bigk}=\begin{bmatrix}
xk11a & xk12a & xk13a & xk14a & 0 & 0 & 0 & 0\\
xk21a & xk22a & xk23a & xk24a & 0 & 0 & 0 & 0\\
xk31a & xk32a & xk33a & xk34a & 0 & 0 & 0 & 0\\
xk41a & xk42a & xk43a & xk44a & 0 & 0 & 0 & 0\\
0 & 0 & 0 & 0 & 0 & 0 & 0 & 0\\
0 & 0 & 0 & 0 & 0 & 0 & 0 & 0\\
0 & 0 & 0 & 0 & 0 & 0 & 0 & 0\\
0 & 0 & 0 & 0 & 0 & 0 & 0 & 0
\end{bmatrix}+
$$

$$
\begin{bmatrix}
0 & 0 & 0 & 0 & 0 & 0 & 0 & 0\\
0 & 0 & 0 & 0 & 0 & 0 & 0 & 0\\
0 & 0 & xk11b & xk12b & xk13b & xk14b & 0 & 0\\
0 & 0 & xk21b & xk22b & xk23b & xk24b & 0 & 0\\
0 & 0 & xk31b & xk32b & xk33b & xk34b & 0 & 0\\
0 & 0 & xk41b & xk42b & xk43b & xk44b & 0 & 0\\
0 & 0 & 0 & 0 & 0 & 0 & 0 & 0\\
0 & 0 & 0 & 0 & 0 & 0 & 0 & 0
\end{bmatrix}+
$$

$$
\begin{bmatrix}
0 & 0 & 0 & 0 & 0 & 0 & 0 & 0\\
0 & 0 & 0 & 0 & 0 & 0 & 0 & 0\\
0 & 0 & 0 & 0 & 0 & 0 & 0 & 0\\
0 & 0 & 0 & 0 & 0 & 0 & 0 & 0\\
0 & 0 & 0 & 0 & xk11c & xk12c & xk13c & xk14c\\
0 & 0 & 0 & 0 & xk21c & xk22c & xk23c & xk24c\\
0 & 0 & 0 & 0 & xk31c & xk32c & xk33c & xk34c\\
0 & 0 & 0 & 0 & xk41c & xk42c & xk43c & xk44c
\end{bmatrix}
$$

$$\text{bigm} = \begin{bmatrix} xm11a & xm12a & xm13a & xm14a & 0 & 0 & 0 & 0 \\ xm21a & xm22a & xm23a & xm24a & 0 & 0 & 0 & 0 \\ xm31a & xm32a & xm33a + xm11b & xm34a + xm12b & xm13b & xm14b & 0 & 0 \\ xm41a & xm42a & xm43a + xm21b & xm44a + xm22b & xm23b & xm24b & 0 & 0 \\ 0 & 0 & xm31b & xm32b & xm33b + xm11c & xm34b + xm12c & xm13c & xm14c \\ 0 & 0 & xm41b & xm42b & xm43b + xm21c & xm44b + xm22c & xm23c & xm24c \\ 0 & 0 & 0 & 0 & xm31c & xm32c & xm33c & xm34c \\ 0 & 0 & 0 & 0 & xm41c & xm42c & xm43c & xm44c \end{bmatrix}$$

$$\text{bigk} = \begin{bmatrix} xk11a & xk12a & xk13a & xk14a & 0 & 0 & 0 & 0 \\ xk21a & xk22a & xk23a & xk24a & 0 & 0 & 0 & 0 \\ xk31a & xk32a & xk33a + xk11b & xk34a + xk12b & xk13b & xk14b & 0 & 0 \\ xk41a & xk42a & xk43a + xk21b & xk44a + xk22b & xk23b & xk24b & 0 & 0 \\ 0 & 0 & xk31b & xk32b & xk33b + xk11c & xk34b + xk12c & xk13c & xk14c \\ 0 & 0 & xk41b & xk42b & xk43b + xk21c & xk44b + xk22c & xk23c & xk24c \\ 0 & 0 & 0 & 0 & xk31c & xk32c & xk33c & xk34c \\ 0 & 0 & 0 & 0 & xk41c & xk42c & xk43c & xk44c \end{bmatrix}$$

```
bigk(1:2,:) = [];
bigk(:,1:2) = [];

bigm(1:2,:) = [];
bigm(:,1:2) = [];
```

$$bigm=\begin{bmatrix} xm33a+xm11b & xm34a+xm12b & xm13b & xm14b & 0 & 0 \\ xm43a+xm21b & xm44a+xm22b & xm23b & xm24b & 0 & 0 \\ xm31b & xm32b & xm33b+xm11c & xm34b+xm12c & xm13c & xm14c \\ xm41b & xm42b & xm43b+xm21c & xm44b+xm22c & xm23c & xm24c \\ 0 & 0 & xm31c & xm32c & xm33c & xm34c \\ 0 & 0 & xm41c & xm42c & xm43c & xm44c \end{bmatrix}$$

$$bigk=\begin{bmatrix} xk33a+xk11b & xk34a+xk12b & xk13b & xk14b & 0 & 0 \\ xk43a+xk21b & xk44a+xk22b & xk23b & xk24b & 0 & 0 \\ xk31b & xk32b & xk33b+xk11c & xk34b+xk12c & xk13c & xk14c \\ xk41b & xk42b & xk43b+xk21c & xk44b+xk22c & xk23c & xk24c \\ 0 & 0 & xk31c & xk32c & xk33c & xk34c \\ 0 & 0 & xk41c & xk42c & xk43c & xk44c \end{bmatrix}$$

Appendix D: MATLAB program for VARIBLADE

% INPUT DATA

```
%*************************************************************************
%*************************************************************************
%********************VARIBLADEANALYSIS ***********************************
%*************************************************************************
%************************** Written by ***********************************
%*************************************************************************
%******************** TARTIBU KWANDA 2008*********************************
%*************************************************************************
%*************************************************************************
%*************************************************************************
%Variable length blade finite element program.  Two portions of beam: hollow beam %(fixed portion) and solid beam (moveable portion). Solves for eigenvalues and eigenvectors of %stepped beam with user defined dimensions and configurations. This program can calculate the %natural frequencies of different beam geometries and configurations ( position of moveable portion)
%default values are included in the program for the purpose of showing how to input data.
   echo off
   clf;
   clear all;
      inp = input('Input "1" to enter beam dimensions, "Enter" to use default ... ');
   if (isempty(inp))
      inp = 0;
   else
   end

   if inp == 0
%   input beam's geometries and material's properties
%   xl(i) = length of element (step)i
%   w(i) = width of element (step)i
%   t(i) = thickness of element (step)i
%   e = Young's modulus
%   bj = global degree of freedom number corresponding to the jth local degree
%   of freedom of element i
%   a(i) = area of cross section of element i
%   ne = number of elements
%   n = total number of degree of freedom
%   no = number of nodes
%   wa = width of hollow for the first portion of stepped beam
%   ta = thickness of hollow for the first portion of stepped beam
```

```
format long
beamconfiguration = 1;
n1 = 10;
n2 = 10;
l1 = 1000;
l2 = 1000;
h1 = 1000/10;
h2 = 1000/10;
xl = [h1*ones(1,n1) h2*ones(1,beamconfiguration-1)];
w1 = 60;
w2 = 50;
w = [w1*ones(1,n1) w2*ones(1,beamconfiguration-1)];
t1 = 20;
t2 = 10;
t = [t1*ones(1,n1) t2*ones(1,beamconfiguration-1)];
wh = 50;
th = 10;
wa = [wh*ones(1,beamconfiguration-1) 0*ones(1,n2)];
ta = [th*ones(1,beamconfiguration-1) 0*ones(1,n2)];
%   configurations of stepped beam:
%   beamconfiguration ≤ n1 & n2
%   for configuration 1, w = [w1*ones(1,n1) w2*ones(1,1-1)],
%   t = [t1*ones(1,n1) t2*ones(1,1-1)]
%   wa = [wh*ones(1,1-1) 0*ones(1,n2)],
%   ta = [th*ones(1,1-1) 0*ones(1,n2)]
%   for configuration 2, w = [w1*ones(1,n1) w2*ones(1,2-1)]
%   t = [t1*ones(1,n1) t2*ones(1,2-1)]
%   wa = [wh*ones(1,2-1) 0*ones(1,n2)]
%   ta = [th*ones(1,2-1) 0*ones(1,n2)]
%   for configuration 3, w = [w1*ones(1,n1) w2*ones(1,3-1)]
%   t = [t1*ones(1,n1) t2*ones(1,3-1)]
%   wa = [wh*ones(1,3-1) 0*ones(1,n2)]
%   ta = [th*ones(1,3-1) 0*ones(1,n2)]
%   for configuration 4, w = [w1*ones(1,n1) w2*ones(1,4-1)]
%   t = [t1*ones(1,n1) t2*ones(1,4-1)]
%   wa = [wh*ones(1,4-1) 0*ones(1,n2)]
%   ta = [th*ones(1,4-1) 0*ones(1,n2)]
%   for configuration 5, w = [w1*ones(1,n1) w2*ones(1,5-1)]
```

```
%   t = [t1*ones(1,n1) t2*ones(1,5-1)]
%   wa = [wh*ones(1,5-1) 0*ones(1,n2)]
%   ta = [th*ones(1,5-1) 0*ones(1,n2)]
   xi = [40000 40000 40000 40000 40000 40000 40000 40000 40000 40000];
   a = [1200 1200 1200 1200 1200 1200 1200 1200 1200 1200];
   e = 206e+6;
   rho = 7.85e-6;
   bj = [1 2 3 4;3 4 5 6;5 6 7 8;7 8 9 10;9 10 11 12;11 12 13 14;13 14 15 16;15 16 17 18;17 18 19
20;19 20 21 22;21 22 23 24;23 24 25 26;25 26 27 28;27 28 29 30;29 30 31 32; 31 32 33 34;33 34 35
36;35 36 37 38;37 38 39 40;39 40 41 42];
   ne = 20;
   n = 22;
   else
```

% INPUT SIZE OF STEPPED BEAM AND MATERIAL

```
   beamconfiguration = input ('Input beamconfiguration of stepped beam, default 1 ... ');
   if (isempty(beamconfiguration))
      beamconfiguration = 1;
   else
   end

   n1 = input ('Input number of elements for the first portion of stepped beam, default 10 ... ');
   if (isempty(n1))
      n1 = 10;
   else
   end

   n2 = input ('Input number of elements for the second portion of stepped beam, default 10 ... ');
   if (isempty(n2))
      n2 = 10;
   else
   end

   l1 = input ('Input length of first portion of stepped beam, default 1000, ... ');
   if (isempty(l1))
      l1 = 1000;
   else
```

```
end

 l2 = input ('Input length of second portion of stepped beam, default 1000, ... ');
if (isempty(l2))
   l2 = 1000;
else
end

w1 = input ('Input width of first portion of stepped beam, default 60, ... ');
if (isempty(w1))
       w1 = 60;
else
end

 w2 = input ('Input width of second portion of stepped beam, default 50, ... ');
if (isempty(w2))
       w2 = 50;
else
end

t1 = input ('Input thickness of first portion of stepped beam, default 20 , ... ');
if (isempty(t1))
     t1 = 20;
else
end

t2 = input ('Input thickness of second portion of stepped beam, default 10 , ... ');
if (isempty(t2))
     t2 = 10;
else
end

wh = input ('input width of hollow of first portion of stepped beam, default 50, ... ');
if (isempty(wh))
   wh = 50;
else
end
```

```
th = input ('input thickness of hollow of first portion of stepped beam, default 10, ... ');
if (isempty(th))
   th = 10;
else
end

e = input('Input modulus of material, mN/mm^2, default mild steel 206e+6 ... ');
if (isempty(e))
   e=206e+6;
else
end

rho = input('Input density of material,kg/mm^3 , default mild steel 7.85e-6 ... ');
if (isempty(rho))
   rho = 7.85e-6;
else
end

bj = input('Input global degree of freedom, default global degree of freedom [1 2 3 4;3 4 5 6;5 6 7 8;7 8 9 10;9 10 11 12;11 12 13 14;13 14 15 16;15 16 17 18;17 18 19 20;19 20 21 22;21 22 23 24;23 24 25 26;25 26 27 28;27 28 29 30;29 30 31 32; 31 32 33 34;33 34 35 36;35 36 37 38;37 38 39 40;39 40 41 42]; ... ');
if (isempty(bj))
   bj =[1 2 3 4;3 4 5 6;5 6 7 8;7 8 9 10;9 10 11 12;11 12 13 14;13 14 15 16;15 16 17 18;17 18 19 20;19 20 21 22;21 22 23 24;23 24 25 26;25 26 27 28;27 28 29 30;29 30 31 32; 31 32 33 34;33 34 35 36;35 36 37 38;37 38 39 40;39 40 41 42];
else
end
end
```

% CALCULATION

```
ne = n1+beamconfiguration-1;
h1 = l1/n1;
h2 = l2/n2;
xl = [h1*ones(1,n1) h2*ones(1,beamconfiguration-1)];
w = [w1*ones(1,n1) w2*ones(1,beamconfiguration-1)];
t = [t1*ones(1,n1) t2*ones(1,beamconfiguration-1)];
```

```
    wa = [wh*ones(1,beamconfiguration-1) 0*ones(1,n2)];
    ta = [th*ones(1,beamconfiguration-1) 0*ones(1,n2)];

%   calculate area (a), area moment of Inertia (xi) and mass per unit of length (xmas) of
%   the stepped beam
    a = (w.*t)-(wa.*ta);
%   define area moment of inertia according to flap-wise or edge-wise
%   vibration of the stepped beam.
    vibrationdirection = input('enter "1" for edge-wise vibration, "enter" for flap-wise vibration ... ');
    if (isempty(vibrationdirection))
        vibrationdirection = 0;
    else
    end
    if vibrationdirection == 0
        xi=((w.*t.^3)-(wa.*ta.^3))/12;
    else
        xi=((t.*w.^3)-(ta.*wa.^3))/12;
    end

    for i=1:ne
      xmas(i)=a(i)*rho;
    end
```

% BUILDING OF MATRICES

```
%   Size the stiffness and mass matrices
    no = ne+1;
    n = 2*no;
   bigm = zeros(n,n);
   bigk = zeros(n,n);
%   Now build up the global stiffness and consistent mass matrices, element
%   by element
   ai = zeros(4,n);
       i1=bj(ii,1);
       i2=bj(ii,2);
       i3=bj(ii,3);
       i4=bj(ii,4);
       ai(1,i1)=1;
```

```
ai(2,i2)=1;
ai(3,i3)=1;
ai(4,i4)=1;
xm(1,1)=156;
xm(1,2)=22*xl(ii);
xm(1,3)=54;
xm(1,4)=-13*xl(ii);
xm(2,2)=4*xl(ii)^2;
xm(2,3)=13*xl(ii);
xm(2,4)=-3*xl(ii)^2;
xm(3,3)=156;
xm(3,4)=-22*xl(ii);
xm(4,4)=4*xl(ii)^2;
xk(1,1)=12;
xk(1,2)=6*xl(ii);
xk(1,3)=-12;
xk(1,4)=6*xl(ii);
xk(2,2)=4*xl(ii)^2;
xk(2,3)=-6*xl(ii);
xk(2,4)=2*xl(ii)^2;
xk(3,3)=12;
xk(3,4)=-6*xl(ii);
xk(4,4)=4*xl(ii)^2;
for i=1:4
  for j=1:4
    xm(j,i)=xm(i,j);
    xk(j,i)=xk(i,j);
  end
end
for i=1:4
  for j=1:4
    xm(i,j)=(((xmas(ii)*xl(ii))/420))*xm(i,j);
    xk(i,j)=((e*xi(ii))/(xl(ii)^3))*xk(i,j);
  end
end
for i=1:n
  for j=1:4
    ait(i,j)=ai(j,i);
```

```
      end
    end
    xka=xk*ai;
    xma=xm*ai;
    aka=ait*xka;
    ama=ait*xma;
   for i=1:n
      for j=1:n
        bigm(i,j)=bigm(i,j)+ama(i,j);
        bigk(i,j)=bigk(i,j)+aka(i,j);
      end
    end

  end
% Application of boundary conditions
% Rows and columns corresponding to zero displacements are deleted

   bigk(1:2,:) = [];
   bigk(:,1:2) = [];

   bigm(1:2,:) = [];
   bigm(:,1:2) = [];
```

% CALCULATION OF NATURAL FREQUENCY

```
% Calculation of eigenvector and eigenvalue
  [L, V] = eig (bigk,bigm)
% Natural frequency
  V1 = V.^(1/2)
  W = diag(V1)
   f =W/(2*pi)
```

Appendix E: NX5 results

A. Configuration1

Mode1 (flap-wise)

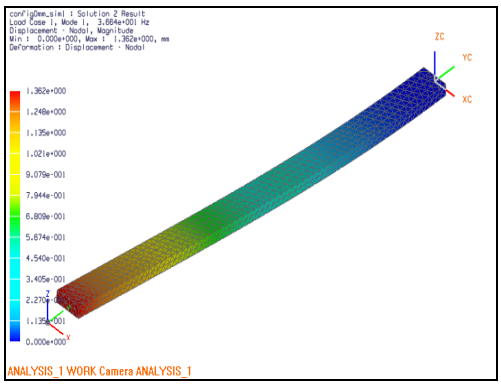

Mode2 (Edge-wise)

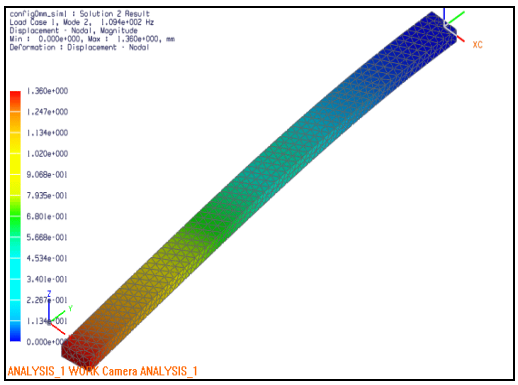

Mode3 (Flap-wise)

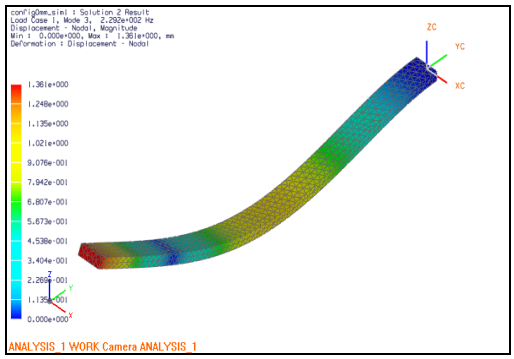

Mode4 (Flap-wise)

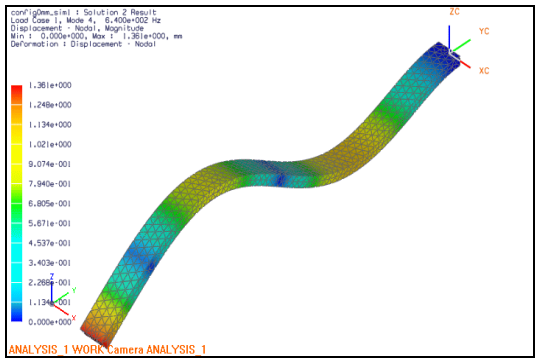

Mode5 (Edge-wise)

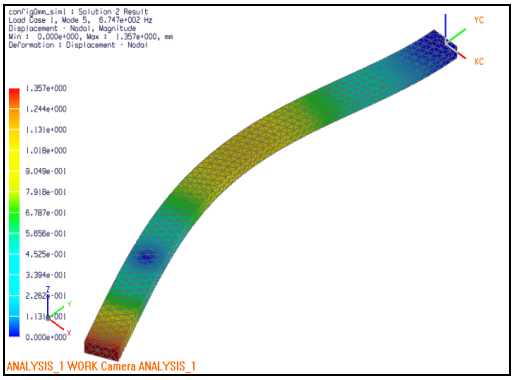

Mode6 (Torsional): 985.3 Hz

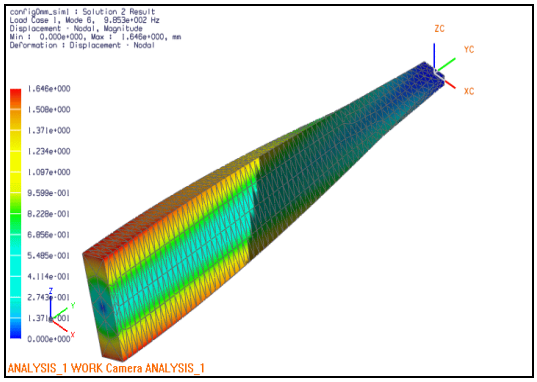

B. Configuration2

Mode1 (Flap-wise)

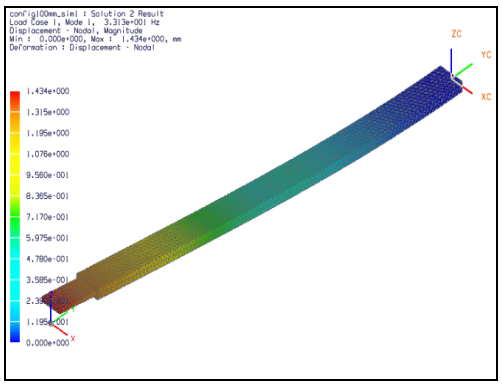

Mode2 (Edge-wise)

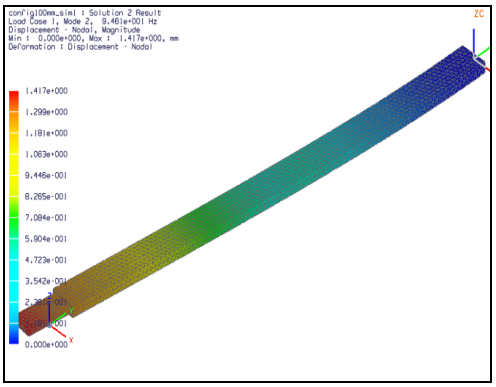

Mode3 (Flap-wise)

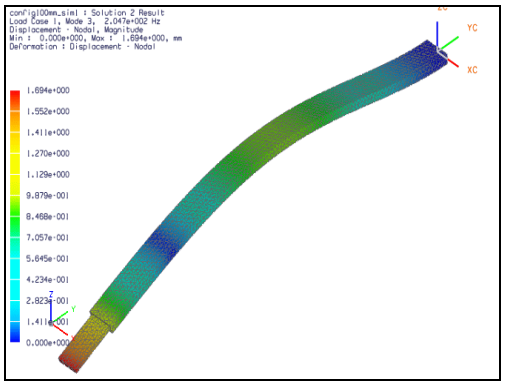

Mode4 (Flap-wise)

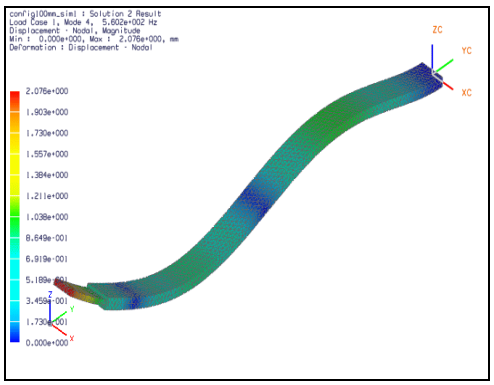

Mode5 (Edge-wise)

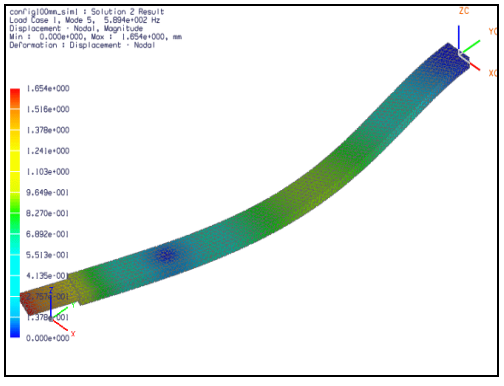

Mode6 (Torsional): 947.6 Hz

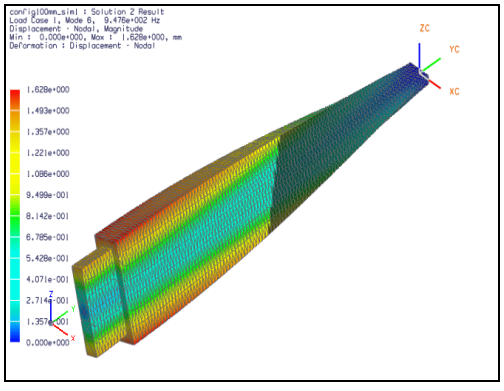

C. Configuration3

Mode1 (Flap-wise)

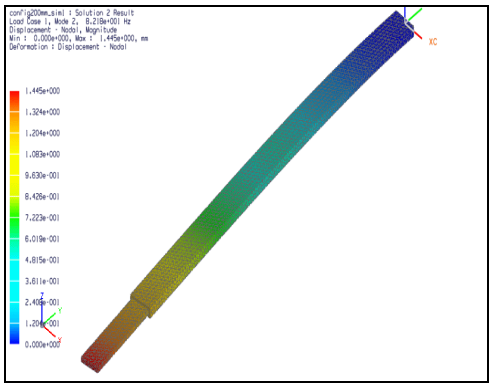

Mode2 (Edge-wise)

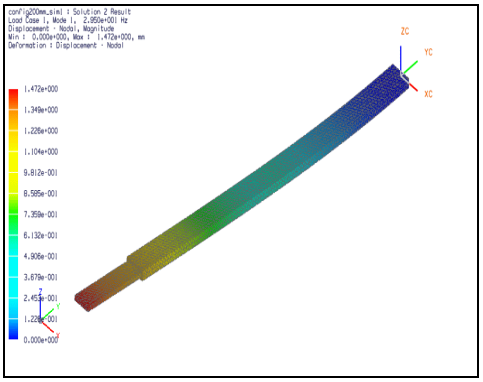

Mode3 (Flap-wise)

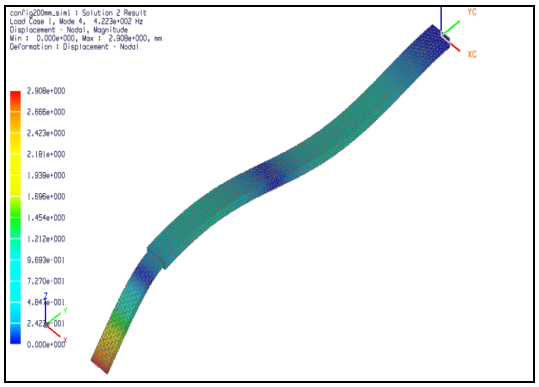

Mode4 (Flap-wise)

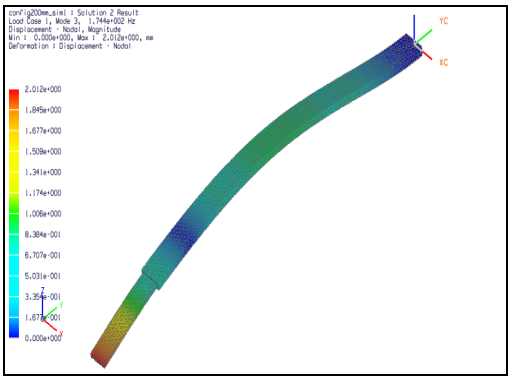

Mode5 (Edge-wise)

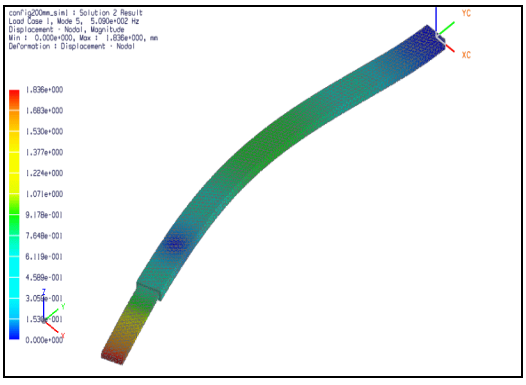

Mode7 (Torsional) : 905.4 Hz

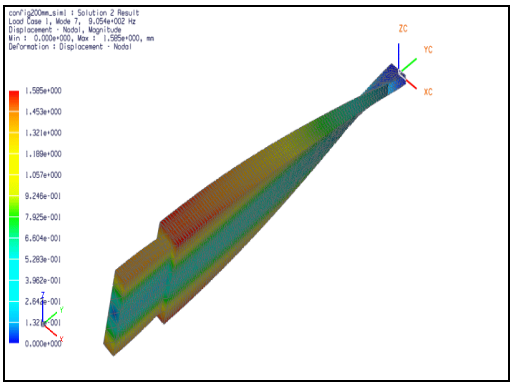

D. Configuration4

Mode1 (Flap-wise)

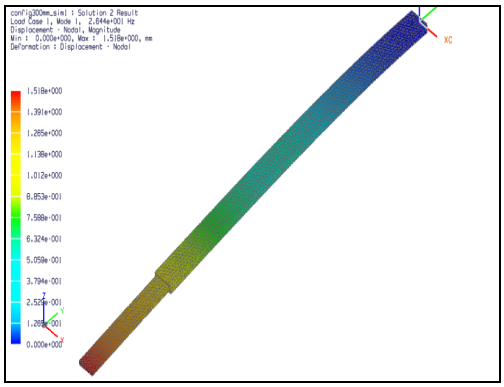

Mode2 (Edge-wise)

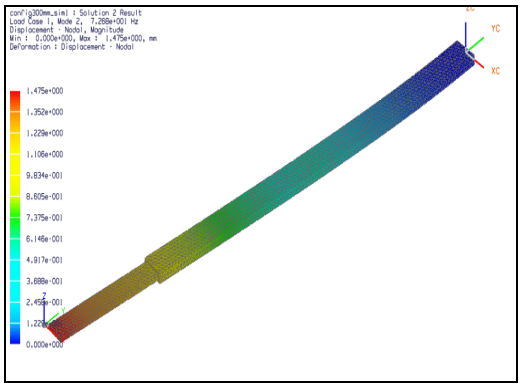

Mode3 (Flap-wise)

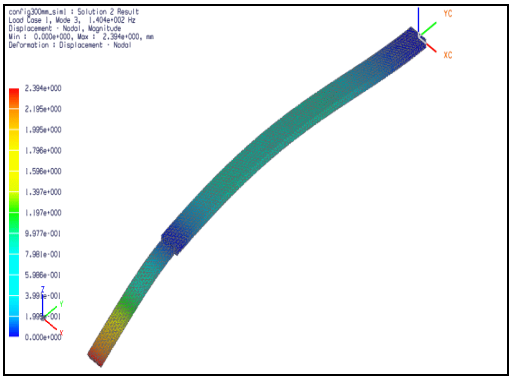

Mode4 (Flap-wise)

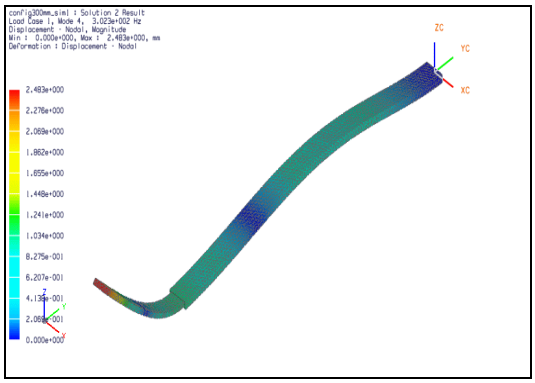

Mode5 (Edge-wise)

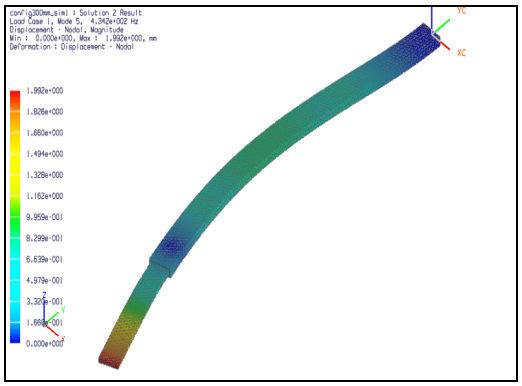

Mode7 (Torsional): 867.8 Hz

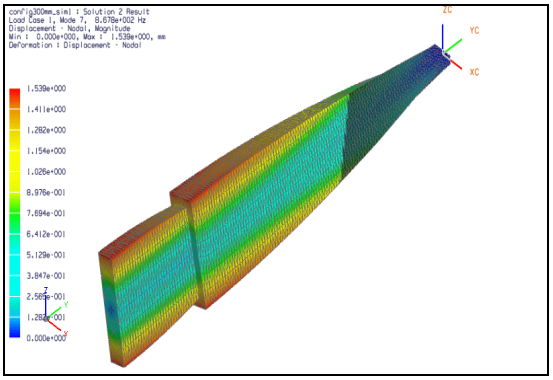

E. Configuration5

Mode1 (Flap-wise)

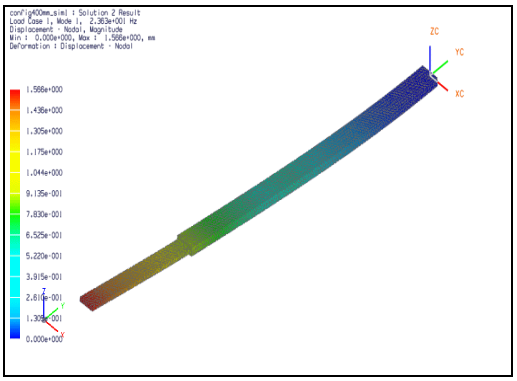

Mode2 (Edge-wise)

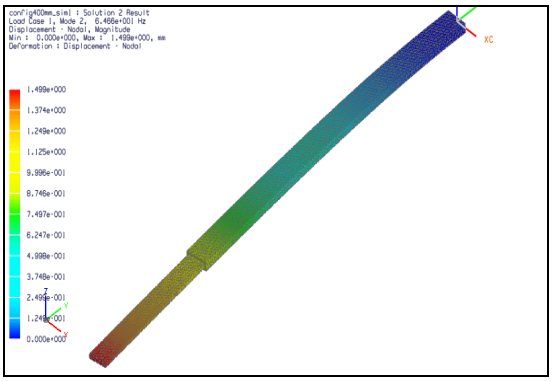

Mode3 (Flap-wise)

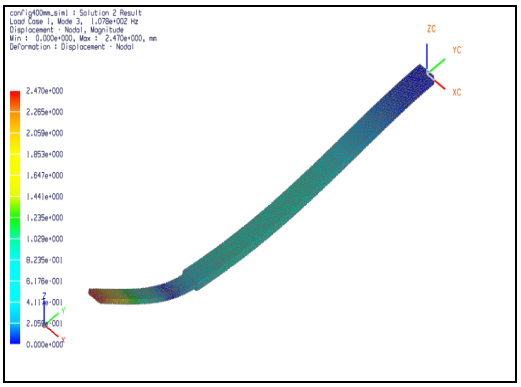

Mode4 (Flap-wise)

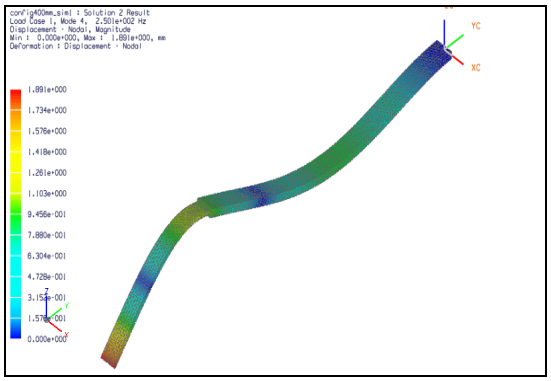

Mode5 (Edge-wise)

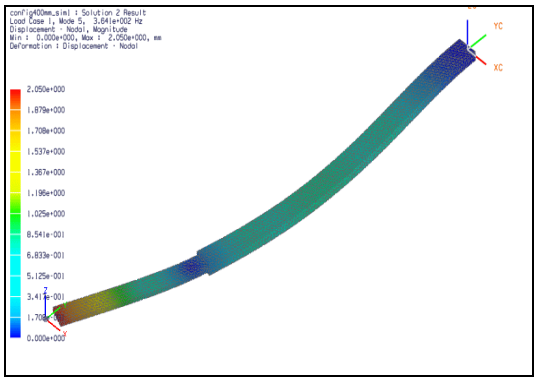

Mode7 (Torsional) : 829.9 Hz

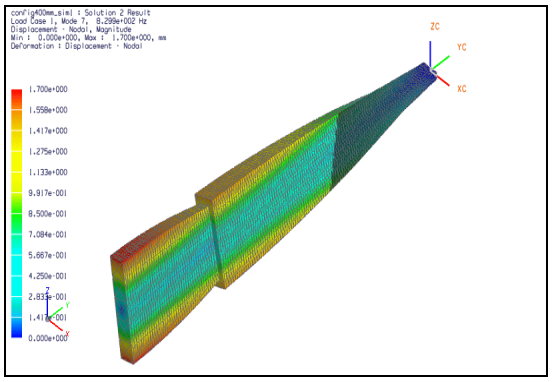

F. Configuration6

Mode1 (Flap-wise)

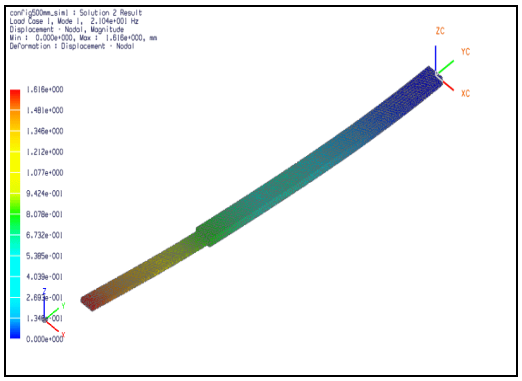

Mode2 (Edge-wise)

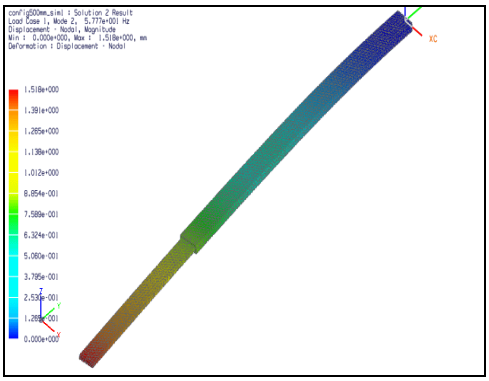

Mode3 (Flap-wise)

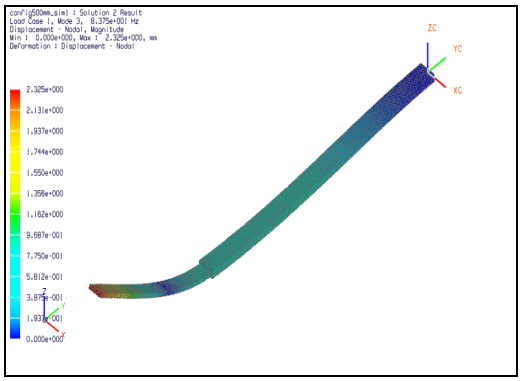

Mode4 (Flap-wise)

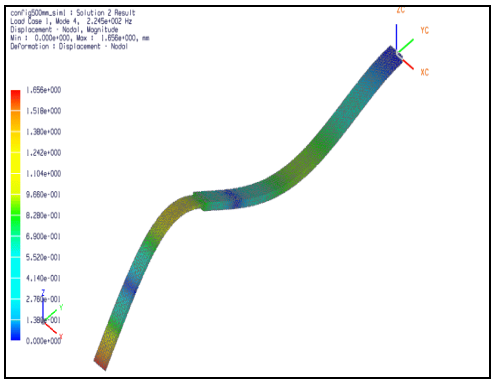

Mode5 (Edge-wise)

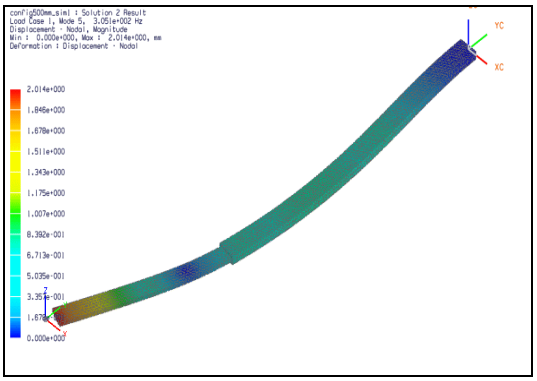

Mode9 (Torsional): 788.8 Hz

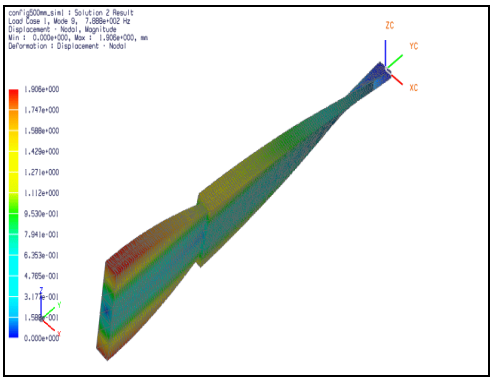

G. Configuration7

Mode1 (Flap-wise)

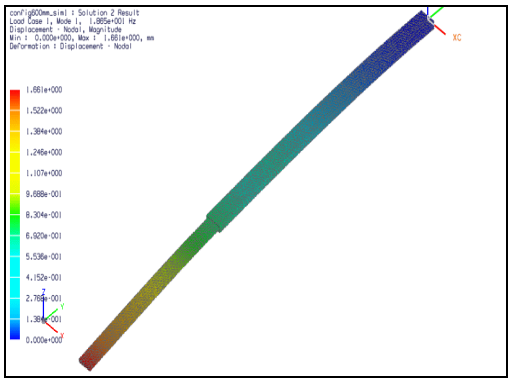

Mode2 (Edge-wise)

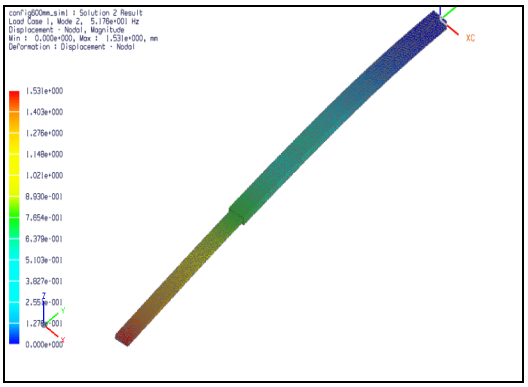

Mode3 (Flap-wise)

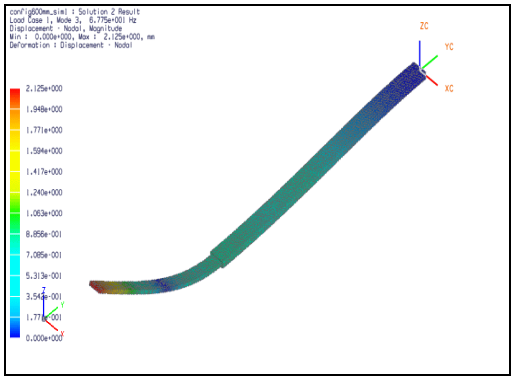

Mode4 (Flap-wise)

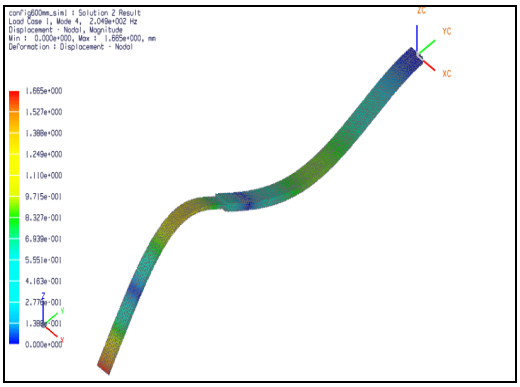

Mode5 (Edge-wise)

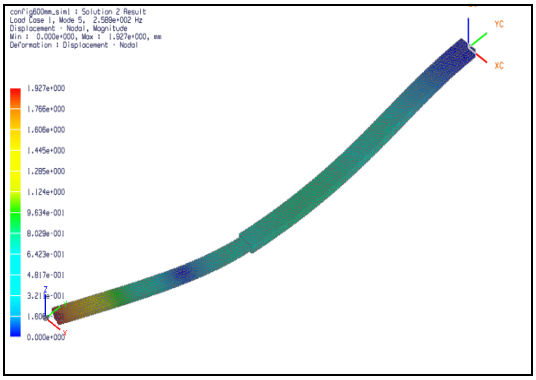

Mode9 (Torsional): 743 Hz

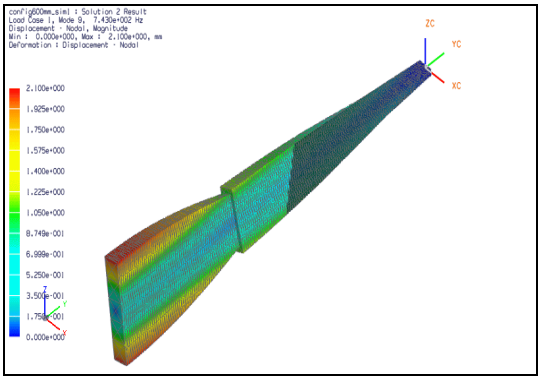

H. Configuration8

Mode1 (Flap-wise)

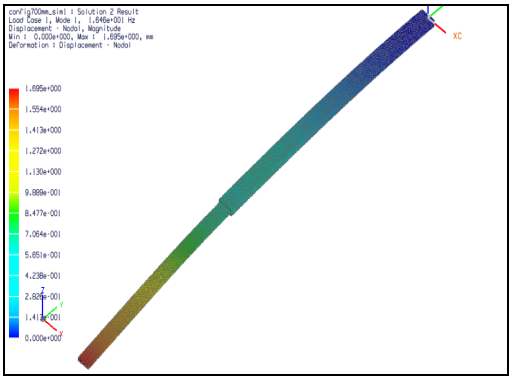

Mode2 (Edge-wise)

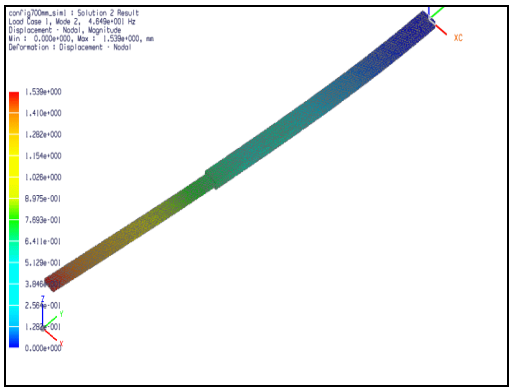

Mode3 (Flap-wise)

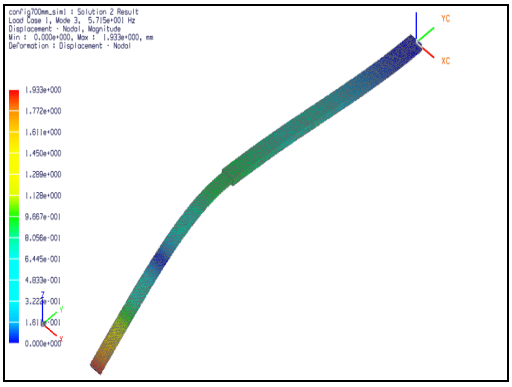

Mode4 (Flap-wise)

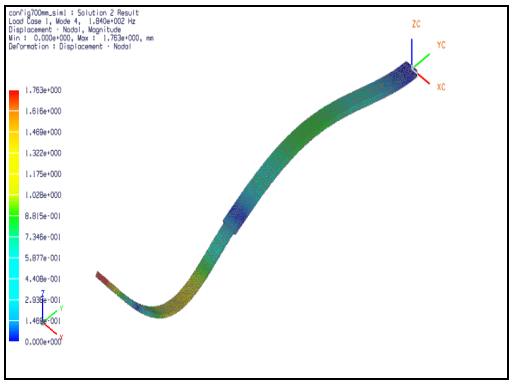

Mode5 (Edge-wise)

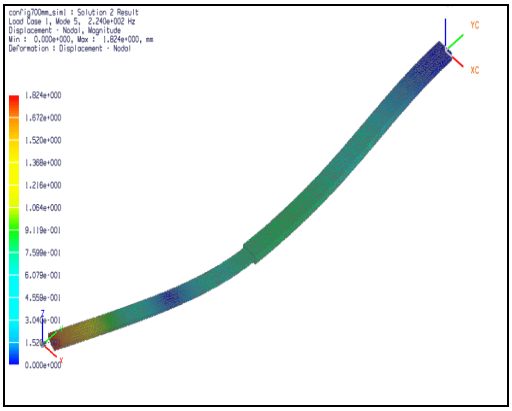

Mode9 (Torsional) : 693.5 Hz

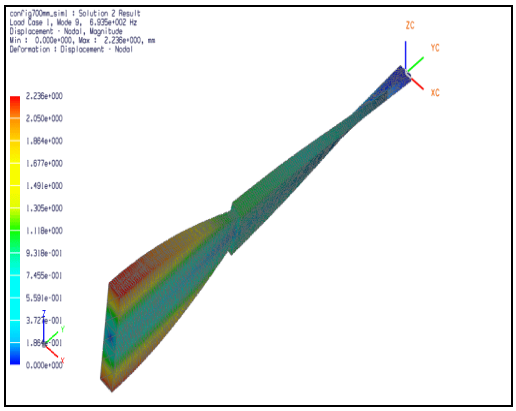

I. Configuration9

Mode1 (Flap-wise)

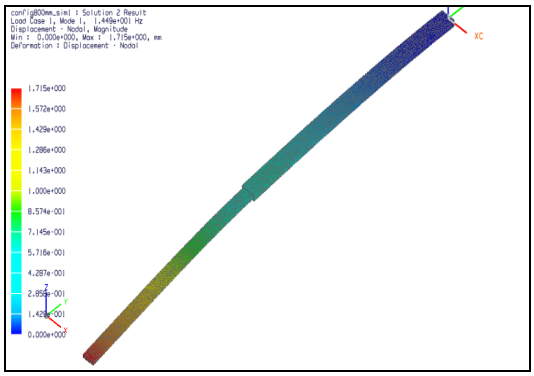

Mode2 (Edge-wise)

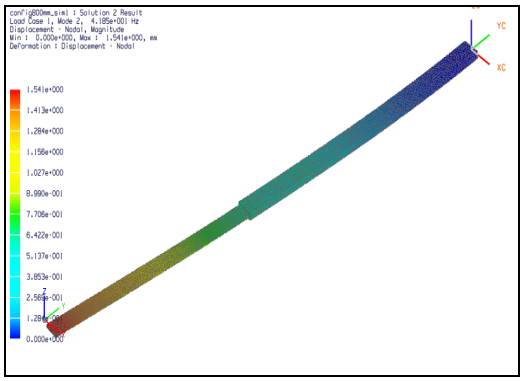

Mode3 (Flap-wise)

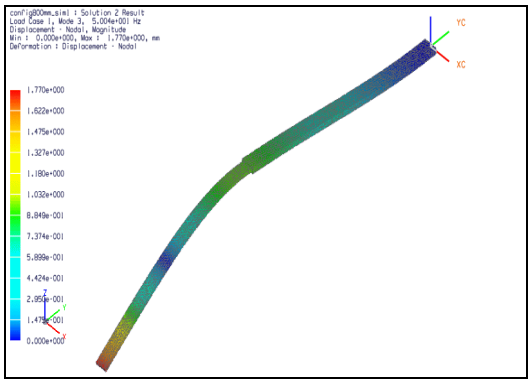

Mode4 (Flap-wise)

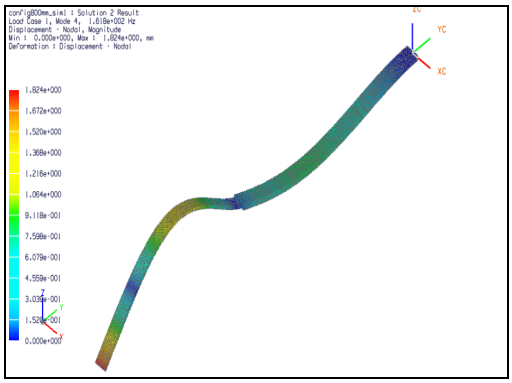

Mode5 (Edge-wise)

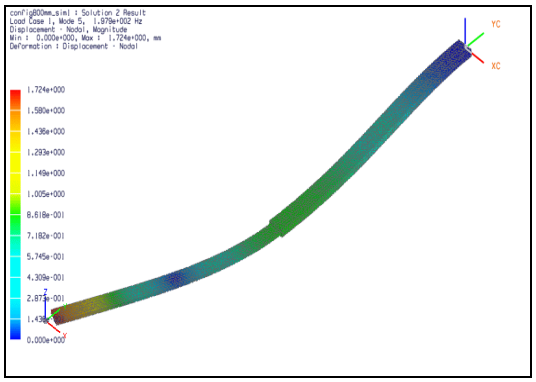

Mode9 (Torsional) : 643.2 Hz

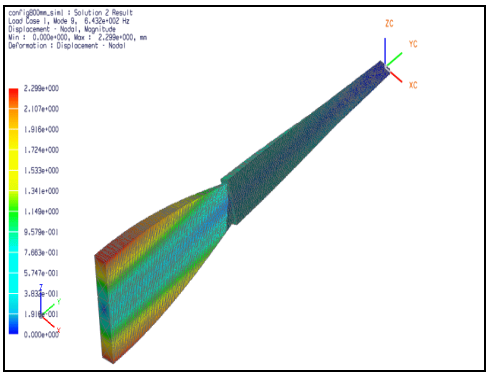

J. Configuration10

Mode1 (Flap-wise)

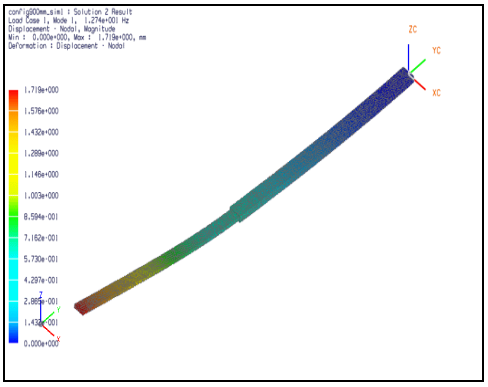

Mode2 (Edge-wise)

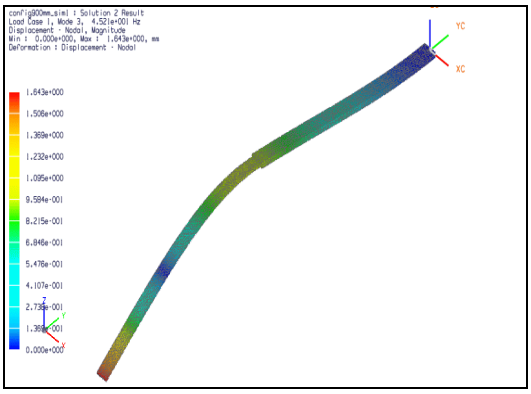

Mode3 (Flap-wise)

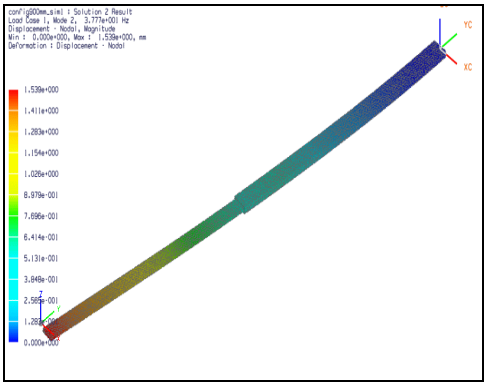

Mode4 (Flap-wise)

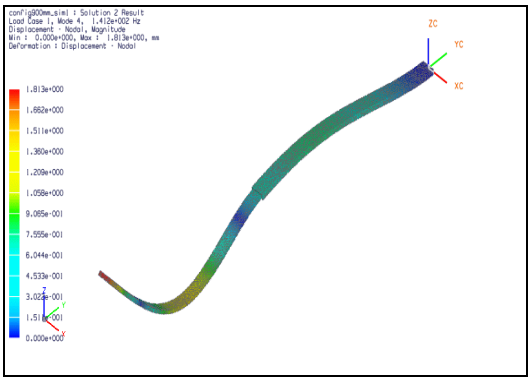

Mode5 (Edge-wise)

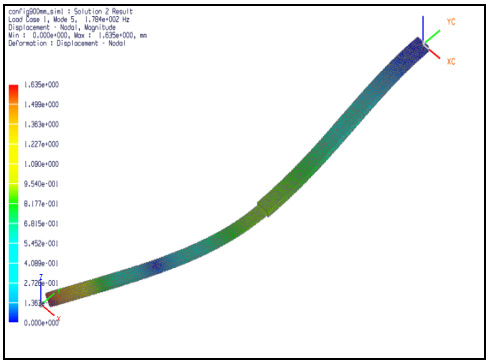

Mode9 (Torsional) : 595 Hz

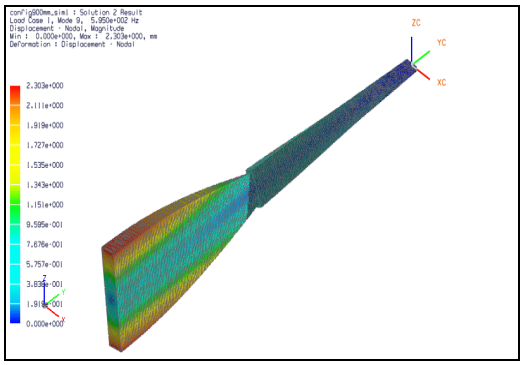

Appendix F: NX5 and MATLAB results comparison

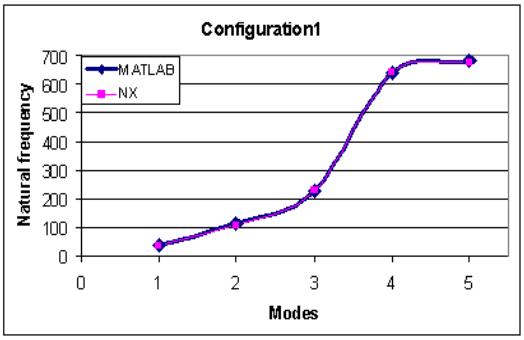

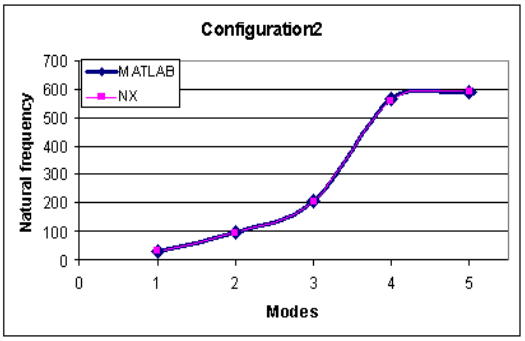

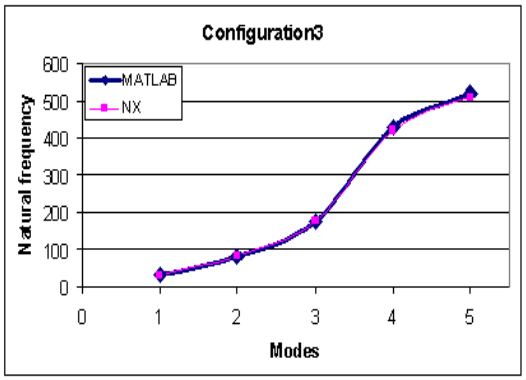

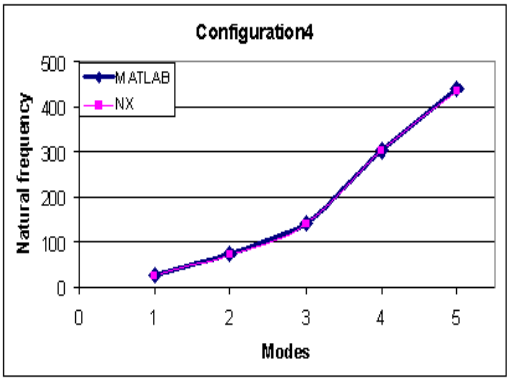

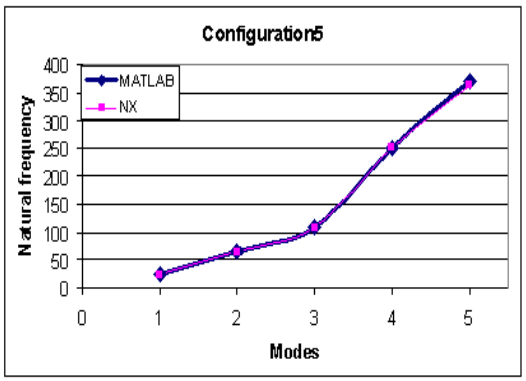

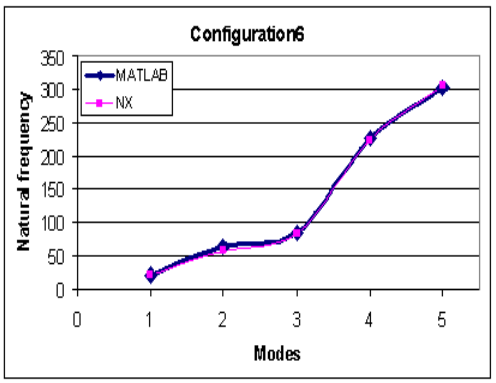

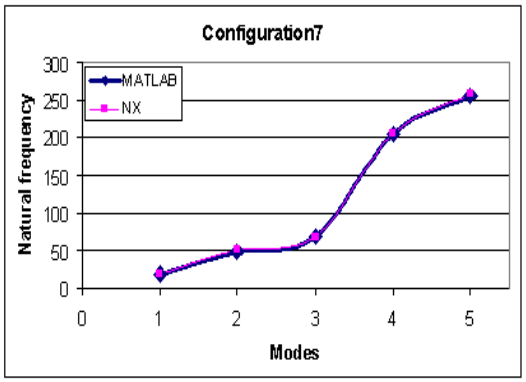

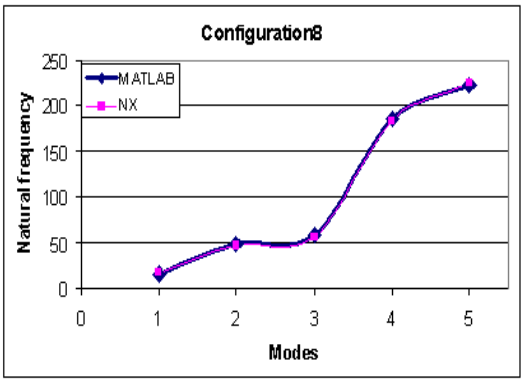

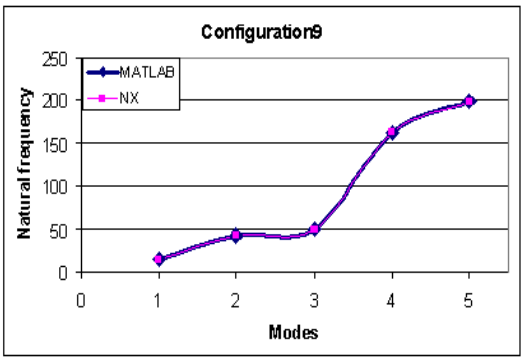
Configuration9
MATLAB
NX
Natural frequency
250
200
150
100
50
0
0
1
2
3
4
5
Modes

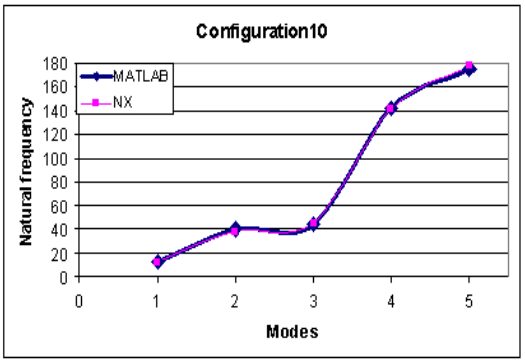
Configuration10
MATLAB
NX
Natural frequency
180
160
140
120
100
80
60
40
20
0
0
1
2
3
4
5
Modes